14. Diseases of the retinal pigment epithelium–photoreceptor complex in nonrodent animal models

GUSTAVO D. AGUIRRE, JHARNA RAY AND LAWRENCE E. STRAMM

The retinal pigment epithelium (RPE) is strategically situated between the photoreceptor cells and the choroid to mediate a number of activities which are essential for normal photoreceptor function and viability. Traditionally, these activities are considered to involve retinoid transport, esterification and isomerization, the phagocytosis and degradation of shed outer segments, and the regulation of ion and metabolite transport. Additionally, evidence for the critical role played by the RPE in sustaining the visual cells has been supported by studies carried out in the Royal College of Surgeons (RCS) strain of retinal-dystrophic rats. In these animals, postnatal retinal development is initially normal, but degeneration begins soon after photoreceptor cells have differentiated normally. Disease occurs because the mutant RPE is unable to internalize and degrade the outer segment membranes that are discarded on a daily basis from the distal tips of the photoreceptors (Herron et al., 1969). This material appears as whorls of membranes whose accumulation in the interphotoreceptor space presages the degeneration and death of the visual cells. Elegant studies by Mullen and LaVail (1976) have established that the target tissue for mutation is the RPE and not the photoreceptors, and the phagocytic defect can be examined in cell (Edwards and Szamier, 1977) or organ (Tamai and O'Brien, 1979) culture, and the photoreceptor disease prevented by the transplantation of genetically normal RPE cells (Li and Turner, 1988).

These and other studies carried out over the past twenty years have identified the critical photoreceptor-supportive roles played by the RPE. It has been established that primary dysfunction in the RPE can result in visual cell pathology and cell loss. Similarly, abnormalities in the photoreceptor cells can elicit a pathologic response in the RPE, either very early in the disease process or late, once the photoreceptor cells have degenerated and disappeared. In other cases, however, the RPE plays a passive role, demonstrating minimal response to the very severe disease that is occurring in its surround. An explanation for the varied repertoire of disease and responsiveness demonstrated by the RPE lies in its complexity and varied functional roles. The RPE can no longer be considered a simple epithelial monolayer with uniform function and behavior. Instead, it must be regarded as a highly complex cell whose cytologic and functional properties are determined or modified by positional and topographic factors. This chapter examines the role of the RPE in diseases of the pigment epithelial–photoreceptor complex in selected domestic animal species. In some cases, the diseases occur sporadically in animals, but the RPE response is so unique that it provides insights into RPE biology or pathology. In other cases, the diseases, which were once identified as naturally occurring primarily in the dog and cat, are now maintained in laboratory colonies. As a result, the models have the same gene defect and demonstrate a consistent disease phenotype that lends itself readily to experimental study and analysis.

NORMAL ANATOMY

The histology of the RPE of domestic animals is influenced by its relationship to the tapetum lucidum, a choroidal modification that is located between the large choroidal vessels and the choriocapillaris. In dog and cat, the tapetum consists of rows of multilayered, flat, often irregularly shaped cells (tapetum cellulosum; Fig. 14-1). Ultrastructurally, the cytoplasm of the tapetal cells contains groups of elongated membrane-bound rods that are electron-dense, are oriented parallel to each other, and are uniform in size and spacing. The rods are separated from each other by amorphous ground substance, and by very fine fibrils and filaments. Within each cell, there are several groups of rods, each group having its own characteristic and independent orientation (Bernstein and Pease 1959). However, the rods are all arranged in a plane parallel to the pigment epithelial basement membrane (Fig. 14-2).

Differences in tapetal structure, organization, and

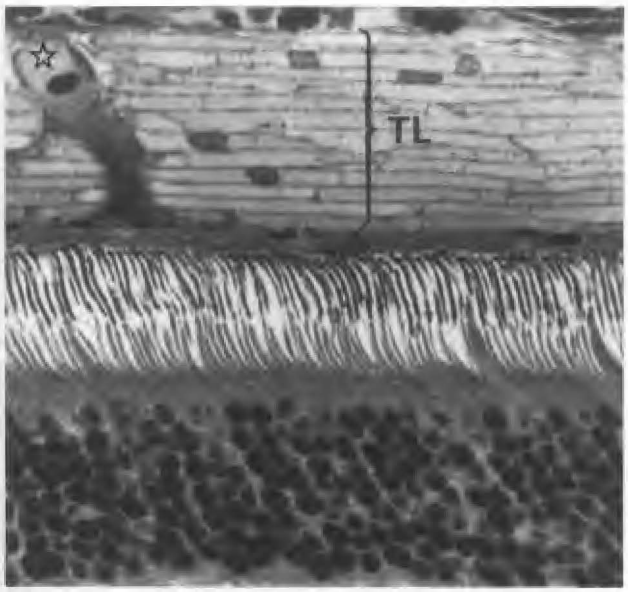

FIGURE 14-1. Anatomic relationship of the tapetum lucidum (TL), retinal pigment epithelium, and photoreceptor cells in the posterior pole of the dog eye. The outer retina is nourished by arterioles from the choroid *(open star, left)* which penetrate through the tapetum and spread horizontally between the tapetum and retinal pigment epithelium to form the choriocapillaris. Magnification ×650.

composition have been noted in the past by several investigators, and these differences appear to be species specific (see Pirie, 1966 for review). Recent studies have examined the tapetum lucidum in the dog and cat (Bussow, 1980; Burns et al., 1988; Wen et al., 1985) and found that, although superficially similar in the two species, there are many differences in structure, cell number, and chemical composition (Table 14-1). Unlike in the dog, the tapetal rodlets in the cat retain an electron-dense core after fixation, and have a single ring rather than concentric rings of zinc deposition, as visualized with a sulfide-silver histochemical method (Wen et al., 1982; 1985). The peripheral rather than internal distribution of zinc around the tapetal rodlets of the cat may account for the tenfold-lower concentration of this divalent cation in the tapetum in comparison to the dog. In the latter species, the zinc is complexed to cysteine, which occurs in higher concentration in the dog tapetum than in any other tissue (Wen et al., 1982).

In contrast to carnivores, herbivores have a fibrous tapetum (tapetum fibrosum), consisting of bundles of undulating collagenous fibers arranged somewhat concentrically and with an iridescent surface. Except for an occasional fibrocyte, the fibrous tapetum is basically

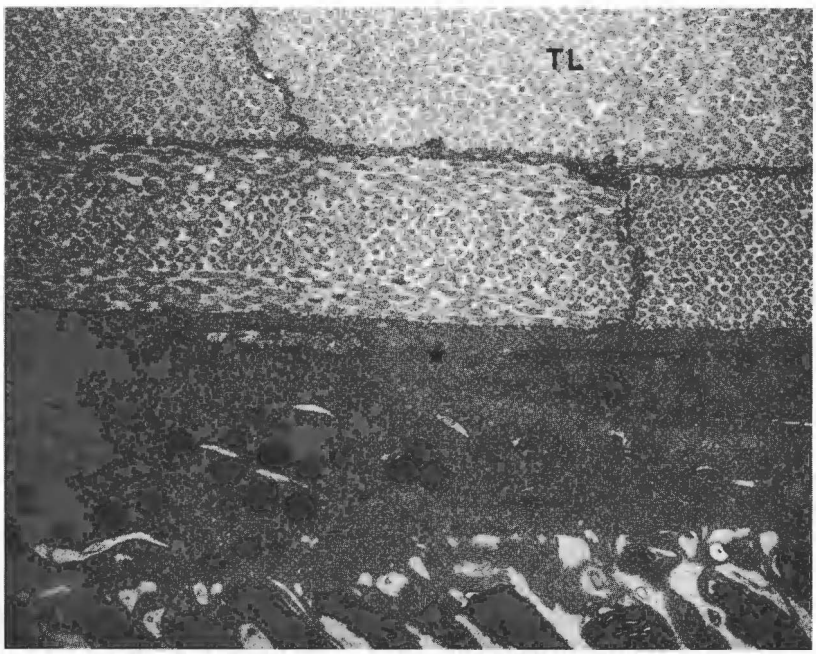

FIGURE 14-2. The tapetum lucidum (TL) consists of a multilayer of flattened cells. Each cell contains groups of membrane bound rods oriented parallel the basement membrane of the retinal pigment epithelium. Note the prominent choriocapillaris layer *(star)*. In the tapetal zone, the pigment epithelium is not pigmented; the cytoplasmic granules are lipofuscin. Magnification ×5,800.

TABLE 14-1. *Comparison of the morphological and histochemical parameters of the mature tapetum lucidum of the dog and cat*

Parameters	Dog	Cat
Number of tapetal cell layers (central)	9–11	16–20
Thickness of central tapetum	26–33 μm	61–67 μm
Thickness of retina from the area of center tapetum	151–184 μm	145–150 μm
Presence of a microtubule-like structure in each tapetal rod	present	absent
Presence of electron-dense cores in tapetal rods after prolonged glutaraldehyde fixation	absent	present
Distribution pattern of zinc in tapetal rod	two concentric rings	one outer ring
Zinc in tapetum (PPM)	26,000 ± 1,100	1,497 ± 152
Cysteine in tapetum (μM/g tissue) (n = 6–8)	241 ± 18	0

Modified from Wen et al., 1982; 1985

acellular (Bellairs et al., 1975). In the cow, this layer can be up to 50 μm thick, with the collagenous bundles oriented in a plane parallel to the RPE basement membrane (Nakaizumi 1964). Pig, rabbit, rat, guinea pig, and most higher primates lack a tapetum.

Blood supply to the RPE and outer retinal layer in the tapetal regions is derived from the large choroidal vessels external to the tapetum. Smaller vessels penetrate this layer and branch extensively under the tapetum, forming an incomplete choriocapillaris layer. In the dog and cat, the choriocapillaris forms a thin vascular zone interposed between the tapetal cells and the basal surface of the RPE. Occasionally, however, deep invaginations of the choriocapillaris into the basal RPE are seen. In the nontapetal regions, the choriocapillaris is adjacent to the larger choroidal vessels. In both tapetal and nontapetal regions, there are multiple fenestrations in the thin endothelial wall of the choriocapillaris adjacent to the RPE.

Unlike the human, the dog and cat lack a well-defined Bruch's membrane. The RPE and choriocapillaris basement membranes are apposed, with infrequent collagenous and elastic fibers present between the two. In the intercapillary space of the tapetal and nontapetal regions, more collagenous and elastic fibers are present, and a more classical Bruch's membrane is occasionally recognized. Of all the domestic species, the pig has the most prominent Bruch's membrane (Prince et al., 1960).

The topographic variation in tapetal distribution is reflected in the differing cytologic characteristics of the RPE. The most obvious of these is the presence of melanin granules. Melanin is absent in areas overlying the tapetum, although sparse pigmentation begins to appear in junctional zones, either centrally or peripherally. In these areas, the tapetal thickness gradually decreases to one or two cells, and melanin granules are present. As the tapetal cells disappear, the degree of pigmentation increases. In general, RPE cells are smaller and have less-dense pigmentation in the posterior pole, and increase both in size and in extent of melanin pigmentation peripherally. The topographic distribution of pigmentation in relation to the tapetum is illustrated in Figure 14-3. However, the elegant studies of the human RPE, which examine the cell number and size, and the degree of pigmentation and lipofuscin accumulation in relation to age and topographic position have not been done in nonprimate species (see Dorey et al., 1989; Gao et al., 1992; Feeney-Burns and Ellersieck, 1985; Feeney-Burns et al., 1984). This limitation interferes with studies examining disease processes in the RPE–photoreceptor interface.

THE RPE IN DISEASES OF THE TAPETUM LUCIDUM

Hereditary Diseases

Hereditary abnormalities of the tapetum lucidum have been described in beagle dogs (Bellhorn et al., 1975; Burns et al., 1988) and Siamese cats (Wen et al., 1982; Collier et al., 1985a). In dogs, the disease is autosomal recessive, and affected animals lack the normal tapetal reflex visible on ophthalmoscopy; instead, the fundus has a uniform red appearance without the topographic separation of tapetal and nontapetal zones (Burns et al., 1988) (Plates 14-I, 14-2). Unlike the albino fundus, where the lack of RPE and choroidal pigmentation permit visualization of the choroidal vasculature overlying the white sclera (Plate 14-III), dogs with the hereditary tapetal defect have a light, uniform choroidal pigmentation which precludes visualization of the choroidal vessels. With the exception of the foveomacular region, which is not present in nonprimate species, the fundus appearance is quite similar to that of a lightly pigmented human.

In affected dogs, there are normal numbers of tapetal cells at birth, but, with time, there is a progressive degeneration of this layer; in adult animals, the remaining layer of dysmorphic tapetal cells is only 1–2 cells thick (Fig. 14-4; Burns et al., 1988). Ultrastructural disease is evident in cells as early as 46 days after birth by the loss of the normal complement of tapetal rodlets, and the accumulation of cytoplasmic membranous whorls (Fig. 14-5). At this age, the normal tapetal cells are in the

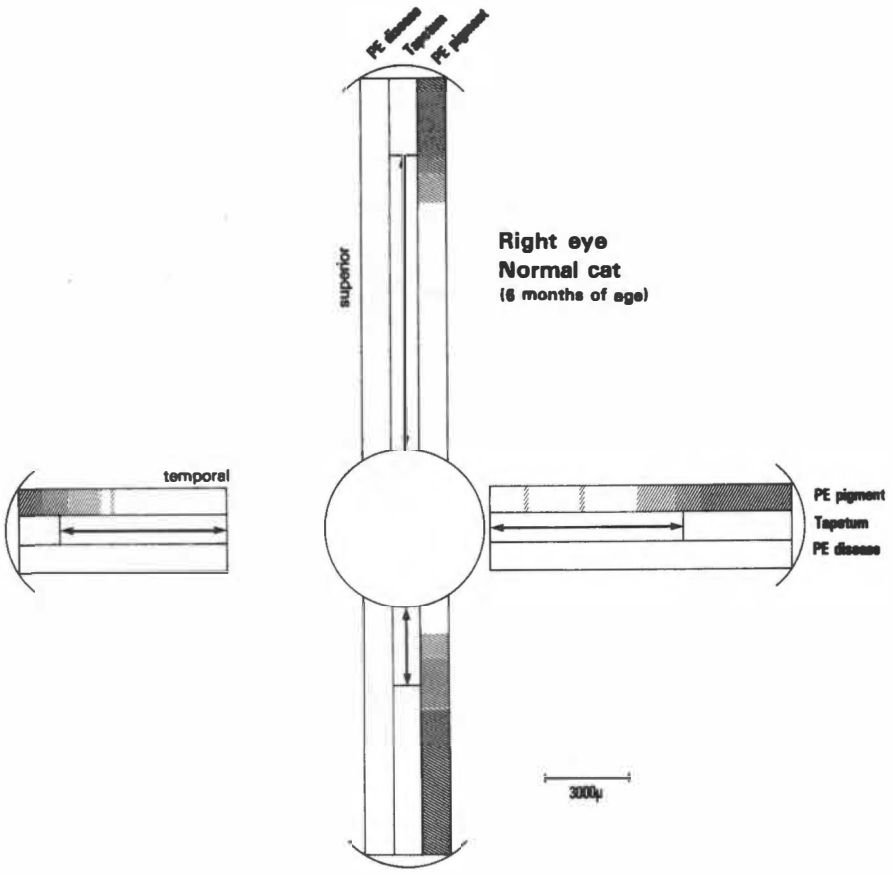

FIGURE 14-3. Schematic representation of the distribution of PE pigmentation and the presence of the tapetum lucidum in the eye of a normal cat. For comparison with the disease (MPS VI) see Figure 14-26. The eye is drawn to scale based on observations of sequential 150 μm fields extending from the disc to the ora serrata *(curved line)*. Note that the tapetum is present primarily in the superior, nasal, and temporal meridians. The pigment epithelium is not pigmented in areas where the tapetum is present. *Key:* arrows indicate the presence of tapetum; RPE pigmentation varies from absent (empty) to moderate (density present in the far periphery). (For details refer to Aguirre et al., 1983, from which this figure was reprinted.)

process of postnatal differentiation. By 13 weeks of age, the abnormal tapetal cells contain only membranous whorls and membrane-limited inclusions. These abnormalities are characteristic of the process of tapetal cell degeneration. Associated with the cytologic abnormalities, the tapetal rodlets fail to show an identifiable zinc signal by X-ray microanalysis, either in very young (21 days) or adult animals (17 months) (Burns et al., 1988). In spite of the severe disease that is occurring in the tapetal layer, the RPE remains normal, and retinal function and structure are preserved.

Similar tapetal degenerative changes have been identified in cats with Chediak-Higashi syndrome (CHS; Collier et al., 1985a), and, in both diseases, there is a striking absence of phagocytic cells during the active process of tapetal cell degeneration. As in the atapetal beagle, tapetal cells in CHS cats develop normally during the early postnatal period. However, the intracellular rods begin to degenerate by four weeks of age, and are completely degenerated by two months of age, a time by which postnatal retinal differentiation is completed (Vogel, 1970). Thereafter, the disrupted tapetal cells begin to degenerate, and this choroidal layer is lost by one year of age.

The tapetal pathology identified in cats with CHS is presumably unrelated to abnormalities in the RPE, since these occur uniformly across the monolayer as well as in other tissues (Collier et al., 1984). The disease is characterized by greatly enlarged cytoplasmic granules, including melanosomes and lysosomes. In the RPE of young affected animals, very few melanosomes are present, and most of the melanin granules are giant sized. These giant granules are composed of several melanosomes and premelanosomes in different stages of

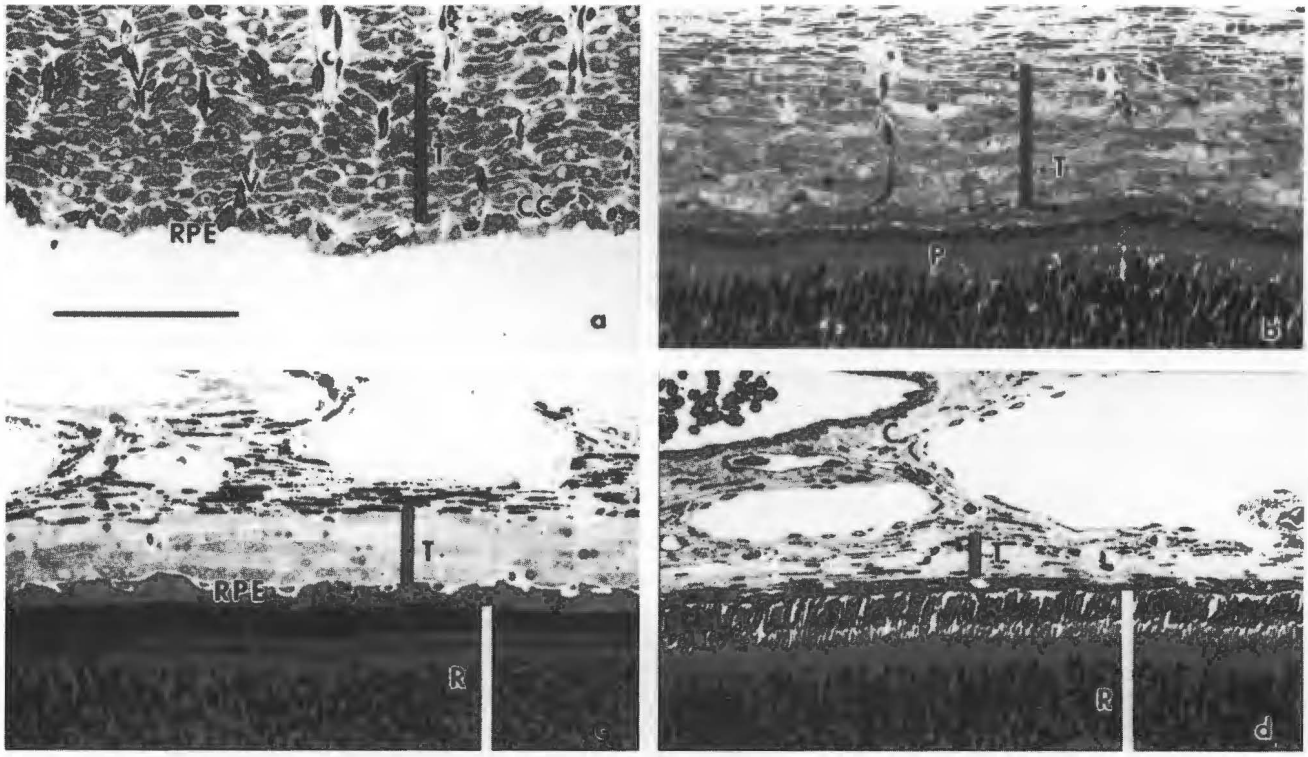

FIGURE 14-4. Tapetal region from beagles affected with a hereditary degeneration of the tapetum lucidum at different stages of the disease. (a) 7 days old. The tapetal cells (T) form a loose, irregular meshwork between the RPE and choroid (C). Vessels (V) penetrate the tapetum and form the choriocapillaris (CC). (b) 21 days. The tapetal layer (T) is more regular, and the photoreceptors (P) are differentiating. (c) 46 days. The retina (R) and RPE are normal. The tapetal layer (T) is thinner, but the remaining cells, although lightly staining, retain normal shape. (d) 17 months old. The tapetum (T) has almost disappeared, but the RPE and retina (R) are normal. Bar = 100 μm. (Reprinted from Burns et al., 1988.)

maturation, and contain lysosomal and melanosomal components (Collier et al, 1985b). The giant granules appear to form by inappropriate fusion of cytoplasmic structures, and the hypopigmentation of the RPE likely results from fusion of premelanosomes and lysosomes, with resultant destruction of the former. In the RPE of older animals (>7 years), numerous variably sized autofluorescent inclusions accumulate which, on ultrastructural examination, are identified as secondary lysosomes. Additionally, extracellular giant residual bodies form drusenoid accumulations beneath the basal lamina of the RPE. These abnormalities are associated with focal reactive and degenerative changes of the RPE, characterized as focal cells loss, detachment, and migration into the interphotoreceptor space (Collier et al., 1986).

Although the involvement of the lysosomal system in CHS is evident by the abnormal fusion of lysosomes, it is clear that lysosomal function is normal, at least in regards to the degradation of proteoglycans associated with the RPE extracellular matrices, or of glycoproteins internalized during phagocytosis of photoreceptor outer segments (see below). This has been confirmed by studies which demonstrate that there is little effect on endocytic and degradative functions, even though disease affects the late endosomes and lysosomes and may result in the abnormal secretion of some lysosomal enzymes into the media by cultured cells (Burkhardt et al., 1993; Zhao et al., 1994). Of interest have been the recent complementation studies using normal fibroblasts and fibroblasts from CHS-affected humans, mink, and mice. The normal human fibroblasts complemented the CHS fibroblasts regardless of the species, resulting in restoration of normal lysosomal size and distribution; this finding suggests the homology between the diseases occurring in the different species (Perou and Kaplan, 1993).

The tapetal defect described in the Siamese cats is not a specific hereditary defect within the breed, but appears to be part of the overall genetic makeup of the breed.

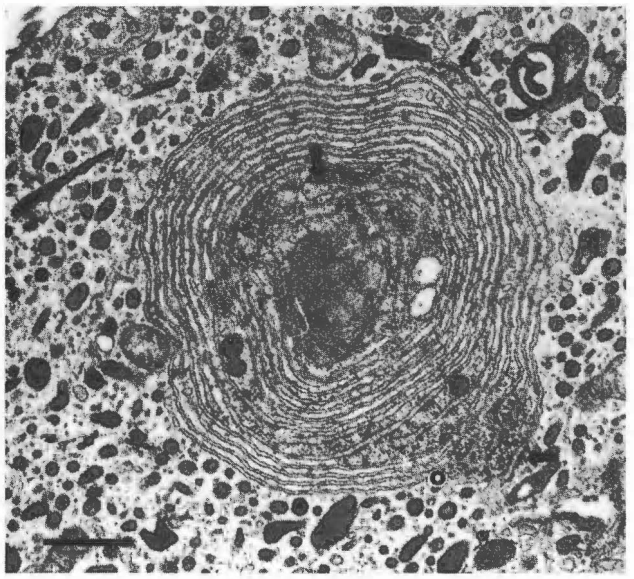

FIGURE 14-5. Degenerating tapetal cell from a 46-day-old beagle with hereditary tapetal degeneration. The tapetal rods have degenerated and the cell is filled with inclusions. The membrane whorl appears to have originated from the rough endoplasmic reticulum, and ribosomes are present inside or at the outer border *(arrows)* of the whorl. Bar = 1 μm. (Reprinted in part from Burns et al., 1988.)

Other breed-specific characteristics reported are differences in fur and ocular pigmentation, strabismus, and abnormalities in the retinogeniculate and cortical projections (see Wen et al., 1982 for review). Even though the ophthalmoscopic appearance of the tapetum is normal in Siamese cats, microscopic abnormalities have been identified in some animals, and consist of weakly staining tapetal cells on light microscopic examinations. On ultrastructural examination, the abnormal cells are filled with irregular and disoriented tapetal rods whose membranes are enlarged or disrupted. The cores of the tapetal rods appear empty, or are filled with an electron-dense material. These abnormalities are not present uniformly in all tapetal cells, but vary in different layers. Overall, however, disease of individual tapetal cells is most severe in the retinal aspect of the tapetum. Associated with the tapetal abnormality is a significant reduction in the amount of zinc in the tapetal rods (Wen et al., 1982). The causal association between the lower levels of zinc and the tapetal cell degeneration is not clear at this time. In spite of the damage to the tapetal cells, the RPE remains normal (Aguirre, unpublished).

Acquired Defects: Nutritional and Toxic Damage

Tapetal defects in cats have been reported secondary to a nutritional deficiency of taurine (Wen et al., 1979). In affected cats there is a marked reduction in thickness associated with a decrease in cell number. Additionally, there is a marked disorganization of the lattice arrangement of the tapetal rods. This abnormality is associated with a taurine-associated progressive degeneration of the cone and rod photoreceptors, with sparing of the RPE (Aguirre and Rubin, 1979: Fig. 19.23).

The most common causes of acquired tapetal defects have been reported in ophthalmic toxicology studies, particularly of dogs, where administration of various compounds results in dramatic changes in the tapetum which are visible on ophthalmoscopy, histopathology, and ultrastructural examination (Figs. 14-6, 14-7). The prototype compound to produce this effect is the antitubercular drug ethambutol. Administration of this compound to dogs causes a decoloration of the tapetum and a reversible disorientation of the tapetal rods with no RPE or retinal damage (Kaiser, 1963; Vogel and Kaiser, 1963). More-severe tapetal damage occurs in the dog following administration of the potent zinc chelator diphenylthiocarbazone (dithizone). There is retinal edema, pigmentary disruption, and end-stage retinal degeneration with intraretinal pigmentation at the higher doses. It appears, however, that the tapetum may play a protective role in ameliorating dithizone toxicity of the retina. In the tapetal area, dithizone causes tapetal necrosis while sparing the underlying RPE and retinal layers. In contrast, areas devoid of tapetum show severe RPE and retinal degeneration (Aguirre and Rubin, 1979). Similar neuroretinal damage has been reported in animals without a tapetum (Budinger, 1961, Butturini et al., 1953).

Tapetal lesions also have been reported with various classes of compounds, not all of which are known zinc chelators. For example, administration of zinc pyridinethione (Cloyd et al., 1978), selected beta-adrenergic blocking agents (Schiavo et al., 1984), macrolide antibiotics (Massa et al., 1984), aromatase inhibitors (Schiavo et al., 1988), and other compounds can cause varying degrees of tapetal damage in the dog or cat (Cloyd et al., 1978). Where damage is acute and severe, such as with zinc pyridinethione, the necrotic changes in the tapetum result in damage to the penetrating tapetal arterioles. This causes focal lesions, presumably infarcts in the RPE and retina, which are evident as focal areas of subretinal edema and hemorrhage. When the lesions are more severe, there is diffuse subretinal edema, retinal detachment, and blindness (Cloyd et al., 1978). In this case the RPE appears to be damaged secondarily by the severe changes occurring in the adjacent tapetal layer, and displays a breakdown of the outer blood–retina barrier. In other cases, for instance following the administration of an aromatase inhibitor (Schiavo et al., 1988), tapetal damage is selective and limited to this cell

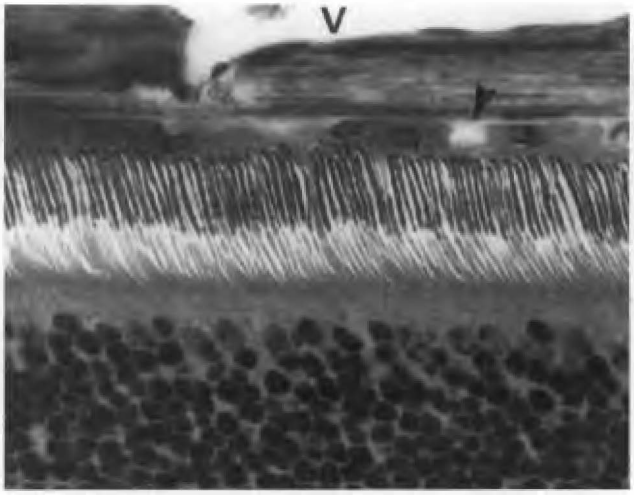

A

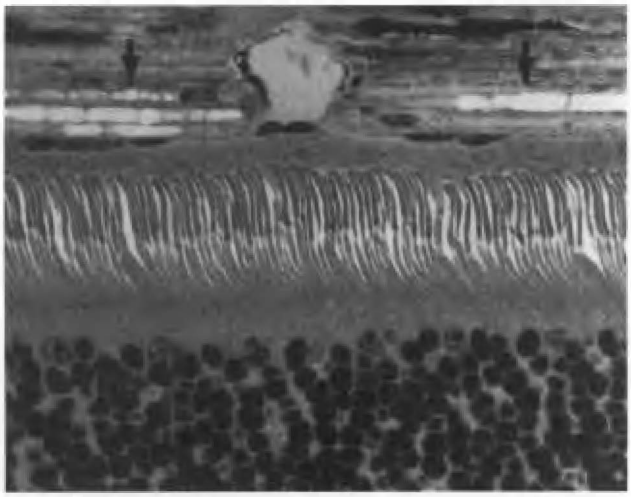

B

FIGURE 14-6. Chronic administration of a tapetotoxic compound results in tapetal degeneration in the dog. In some areas there is loss of tapetal cells *(A)* and the RPE abuts the vascular choroid (v). In other areas, the few remaining tapetal cells have vacuolated inclusions *(arrows, B)*. Arrowhead indicates indentation of the normal RPE by the choriocapillaris. Magnification ×680.

layer; thus the RPE and retina remain normal. The differential expression of the compound-associated damage between the tapetal and nontapetal areas is intriguing, and raises concerns about the interpretation of tapetal lesions in animals used in toxicologic studies. For that reason, several studies of potentially tapetotoxic compounds also use atapetal dogs having the hereditary absence of this structure (Burns et al., 1988). It has been clearly demonstrated that, in contrast to the findings in normal dogs, these compounds cause no ocular abnormalities in dogs lacking a tapetum (Cloyd et al., 1978; Massa et al., 1984; Schiavo et al., 1984).

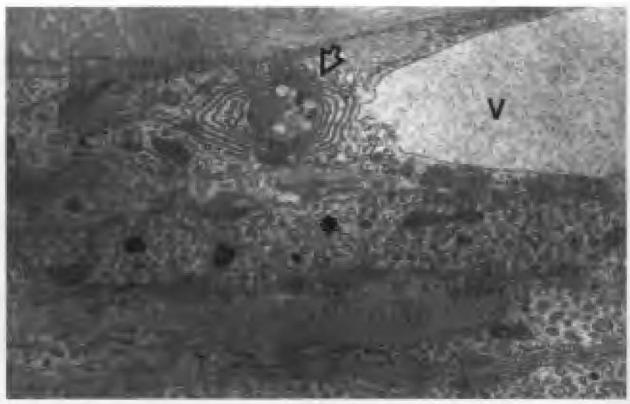

FIGURE 14-7. Ultrastructural appearance of tapetal degeneration induced by chronic administration of a tapetotoxic compound. There is loss of tapetal cells. Remaining cells have disorientation of the rodlets (*), and accumulation of vacuoles (V) and membrane whorls *(open arrow)*. Magnification ×10,000. Compare with Figure 14-5.

THE RPE IN HEREDITARY PHOTORECEPTOR DISEASES

Hereditary diseases affecting the rods and cones, either primarily or secondary to an RPE defect, are recognized in a number of different species including man. Regardless of the underlying cause, the diseases appear to affect the photoreceptors early and progressively; in the advanced stages, the entire visual cell layer is destroyed, and there is damage also to the inner retinal layers and the RPE. In man, this class of diseases is referred to, collectively, as retinitis pigmentosa (RP). Multiple loci for RP have been recognized, but few genes have been identified (see Dryja and Li, 1995 for review). Recent studies of retinal degeneration in human patients and animal models have identified mutations in six different genes (rhodopsin, peripherin/rds, rom-1, a and β subunits of rod cyclic GMP-phosphodiesterase [PDEA and PDEB], and the cyclic GMP-gated channel) as causally associated with RP (Humphries et al., 1992; Kajiwara et al., 1991; 1994; Travis et al., 1989; Bowes et al., 1990; Suber et al., 1993; McLaughlin et al., 1993; Dryja et al., 1995; Huang et al., 1995). Some of these genes—rhodopsin, rom-1, PDEB—are expressed exclusively in the rod photoreceptor cells, yet the clinical and pathologic phenotype of RP and related diseases indicates that there is progressive rod and cone degeneration with a late and secondary involvement of the RPE. It appears that all defects that cause widespread disease and de-

generation of rods, regardless of the selective expression of the gene product in rods, result in the concomitant loss of cones, and progressive retinal degenerative disease.

The manner in which cellular dysfunction, disease, and degeneration are expressed in the visual cell layer is dependent, to a large extent, on the gene affected and the nature of the mutation. However, different mutations of the same gene can result in a varied clinical phenotype, for example with opsin (Berson et al., 1991; Dryja et al., 1993) and peripherin/rds (Weleber et al., 1993) genes, and factors external to the visual cell may also play a modulatory role to influence the temporal, topographic, or cellular distribution of the disease. In this brief overview, we discuss different aspects of photoreceptor disease from the perspective of the RPE.

Progressive Retinal Atrophy (PRA) in the Dog

The PRA class of diseases represents a heterogeneous grouping of retinal disorders having similar disease phenotype. Like RP in man, the term PRA represents an aggregate of different genetic defects having a broadly similar clinical phenotype. All show the same general ophthalmoscopic abnormalities (Plate 14-IV) and visual deficits characterized initially by rod dysfunction followed by loss of day vision; in the late stages of the disease, the animals are blind, have end-stage retinal degenerative changes, and secondary cataracts. Excluding the absence of intraretinal pigmentation, which appears to be a property unique to the human retina with advanced photoreceptor disease, the clinical phenotype of PRA in dogs is similar to RP in man.

Within this general grouping, PRA is subdivided into developmental and degenerative diseases (Table 14-2). The developmental class represents a large grouping of genetically distinct disorders which are expressed cytologically in the postnatal period, at the time that visual cells are beginning to differentiate. These developmental disorders represent a dysplasia of the rod and/or cone photoreceptors, and each has its own unique disease course and phenotype, as assessed by functional and morphologic criteria (Aguirre, 1978; Acland and Aguirre, 1987; Acland et al., 1989; Parshall et al., 1991). Even though all dysplasias show rather severe structural alterations of the photoreceptor cells, the rate of progression to loss of cones, the hallmark criteria for loss of functional vision, is varied; e.g., this occurs early in the *erd, rcd1* and *rcd2* retinas, but not until the equivalent of middle age in *pd* and *rd*. In contrast, the degenerative class of diseases represents defects in which photoreceptor cells degenerate after having differentiated normally; this class includes diseases at the progressive rod-cone degeneration *(prcd)* and XLPRA gene loci (Aguirre et al., 1982a; Aguirre and Acland, 1988; Acland et al., 1994). Here, disease occurs more slowly, and is modified by temporal and topographic factors (see below). Different alleles have been identified at the *prcd* locus (Aguirre and Acland, 1988), and these segregate independently to regulate the rate, but not the phenotype, of photoreceptor degeneration (Acland and Aguirre, unpublished). Examples are presented below.

TABLE 14-2. *Gene loci for hereditary photoreceptor diseases in dogs*

Disease name	Gene locus	Genes excluded/included
Progressive Retinal Atrophy (PRA)		
I. Abnormal Photoreceptor Development		
Rod-cone dysplasia 1	*rcd1*	*PDEB (codon 807-stop)*
Rod-cone dysplasia 2	*rcd2*	PDEB, transducin α-1
Rod dysplasia	*rd*	
Early retinal degeneration	*erd*	RDS/peripherin, opsin, PDEB, transducin α-1
Photoreceptor dysplasia	*pd*	
II. Photoreceptor Degeneration		
Progressive rod-cone degeneration	*prcd*	RDS/peripherin, opsin, PDEB, transducin α-1
X-linked PRA	XLPRA	
Other Primary Photoreceptor Diseases		
Cone degeneration	*cd*	Transducin β3
Congenital stationary night blindness	*csnb*	

Data from Aguirre and Acland, 1988; Acland et al., 1989; 1994; 1995; Aguirre and Rubin 1974; Akhmedov et al., 1997; Ray et al., 1996, 1997; Wrigstad, 1994.

Photoreceptor Dysplasias, Abnormal Retinal cGMP Metabolism and Retinal Degeneration

Rod-cone dysplasia 1. Rod-cone dysplasia1 *(rcd1)* in the Irish setter is a recessively inherited photoreceptor defect characterized by arrested differentiation of visual cells resulting from an abnormality in retinal cyclic GMP (cGMP) metabolism (Aguirre et al., 1978; 1982b). Beginning at ten days of age, deficient cGMP-phosphodiesterase (cGMP-PDE) activity causes the retinal levels of cGMP to rise sharply to concentrations up to tenfold higher than normal; these biochemical abnormalities are present before degenerative changes are observed in the photoreceptor cells (Fig. 14-8). The morphologic and biochemical phenotype of the disease is similar to that present in the *rd* mouse (Farber and Lolley, 1974). Homology between the dog and mouse diseases, as well as to some forms of RP in man, has been established by identification of mutations in the PDE-Beta (PDEB)

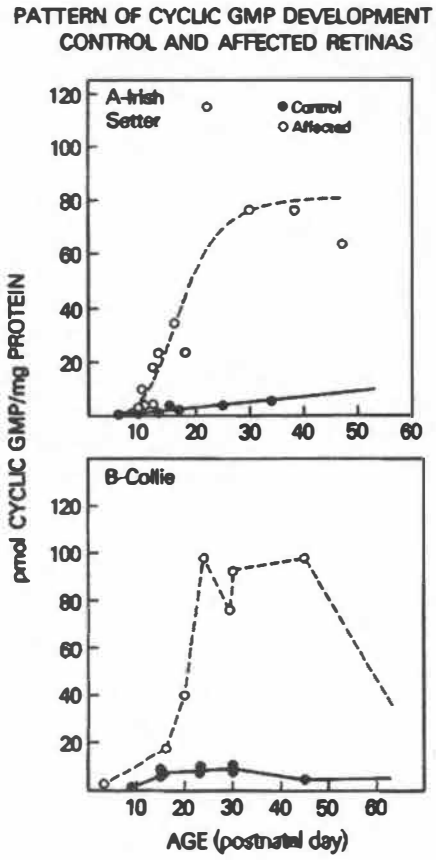

FIGURE 14-8. Developmental pattern of changes in cGMP concentration with age in retinas from dogs affected with *rcd1 (Irish setter, upper panel)* and *rcd2 (collie, lower panel)*. Normal values *(solid circles)* from controls are included in each figure. In both *rcd1* and *rcd2*, levels of cGMP increase early in the postnatal period to values 8–10 times higher than normal. (Modified from Chader et al., 1985.)

subunit gene as being responsible for the diseases in the three different species (McLaughlin et al., 1993; Bowes et al., 1990; Farber et al., 1990; 1992; Suber et al., 1993). Not surprisingly, human RP patients with abnormalities in the PDEB gene show a varied mutation spectrum (McLaughlin et al., 1995). In contrast, the same two different abnormalities have been identified concurrently in all *rd* strains examined (Pittler and Baehr, 1991; Bowes et al., 1993), while all *rcd1*-affected dogs have the same mutation in codon 807 (TRP807X), which presumably results in the premature termination of the PDEB protein by 49 amino acid residues (Clement et al., 1993; Ray et al., 1994 and 1995).

A question arises about the specificity of the abnormal retinal cyclic nucleotide metabolism, and whether it is limited to the visual cells. In our original study, we found that retinal cGMP levels were elevated in retina, but not in the RPE/choroid complex or in nonocular tissues (Aguirre et al., 1978). Subsequently, using the retinal layer microdissection method of Lowry, Barbehenn and colleagues (1988) found that the elevated retinal cGMP levels are confined to the photoreceptor cells. Since the outer segments of the affected visual cells are small, and degenerate early, the elevated cGMP levels are not located in this structure but, rather, are present in the outer nuclear and plexiform layers (Barbehenn et al., 1988). Such abnormally high levels of cGMP in the synaptic terminals are unexplained, but may indicate aberrant sites of synthesis or trafficking of newly synthesized cyclic nucleotides in the dysplastic rod photoreceptors. Additionally, more recent studies indicate that there are no abnormalities in cyclic nucleotide levels in cultured RPE cells of *rcd1*-affected dogs, further confirming the specificity of the defect to the visual cells (Table 14-3; Stramm, Fletcher, Aguirre, and Chader, unpublished).

In *rcd1*-affected dogs, there is normal retinal structure and opsin biosynthesis during the first two weeks of life. However, at the time when photoreceptors begin to differentiate in the normal retina (13–16 days), development of rods in the *rcd1* retina is arrested, and the diseased cells begin to degenerate; by 25 days after birth, photoreceptor cell death begins, and this process continues throughout the first year of life (Fig. 14-9) (Aguirre et al., 1982b; Schmidt and Aguirre, 1985). The degeneration initially affects the rods, and, as these cells degenerate, the proportion of cones in the visual cell layer increases. However, cone degeneration develops eventually, and results in collapse of the interphotoreceptor space, bringing into close apposition the apical surfaces of the RPE and Müller cells. In spite of the severe disease that is occurring in the apposing visual cell layer, the RPE remains normal and minimally reactive, and, as is characteristic of hereditary retinal diseases in nonprimate models, there is a lack of intraretinal pigment migration.

Photoreceptor–RPE interactions occur through the interphotoreceptor matrix (IPM). Until recently, this matrix was ill defined, and its structural and functional characteristics were not clear. The IPM is now known to be a complex and highly ordered structure consisting of soluble and insoluble constituents in which proteins,

TABLE 14-3. *Cyclic nucleotide levels (picomole/mg protein) in primary cultures of RPE cells from ten-week-old normal, carrier, and* rcd1*-affected dogs*

Nucleotide	Normal	Carrier	Affected
cAMP	3.1 ± 1.6	3.9 ± 2.9	2.2 ± 0.2
cGMP	1.8 ± 1.7	1.8 ± 1.1	1.2 ± 0

Unpublished data from Stramm, Fletcher, Aguirre, and Chader.

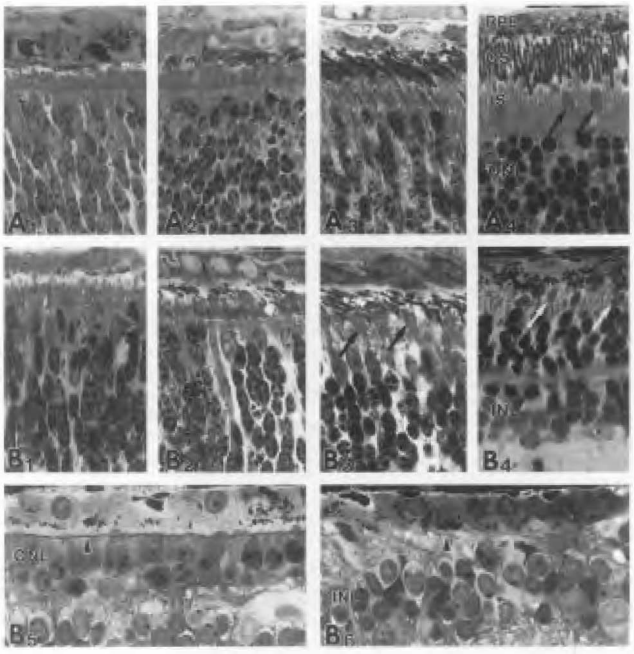

FIGURE 14-9. Retinas from normal (A_{1-4}) and *rcd1*-affected Irish setters (B_{1-6}) of different ages. Normal: A_{1-4} = 10 days, 13 days, 26 days, and adult. Affected: B_{1-4} = 9 days, 16 days, 33 days and 57 days; $B_{5,6}$ = 1 year. In the normal dog, the inner segments are distinct by 10 days, and outer segments have elongated to near adult proportions by 26 days. The adult retina has a high photoreceptor density, and the rods outnumber the cones (arrows in A_4). The *rcd1* retina shows normal development at 9 days of age. At 16 and 33 days of age, the rod inner segments have not elongated, and the outer segments are short and disorganized. Loss of rods results in increased prominence of cones (arrows in $B_{3,4}$), and thinning of the outer nuclear layer. By 1 year of age, photoreceptor loss is extensive. At all stages of the disease, the RPE is normal. Magnification ×400. (Reprinted from Farber et al., 1992.)

glycoproteins, enzymes (acid hydrolases, etc.), glycosaminoglycans (GAGs), proteoglycans, and other molecules are localized (see Hageman and Johnson, 1991 for review). Within the insoluble matrix, individual rods and cones are invested by photoreceptor type specific domains (Hageman and Johnson, 1991; Mieziewska et al., 1991). A matrix disorder that affects either its synthesis or maintenance could adversely affect these two cell layers; alternatively, disease in the photoreceptors or RPE layers could induce secondary changes in the matrix structure to modify the rate of visual cell degeneration.

The complexity of the IPM and the various cell types that border the matrix (rods, cones, RPE, and Müller cells) precludes establishing a cell-specific association between a given component and a cell. Similarly, the contribution of different cell classes to the development of the matrix is also not known. Because of the severe developmental arrest that occurs in *rcd1*-affected photoreceptors, we have examined the matrix to see if abnormalities in photoreceptor differentiation affect the development or maintenance of the insoluble IPM (Mieziewska et al., 1993a). The insoluble matrix domains of the IPM are characterized using lectin cytochemistry (wheat germ agglutinin [WGA] and peanut agglutinin [PNA] lectins) in cryosections of retinal tissues and in extracted insoluble matrix preparations, and examined by epifluorescence and scanning confocal laser microscopy.

In the normals, the insoluble matrix is extracted as a continuous sheet that comprises two photoreceptor-specific matrix domains distinguished both by the size of the domains, and by differential binding of WGA and PNA lectins (Mieziewska et al, 1991). Each domain encloses a photoreceptor inner and outer segment. The PNA lectin primarily labels galactose residues in the cone-associated matrix, with weak binding to the rod matrix; the WGA lectin labels equally the rod- and cone-associated matrices which contain N-acetyl glucosamine and sialic acid residues. The specific matrix domains identified with these lectins are present early in the postnatal developmental period, at the time that the two classes of photoreceptors are recognizable cytologically, and they mature in parallel with visual cell morphogenesis. Since the matrix conforms to the shape of the individual rods and cones it surrounds, the structural changes associated with normal photoreceptor development also occur in the matrix (Fig. 14-10$A_{1,2}$) (Mieziewska et al., 1993a).

As noted previously, the *rcd1* retina shows normal development of the photoreceptors during the first two weeks of life, and during this time period the IPM also develops normally. However, no change in matrix structure or carbohydrate specificity is found during the period of developmental arrest (13–24 days postnatal), or after the onset of photoreceptor degeneration (after 25 days of age; Schmidt and Aguirre, 1985). The only changes in the IPM that occur during this time are conformational, i.e. distortion, adherence of cellular debris, and loss of continuity, abnormalities that are presumably secondary to the severe pathology occurring in the visual cells within the individual domains. These occur in older affected retinas as the abnormally developed outer segments disappear and the inner segments shorten and broaden concomitant with cell loss in the photoreceptor layer (Fig. 14-10B_{1-4}, $C_{1,2}$). Survival of cones late in the disease is a feature of *rcd1*, and PNA labeled cone domains remain intact, even when surrounding severely degenerated cone cells (Mieziewska et al., 1993a).

The cellular origin of the matrix constituents has not been established (Mieziewska, 1993). Due to the close relationship between matrix and photoreceptor cells in

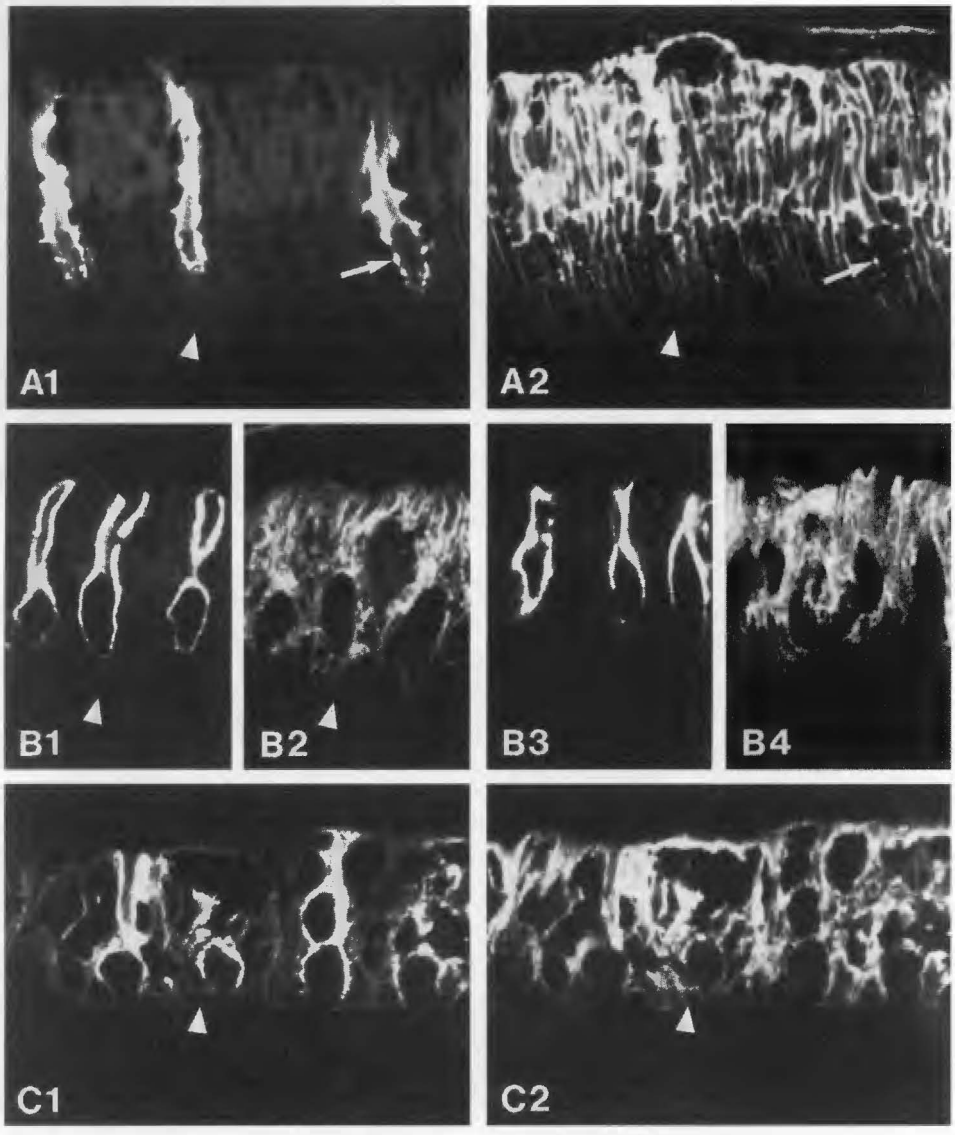

FIGURE 14-10. Optical sections normal and *rcd1*-affected retinas viewed with a confocal scanning laser microscope. Sections were collected in 0.5 μm increments, and each picture represents one section. Normal retina 60 days old shows the distribution of PNA (A_1) and WGA (A_2) label in both rod and cone matrices. A substructure of the cone matrix is labeled by both PNA and WGA *(arrow)*. The WGA matrix label is stronger in the OS layer than in the IS layer. In the 40-day-old *rcd1*-affected retina ($B_{1,3}$ = PNA, central [1] and peripheral [3] retina; $B_{2,4}$ = WGA, central [2] and peripheral [4] retina) the CIS appear to be displaced sclerally in relation to the small RIS. At 60 days (C1 = PNA, C2 = WGA) substantial cell loss has occurred and the cone inner segments are close to the OLM *(arrowhead)*, but label specificity is comparable to the normal retina (C_1). The WGA lectin labels a domain that is irregular and distorted secondary to the rod disease (C_2). Magnification ×1200. (Reprinted from Mieziewska et al., 1993a.)

normal and diseased retinas, it is reasonable to assume that the photoreceptor cell is synthesizing its own matrix domain. Studies have shown that photoreceptors are likely to synthesize chondroitin sulfate proteoglycans which are parts of the insoluble matrix (Landers et al., 1991). However, the close association between photoreceptor cells, matrix, and RPE does not preclude the involvement of RPE in synthesis of specific matrix components, either directly or via inductive factors. The studies with the *rcd1* mutant show that normal photoreceptor development is not a prerequisite for the insoluble IPM to develop normally. Similarly, normal maintenance of the matrix occurs even when the visual cells are undergoing very rapid and severe degeneration, and the matrix disappears only after there is photoreceptor loss. It is possible, therefore, that the RPE and/or

Müller cells are the principal cells involved in maintaining this elaborate and complex extracellular scaffold once it is synthesized. Alternatively, one could argue that the photoreceptor cells, although severely diseased, still are able to orchestrate the formation of the insoluble IPM, and this structure is maintained normally until the visual cells disappear. These are issues that cannot be resolved at present. What is known, however, is that the RPE plays a critical role in the remodeling and degradation of matrix constituents through the extracellular and intracellular pathways involved in the degradation of the GAG components of matrix proteoglycans. This will be discussed in subsequent sections (see below).

Rod-cone dysplasia 2. A second early-onset photoreceptor dysplasia has been identified which appears to share many phenotypic similarities with *rcd1,* and, as a result, has been given the disease designation of rod-cone dysplasia 2 (*rcd2*) to differentiate it from the disease present in the Irish setter dogs. Based on clinical, electrophysiological, morphological, and biochemical criteria, the two diseases are identical (Chader, 1991; Woodford et al., 1982). In both, there is an equally rapid increase in retinal cGMP levels early in the postnatal period; the magnitude of this elevation, as well as its time course, are the same (Fig. 14-8). In both *rcd1* and *rcd2* there also is deficient cGMP-PDE activity, although in the latter the activity is calmodulin independent (Chader et al., 1985; Chader, 1991). As in *rcd1,* the disease is expressed initially in the photoreceptor cells, and there is sparing of the RPE and inner retinal layers until the end-stages of the disease.

Although *rcd1* and *rcd2* are phenotypically and biochemically identical, there is considerable evidence that the disorders represent mutations of different genes. With the advent of a molecular diagnosis for *rcd1,* we have established that this mutation is *not* present in *rcd2,* and that the nucleotide sequence of exon 21 of the PDEB gene in *rcd2*-affected dogs is normal (Ray et al., 1994). This finding does not by itself rule out the PDEB gene involvement in *rcd2,* as a different mutation may be present elsewhere in the coding sequence, in an intron–exon junction or in the promoter or a regulatory region. The most compelling evidence for nonidentity of the two diseases comes from our group's previous work in which they performed crosses between dogs affected with *rcd1* and *rcd2* and found the progeny to be normal (Acland et al., 1989). Thus *rcd1* and *rcd2* represent nonallelic diseases that have similar effects on retinal cyclic GMP metabolism. It is likely, therefore, that the molecular defect in *rcd2* resides in one of the two remaining PDE subunits, or in the genes coding for proteins involved in PDE activation.

Other photoreceptor dysplasias. Table 14-2 summarizes the developmental and degenerative photoreceptor diseases of the dog. Two of these, *rcd1* and *rcd2* have been discussed above. Of the three remaining diseases, the mutant strain for one, rod dysplasia *(rd),* has been lost, and the disease is no longer extant in the general population, nor is it maintained in experimental research colonies (Aguirre, 1978; Acland and Aguirre, 1987). In all of these diseases there is a minimal RPE response to the degenerative process occurring in the adjacent photoreceptor layer (Fig. 14-11). It is only in the late stages of the disease that the RPE undergoes atrophy and limited intraretinal migration into areas that are gliotic and disorganized (Fig. 14-12). These reactions are secondary and nonspecific. Of interest is the exclusion of abnormalities in retinal cyclic nucleotide metabolism as being causally associated with the diseases. This has been done biochemically in the case of *pd* and *erd* (Acland et al., 1989; Parshall et al., 1991). In the latter disease, mutations in the PDEB gene have been excluded, respectively, by breeding and molecular studies (Acland et al., 1989; Ray et al., 1994). This establishes that abnormalities in retinal cGMP metabolism in the retina are not the only causes of photoreceptor dysplasias, although they are likely to be involved in those diseases that have an early onset and a relatively rapid disease course.

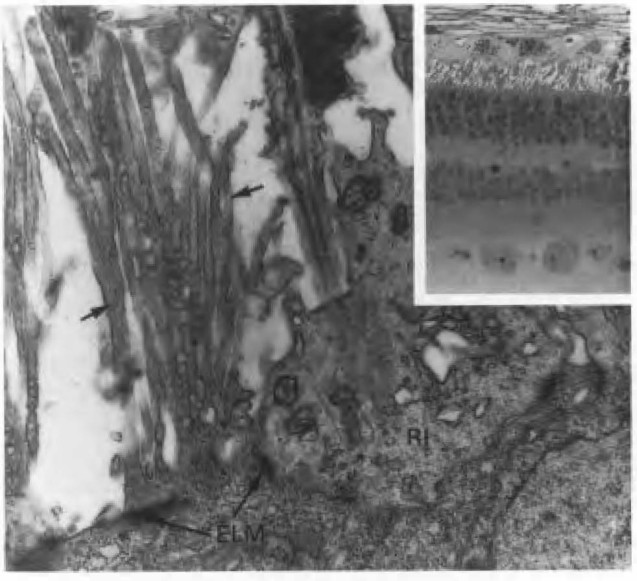

FIGURE 14-11. Müller fiber baskets *(arrows)* projecting through the external limiting membrane (ELM) become prominent after loss of photoreceptor cells in *rd*-affected retina. Inset shows the reduction in photoreceptor number and the shortening of rod inner segments (RI). The RPE is normal. Magnifications: ×17,000 for main figure, ×200 for inset. (Reprinted from Aguirre, 1978.)

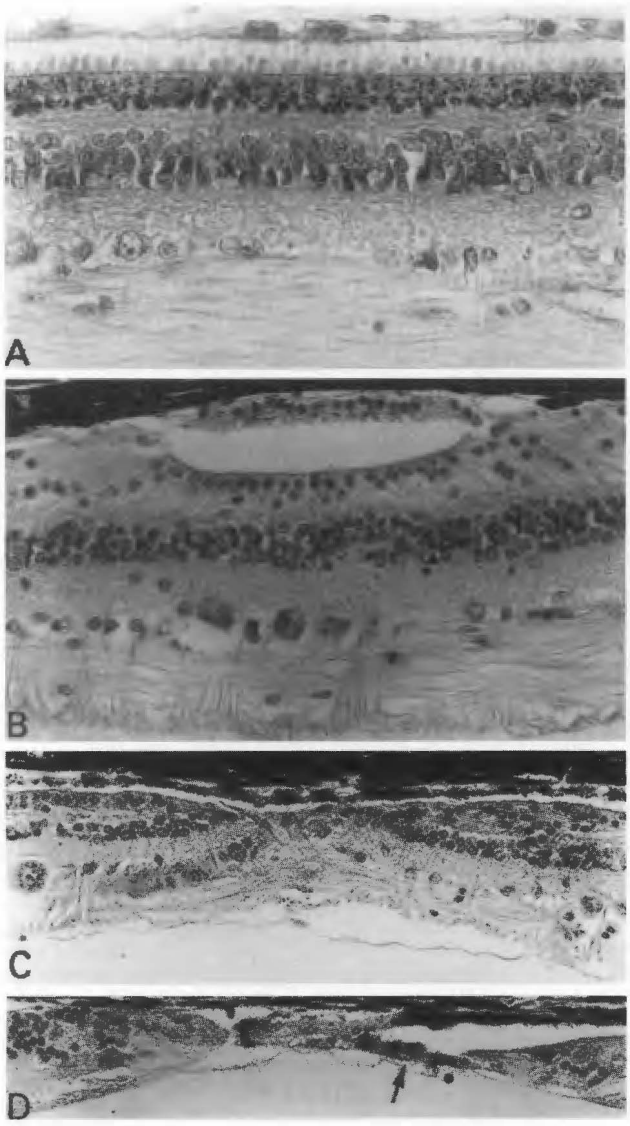

FIGURE 14-12. Different stages of disease in *rd* illustrate the RPE response to the photoreceptor degeneration. (A) In a high-cone-density area of the posterior pole, the loss of rods results in increased prominence of cones. The RPE is normal. (B) An isolated segment of RPE and outer nuclear layer remain. (C) Focal retinal gliosis with loss of retinal layer organization; the RPE is normal. (D) End stage atrophy. The RPE is absent to the left of atrophic focus, but is present to the right and has migrated intraretinally *(arrow)*. Magnifications: (A) ×370; (B) ×100; (C) ×200; (D) ×170. (Reprinted from Aguirre, 1978.)

Photoreceptor degenerations. Of the degenerative group of hereditary retinal diseases, mutations at the *prcd* gene locus account for all of the autosomal disorders recognized to date (Aguirre and Acland, 1988; 1991; unpublished). The *prcd* gene, as well as the different mutations responsible for the defined allelic variants, has yet to be identified. However, very recent studies in our lab have excluded the peripherin/rds, opsin, PDEB rod transducin α1 genes from the *prcd* gene locus (Acland et al., 1995; Wang et al., 1995; Ray et al., 1996; 1997). Thus, *prcd* may represent a mutation of one of the other genes or gene loci that have been identified to cause RP, or, alternatively, of a novel gene not previously associated with the disease.

Photoreceptor disease and degeneration-temporal and topographic factors. As a degenerative disease of the visual cells, structural and functional abnormalities in *prcd* become evident after the cells have developed normally. Pathology occurs first in the rod outer segments, and progresses, with time, to involve the inner segments, and the inner retinal layers. This highly characteristic sequence of disease has allowed us to stage the structural abnormalities into three major phases: a—disease (stages 1*–1); b—degeneration (stages 2–4); c—atrophy (stages 5–8) (Fig. 14-13; Aguirre and Acland, 1988; Long and Aguirre, 1991). Starting at approximately 12–14 weeks of age, all photoreceptor cells begin to develop the stage-specific pathology characteristic of the disease, but the rate of progression is dependent on topographic factors (Aguirre et al., 1982a). In all cases, pathology is more severe in the inferior quadrants, while the visual cells in the superior and temporal retinal quadrants are spared the ravages of the disease until later (Fig. 14-14). Throughout the three phases of the disease, the RPE remains normal and minimally reactive (Fig. 14-13). Only in very advanced disease will the RPE show the nonspecific atrophic and migratory responses illustrated in Figure 14-12D. An additional complexity is the selectivity of the disease, at least initially, for rods. Cone pathology develops late, after rods have begun to degenerate (stage 2 and later). With loss of rods, the cones become the predominant cell remaining in the photoreceptor layer (Fig. 14-15).

This topographic distribution of disease is not unique to *prcd,* but occurs also in other retinal degenerations, particularly in man. The inferior retina appears to be selectively affected in some forms of RP regardless of the molecular basis of the disease. Different rhodopsin mutations have been causally associated with RP, e.g. Pro23His and Gly106Arg (Heckenlively et al., 1991; Fishman et al., 1992), although not all patients with the same molecular defect show the same regionally selective damage to the inferior retina (compare Berson et al., 1991 and Heckenlively et al., 1991). The identification of the factors that modify the topographic expression of the photoreceptor pathology would provide important information on the interaction between the molecular defect, the visual cell, and the local retinal environment, and provide insights of the regulation of the disease phenotype. In order to identify such factors, we have ex-

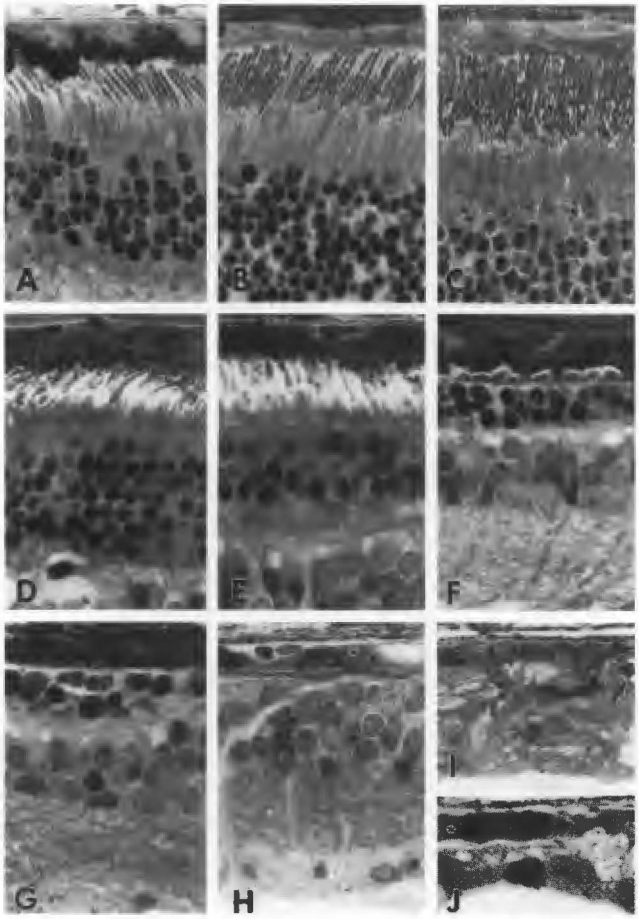

FIGURE 14-13. Disease stages in *prcd*: S-0 (A), S-1* (B), S-1 (C), S-2 (D), S-3 (E), S-4 (F), S-5 (G), S-6 (H), S-7 (I) and S-8 (J). Arrowhead (F) indicated RPE process contacting the external limiting membrane; * (H, I, J) indicate RPE; arrow (I) indicates retinal vessel. At all stages of the disease, the RPE remains structurally normal. Magnification ×430. (For details refer to Aguirre and Acland, 1988, from which this figure was reprinted with permission.)

amined several different parameters that could be involved in modulating the rate and severity of the photoreceptor degeneration. These include: RPE pigmentation (Aguirre and O'Brien, 1986), invasion of pha-gocytic cells into the interphotoreceptor space (Aguirre, 1986), visual cell renewal (Aguirre and O'Brien, 1986), the soluble and insoluble components of the IPM (Wiggert et al., 1991; Mieziewska et al., 1993b), and the expression of photoreceptor-specific proteins and transcripts (Huang et al., 1994). Thus far, no specific properties have been identified in the inferior retinal quadrant that selectively predisposes this area to earlier and more severe disease. Some of these issues are addressed below.

Photoreceptor degeneration, RPE pigmentation and interphotoreceptor space phagocytic cells. As noted in the section on "Normal Anatomy," above, the dog RPE is not pigmented in the tapetal region (Fig. 14-1). Additionally, the density of pigmentation is also not uniform, with pigmentation density being greater in the periphery. Because of the presence of pigmented and nonpigmented RPE regions overlying the photoreceptor mosaic, it is essential to consider topographic effects when evaluating the influence of pigmentation on diseases of the photoreceptor–RPE complex.

We have developed a technique for sampling retinal tissues from topographically defined regions of the eye using tissues embedded either in plastic (following glutaraldehyde/osmium tetroxide fixation) or in diethylene glycol distearate (DGD) wax after paraformaldehyde fixation (Aguirre et al., 1983; 1986; Huang et al., 1993). This permits cutting 1 μm sections which extend from the optic disc to the ora serrata in all four quadrants; the tissue can then be examined by conventional light microscopy after staining (plastic sections), or following

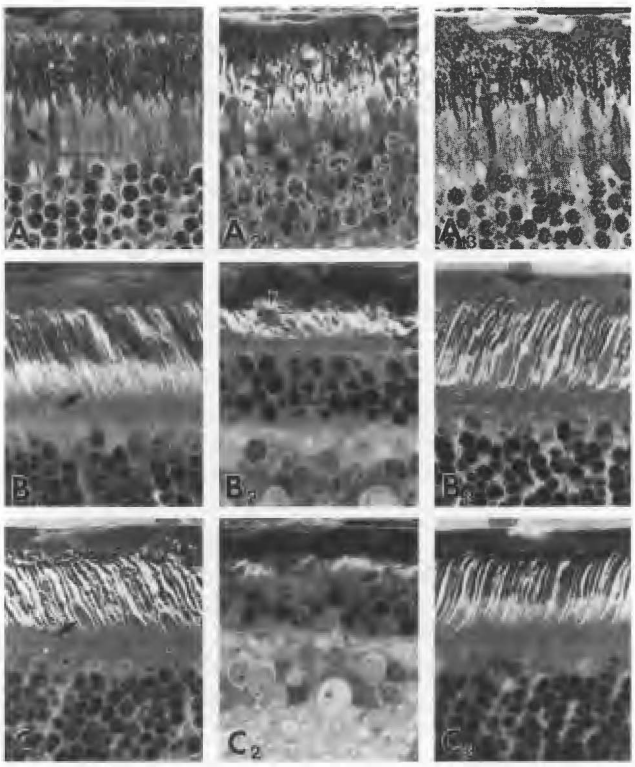

FIGURE 14-14. Variation of *prcd* disease severity by quadrant. All photographs taken 3000 μm from the edge of the optic disc in the superior (A_1, B_1, C_1), inferior (A_2, B_2, C_2) and temporal (A_3, B_3, C_3) quadrants of animals at 1.1 (A_{1-3}), 2.1 (B_{1-3}), and 2.5 (C_{1-3}) years. Disease progresses first in the inferior quadrant; visual cells degenerate, and macrophages *(arrowhead)* invade the interphotoreceptor space. Cones *(arrows)* are generally spared by the disease process and remain normal, particularly in the temporal quadrant. Magnification ×400. (Reprinted from Aguirre and Acland, 1988.)

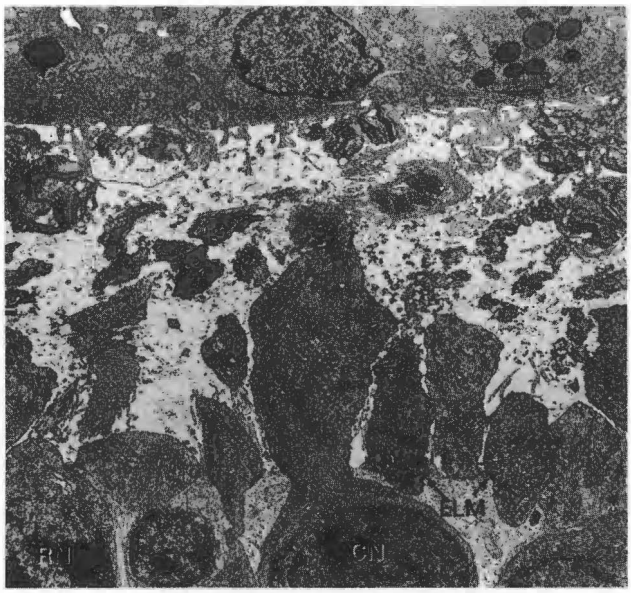

FIGURE 14-15. Stage 2 disease *(prcd)*. There is extensive rod outer and inner segment degeneration and loss which results in the increased prominence of the cones. The RPE is normal. RN = rod nucleus, CN = cone nucleus, ELM = external limiting membrane. Magnification ×4000. (Reprinted from Aguirre and O'Brien, 1986.)

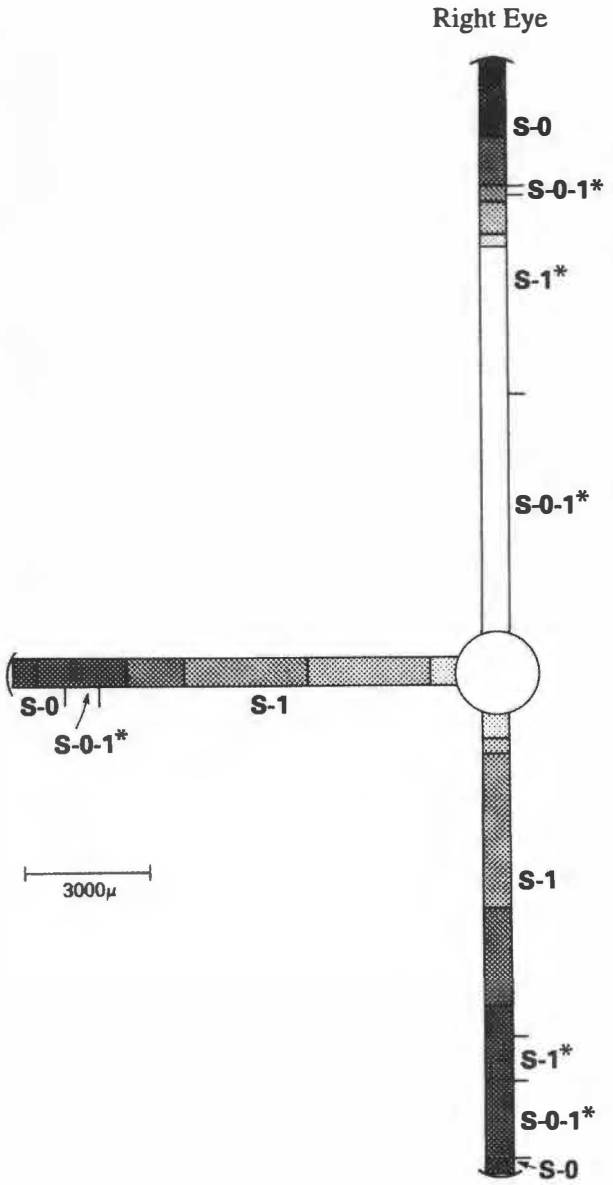

FIGURE 14-16. Illustration of the topographic distribution of retinal disease in the right eye of a 22-week-old *prcd*-affected dog (refer to Figure 14-13 for details of disease stages). The rectangles indicate the exact length of the section and retinal position *(refer to 3000 μm calibration marker)* in relation to the optic nerve *(central circle)* and ora serrata *(curved line)*. Rectangles above and below the optic disc represent, respectively, the superior and inferior retinal quadrants; the temporal quadrant is represented by a horizontal rectangle. The degrees of shading within the rectangles represent the extent of RPE pigment density. Note that the peripheral retina is normal, but the RPE pigmentation density does not ameliorate the severity of the disease. (Reprinted with modification from Aguirre and O'Brien, 1986.)

lectin, immunocytochemical and/or *in situ* hybridization procedures carried out in the same tissue. In this manner, it is possible to correlate disease stage with any of the parameters that are potentially involved in modulating the severity of the visual cell degenerative process.

In young *prcd*-affected animals, the retinas show a central-to-peripheral gradation of disease severity (Fig. 14-16). Early disease (stages -1*, -1) is present throughout the posterior pole and equatorial regions, but stops abruptly in the periphery where the photoreceptors become normal. This change in disease severity could be associated with increasing RPE pigment density, since a gradual change in pigmentation also occurs in a central-to-peripheral gradient. This finding raises the possibility of a pigmentation associated protective effect. However, critical examination of the areas where pigmentation changes abruptly reveals that the change in disease severity (from stage-1 to stage-0) is not associated with a change in pigmentation. Thus, the improvement in disease severity appears to be dependent on topographic position of the visual cells in the photoreceptor mosaic rather than RPE pigmentation. With progression of the disease, the peripheral sparing effect is lost, and disease severity is of equal or greater magnitude to that present more centrally (Fig. 14-17).

In fact, it could be argued that the presence and density of RPE pigmentation *per se* enhances the disease process. After all, the transition from disease (stage-1) to degeneration (stages-2, -3, -4) occurs first in the inferior retinal quadrant, a region characterized by heavy pigmentation in the RPE monolayer (Fig. 14-17). It is this quadrant that shows the degeneration of the pho-

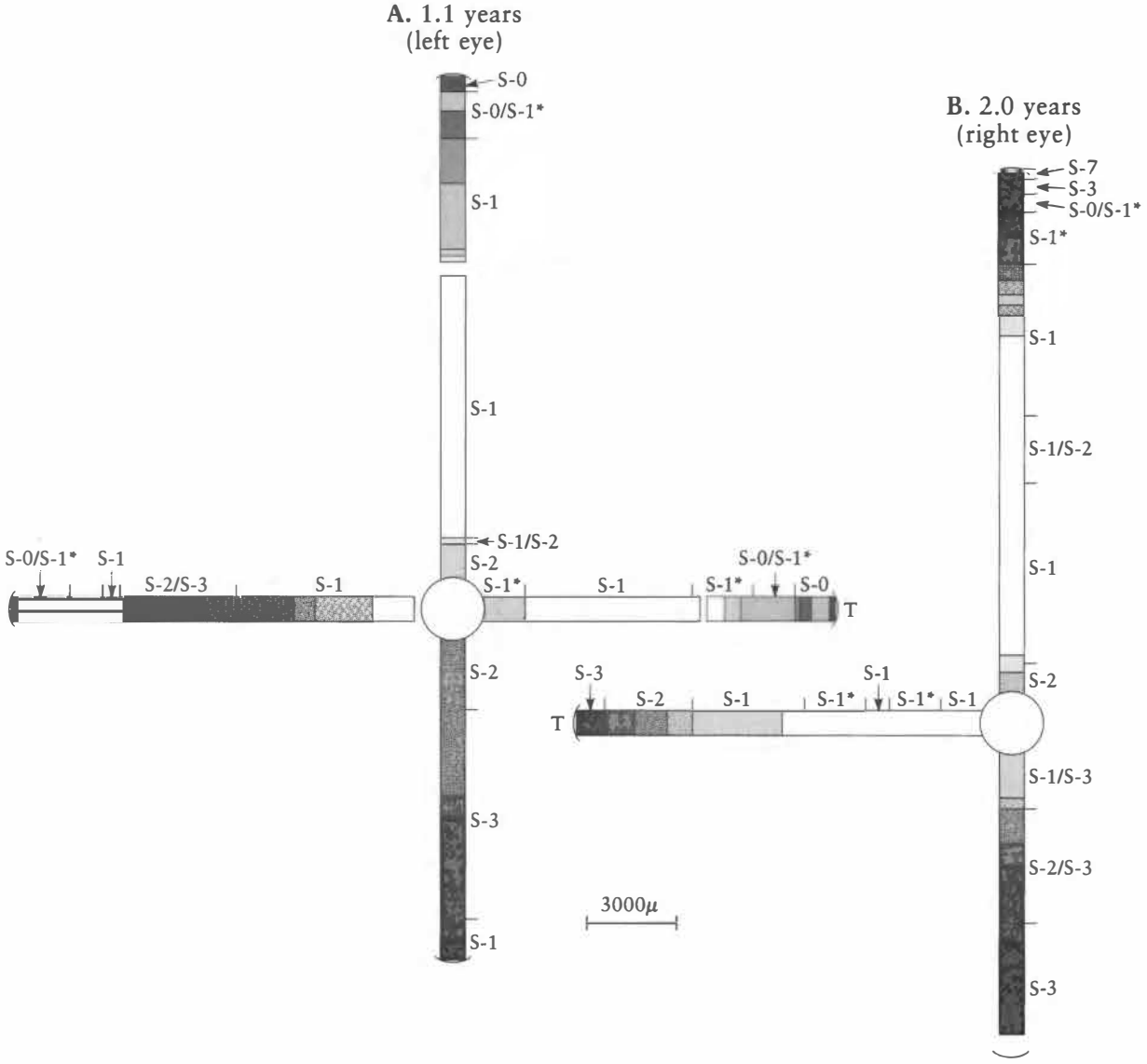

FIGURE 14-17. Comparison of the topographic distribution and progression of retinal disease in both eyes of a *prcd*-affected dog at two different ages (1.1 and 2.0 years). Refer to Figure 14-13 for details of disease stages, and to Figure 14-16 for explanation of the schematic illustration. At the earlier time period (1.1 years), the peripheral retina is normal in the superior, temporal, and nasal quadrants. With time, the disease progresses to involve the periphery. Note that disease is more severe in the inferior quadrants, and that RPE pigmentation does not have a protective effect. (Reprinted with modification from Aguirre and Acland, 1988.)

toreceptors and loss of 75%–80% of the outer nuclear layer at the time that the visual cells in other quadrants of the eye show minimal disease. Thus, the selectivity of the disease process for the inferior retinal quadrant can not be explained on the basis of a protective effect of pigmentation. These results are different from those reported for the RCS rat, where light deprivation or pigmentation have a protective effect, and reduce the rate of the retinal degeneration (LaVail and Battelle, 1975; LaVail, 1980).

A prominent feature of the degenerative phase of the disease is the presence of cells in the interphotoreceptor space (Fig. 14-14B_2). Initially, we suspected that these cells represented activated RPE cells that had detached and migrated into the interphotoreceptor space. However, we found no area of the RPE monolayer that was devoid of RPE cells, or that showed breaks in the apical tight junctions that define the outer blood–retina barrier. Cytological examination showed that these cells likely represented phagocytic rather than RPE cells, because

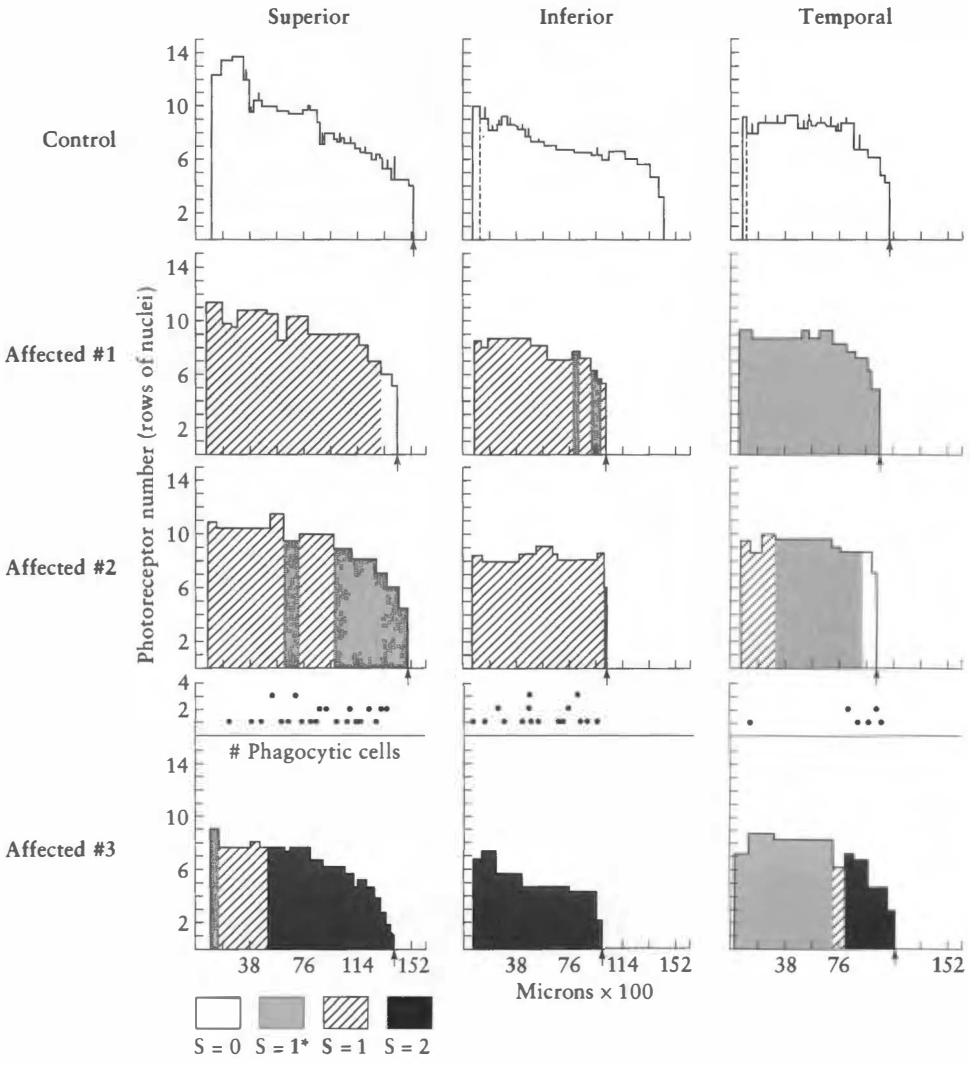

FIGURE 14-18. Histograms correlating photoreceptor numbers *(rows of nuclei)*, disease stage *(refer to shading key below)*, and number of phagocytic cells in the interphotoreceptor space for the superior, inferior and temporal retinal quadrants of control and *prcd*-affected dogs at 22 weeks (#1 and 2) and 36 weeks (#3) of age. In the younger affected dogs, disease is less severe in the periphery, the photoreceptor number remains within normal limits, and phagocytic cells are not present. The older affected dog (#3) shows more advanced disease (S-2), especially in the inferior quadrant. Phagocytic cells are present in the interphotoreceptor space, primarily in areas of S-2 disease. (Reprinted with modification from Aguirre and O'Brien, 1986, and Aguirre, 1986.)

they lacked pigmentation and had irregularly shaped, pale nuclei with dense peripheral chromatin condensation (Aguirre, 1986). Recent studies in the RCS rat indicate that the phagocytic cells that invade the interphotoreceptor space are of microglial origin (Roque et al., 1996).

We have examined the association between photoreceptor disease and the presence of phagocytic cells in the interphotoreceptor space. In young affected dogs, early disease (stages 1* and 1) is present uniformly throughout the eye, and phagocytic cells are absent. With progression to stage 2, however, phagocytic cells appear (Fig. 14-18). It is at this stage of the disease that rod inner and outer segments begin to degenerate rapidly, and the number of outer nuclear layer nuclei decreases. The histogram illustrating disease severity with the number of phagocytic cells in the interphotoreceptor space indicates a direct correlation between the two processes. Almost all the phagocytic cells that are present are restricted to those areas having the more severe stage-2 disease. In the late degenerative (stage-4) and atrophic (stages-5 and -6) phases of the disease, the number of phagocytic cells decrease (Aguirre, unpublished). This would suggest that the debris accumulating in the inter-

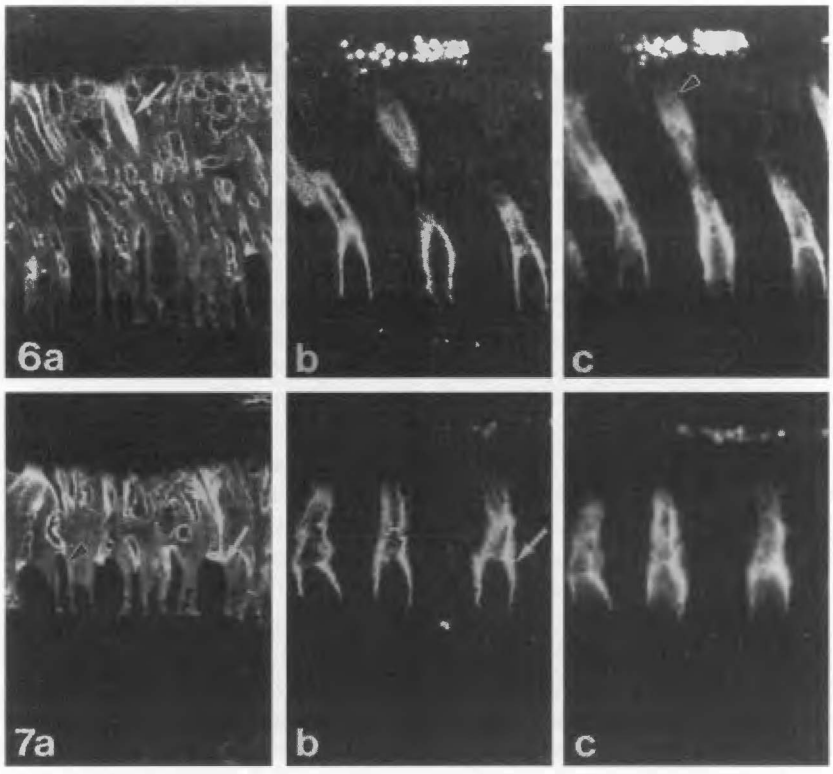

FIGURE 14-19. The central (6_{a-c}) and peripheral (7_{a-c}) retinal areas of a 3 year old *prcd*-affected dog with stage 3 disease. (6a) WGA strongly labels the IPM space adjacent to the outer segments; there is diffuse but weak labeling of the remaining IPM. The surviving photoreceptors are well organized, except for the whorls of OS debris located on the RPE apical surface. WGA labels the RPE cone sheaths strongly *(arrow)*. (6b) The PNA domain is thicker than normal, smooth and slightly "fluffy" in appearance. (6c) The composite shows the diminishing PNA label intensity at the RPE level *(arrowhead)*. RPE lipofuscin granules were brightly labeled. The peripheral retina shows more advanced stage 3 disease. (7a) WGA label is strong immediately around the remaining cells *(rods = arrowhead, cones = white arrow)*. (7b) PNA label is prominent and thick around cone IS and OS *(arrow)*. Note that the cone matrix thickness differs when visualized with the WGA and PNA lectins *(compare Figures 14-7a and b, arrow)*. (7c) The composite shows the circumference and thickness of the PNA domain around the cones. Magnification ×1,000. (Reprinted from Mieziewska et al., 1993b.)

photoreceptor space secondary to photoreceptor degeneration may serve as the signal for the invasion of macrophages.

The interphotoreceptor matrix. Using the techniques of lectin cytochemistry, we have examined the molecular components of the insoluble IPM to determine if abnormalities are present in the *prcd*-affected retina, either before the development of the disease, or after the process of photoreceptor degeneration has been initiated (Mieziewska et al., 1993b; Mieziewska, 1993). Because of the topographic specificity for early degeneration in the inferior quadrant, we examined for differences between this quadrant and other retinal loci. We reasoned that degenerative changes in the visual cells could be initiated in response to a damaged matrix environment, irrespective of the nature of the primary defect that is responsible for the cell dysfunction. Because the slow degeneration present in the *prcd* mutant retina allows diseased photoreceptors to remain viable for a relatively long period of time, the microenvironment of the IPM during degeneration may reflect more accurately that present in RP, the comparable disease in man.

With the exception of the late atrophic stages (stages 5–8) of the disease, the lectin specificity remains normal in all the ages and stages examined. However, a thickening of the rod and cone matrix domains is observed in some samples representing stages 2 and 3 (Fig. 14-19). Since the change in thickness was observed at a relatively advanced stage of degeneration, when substantial cell death had already occurred, the thickening may represent a secondary response of the surviving cells. This response would maintain the structural integrity of the IPM and prevent the disruption of molecular flow through the IPM resulting from discontinuity in the structure. The number of photoreceptors remaining in the IPM compartment has been severely reduced by the time stage 2 is reached. The extra space is presumably occupied by broadened photoreceptors and matrix do-

mains, as seen in later stages. Additionally, we found that the cone domains terminated somewhat more vitreal to the RPE than normal, and, in the older affected animals with shorter PNA cone domains, WGA (wheat germ agglutin) strongly labeled the RPE cone sheath surrounding these cones. The significance of this finding is unclear, but it could be the result of outer segment debris accumulation below the apical surface of the RPE. Extreme displacement of IPM material due to debris accumulation has been shown in the RCS rats (LaVail et al., 1981; Porrello et al., 1986). Our findings in the *prcd* mutant indicates that the photoreceptor-specific IPM constituents which form the insoluble IPM are not primarily involved in this hereditary retinal degeneration.

Progressive Retinal Atrophy (PRA) in the Cat

Similar hereditary retinal disorders have been recognized in other animal species. Brief mention will be made only of the diseases occurring in the cat, where both early- and late-onset hereditary photoreceptor degenerations have been described. Three different early-onset disorders have been identified; two are dominantly inherited (mixed-breed cats [West-Hyde and Buyukmihci, 1982] and Abyssinians [Barnett and Curtis, 1985; Curtis et al., 1987]), and one is recessively inherited in the Persian breed (Rubin and Lipton, 1973; Gaarder and Aguirre, unpublished). Surprisingly, all three diseases have a very early onset and rapid degeneration, and end-stage retinal disease is evident on ophthalmoscopy by the time the animals are only a few months of age (Plates 14-V, 14-VI). This is different from what is found in dogs with the comparable developmental photoreceptor diseases (Table 14-2). A late-onset, slowly progressive disease, also recognized in the Abyssinian breed, is inherited as autosomal recessive (Narfström, 1983). Both of the diseases found in the Abyssinian breed are maintained in experimental colonies by different research groups, and confusion may arise in those not familiar with the profound differences that exist between the two disorders.

Heterozygous Abyssinian cats affected with the early onset rod-cone dysplasia (*Rdy*) show equal structural abnormalities in the rod and cone photoreceptors (Leon and Curtis, 1990). These remain rudimentary, and fail to form organized outer segments; in addition, there is delayed and incomplete photoreceptor synaptogenesis. Degeneration begins in the central retina and progresses to the periphery; by 30 weeks of age, two to five rows of nuclei remain in the outer nuclear layer. In the area centralis, the feline equivalent of the foveomacular region of primates, there is atrophy of the RPE and the choriocapillaris, and thinning of the overlying tapetal layer. These changes are presumably secondary, as they occur late in the disease process. Abnormalities in retinal cyclic nucleotide metabolism have been reported in abstract form for the *Rdy* model (Leon et al., 1988), but not published. In that brief abstract, the authors reported the presence of elevated retinal cGMP levels in affected animals in the earliest stages of the dystrophy, at a time when the cGMP-PDE activity was low.

The late-onset, recessive degenerative photoreceptor disorder is characterized initially by disorientation of the rod disc membranes (Narfström and Nilsson, 1989). This is followed at approximately six months of age by disintegration of the rod outer segments, appearing as vacuolization and clumping of disc material and accumulation of debris. Thereafter, rod cells are lost from the photoreceptor and outer nuclear layers. Cones develop and remain normal until two to three years of age, at which time degeneration begins (Narfström and Nilsson, 1986). In several respects, this disease has many similarities to *prcd* in the dog, among which are the clinical, cytological, and temporal characteristics of photoreceptor degeneration, as well as the presence of abnormalities in plasma lipids, particularly docosahexaenoic acid (22:6n-3; Anderson et al., 1991).

Retinal pigment epithelial defects have not been described in the Abyssinian cat with the late onset recessive disease. Based on normal rhodopsin regeneration as determined *in situ* by imaging fundus reflectometry, the normal participation by the RPE in this aspect of the rhodopsin cycle is implied (Jacobson et al., 1989). Similarly, normal RPE function has been established electrophysiologically by measurements of the DC-recorded c-wave and direct measurements of the standing potential (Narfström et al., 1985). Normal dark-adapted sensitivity (Narfström et al., 1988) and rhodopsin regeneration occur, even though a profound decrease in IRBP gene expression has been reported at both the message and protein levels (Narfström et al., 1989a; Wiggert et al., 1994). It is not clear how this finding relates to the retinal function, or its significance in terms of the identification of the molecular defect of the disease. To date, only the phosducin and peripherin/rds genes have been excluded from the disease (Gorin et al., 1993, 1995).

THE RPE IN INHERITED DEFECTS OF LYSOSOMAL FUNCTION

Our laboratories have been involved in studies of the RPE disease present in animals with lysosomal storage disorders. In both man and animals, these diseases are caused by the inherited deficiency of lysosomal en-

zymes, and represent generalized multisystemic abnormalities of which the ocular lesions are but one component. That selective deficiency of an enzyme results in substrate accumulation indicates that the degradative pathway involved, as well as the substrate accumulating, are critical for the normal function of the tissue studied. These aspects of the diseases lend themselves to be used to define specific catabolic pathways essential for normal RPE function. Disease in the RPE is dramatic, and underscores the importance of the lysosomal system in the function of this cell layer. This is not surprising, because compared with other tissues of the body the RPE shows a higher activity for most of the acid hydrolases and sulfatases (Hayasaka, 1974; Zimmerman et al., 1983; Stramm et al., 1983; Aguirre and Stramm, 1991). Of this group of diseases, our focus has been primarily on those disorders involved in the degradation of glycosaminoglycans (GAGs), known collectively as the *inherited mucopolysaccharidoses*.

Mucopolysaccharide (MPS) Storage Diseases

Severe RPE pathology with no photoreceptor disease. We have examined the RPE in animals with mutations of three different lysosomal enzyme gene loci: arylsulfatase B (ASB; cat), α-L-iduronidase (α-L-id; cat) and β-glucuronidase (GUSB; dog) (see Table 14-4 and Aguirre and Stramm, 1991 for review). The lysosomal enzymes encoded by these genes participate in the degradation of GAGs. Morphologic studies of the three mutations indicate that the accumulation of intracellular inclusions in secondary lysosomes serves as a distinct structural marker of the enzyme deficient RPE. By light microscopy, these inclusions appear vacuolated, or homogeneous and indistinct from the surrounding cytoplasm. Ultrastructurally, the inclusions can vary from electron lucent to granular, lamellar, or mixed (Fig. 14-20). The electron-lucent and granular vacuoles are believed to represent leached and stored GAGs, respectively, while lamellar inclusions result from lipid accumulation secondary to inhibition of ganglioside degradative pathways by the stored GAGs (Rushton and Dawson, 1977).

Accumulation of secondary lysosomal inclusions in the enzyme-deficient RPE is the hallmark structural abnormality. Using the MPS–VI deficient mutant as the prototype disease, we have found that there is RPE hypertrophy subsequent to the accumulation of vacuolated inclusions. In the RPE, single cytoplasmic inclusions are present initially in the early postnatal period. Their number and size increase during the period of photoreceptor differentiation. Subsequently, the RPE cells enlarge, and the monolayer becomes uniformly hypertrophied. In older animals, some of the enlarged cells become massively hypertrophied, and have a uniformly rounded apical border. These hypertrophied cells, which can have an apical–basal height greater than 25 microns, occur either singly or in clusters, and result in loss of the uniformity that is characteristic of the RPE monolayer (Fig. 14-21). Similar disease is present in the MPS VII RPE (Stramm et al., 1990). In contrast, the MPS–I affected RPE accumulates homogeneous inclusions that are not distinct from the surrounding cytoplasm, and RPE hypertrophy is minimal or absent (Stramm et al., 1989). The inclusions represent stored GAGs that accumulate in the diseased RPE cells (Fig. 14-22).

In spite of the severe RPE pathology, there is complete preservation of neuroretinal structure and function. Examination of the ERG rod-and-cone system responses indicates maintenance of normal retinal function at a time when RPE storage is severe (Aguirre et al., 1986). Morphologic examination also shows that the internal lamellar organization of the rod outer segments is preserved, even though they appear disoriented when adjacent to massively hypertrophied RPE cells. In fact, outer segment lengths and renewal rate, an indication of the normal participation of the RPE in the outer segment renewal process, are normal when studied both early and late in the disease (Fig. 14-23). It is apparent, therefore,

TABLE 14-4. *Lysosomal storage diseases in animal models*

Number	Eponym	Animal	Enzyme	Stored GAGs
MPS I*	Hurler	Cat, dog	α-L-Iduronidase	DS, HS
MPS II	Hunter	Dog	Iduronate-2-sulfatase	HS, DS
MPS IIID	Sanfilippo	Goat	N-Acetylglucosamine 6-Sulfatase	HS
MPS VI*	Maroteaux-Lamy	Cat, dog, rat	Arylsulfatase B	DS
MPS VII*	Sly	Dog, mouse, cat	β-Glucuronidase	DS, HS, CS

DS = dermatan sulfate HS = heparan sulfate CS = chondroitin sulfate
*Extensive RPE storage of substrate has been reported; refer to text for details.

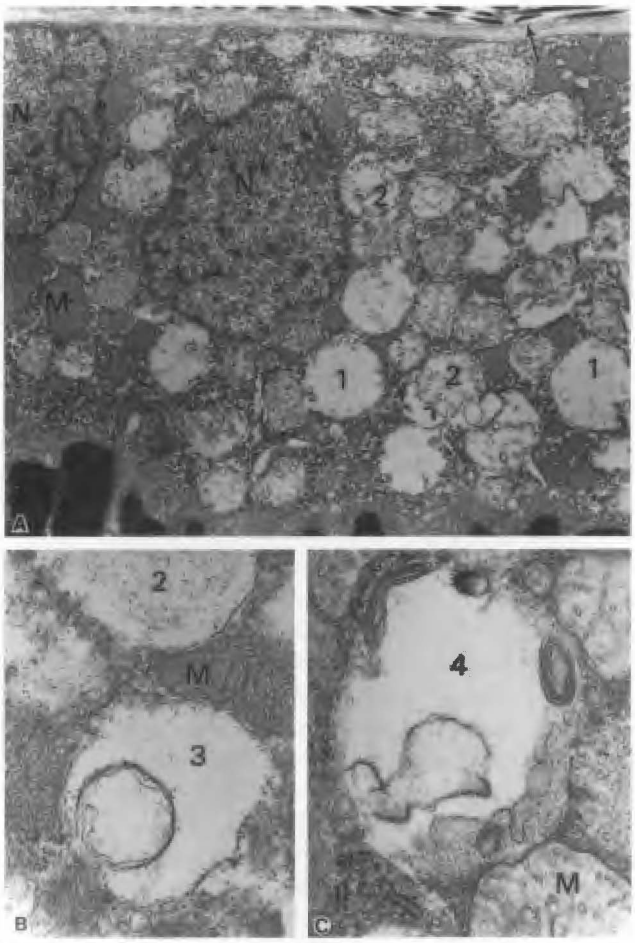

FIGURE 14-20. Nonpigmented RPE cell from the tapetal zone *(arrow)* of an MPS VI–affected cat (ASB deficiency) accumulates electron lucent (1), granular (2), lamellar (3), and mixed (4) inclusions in secondary lysosomes. The inclusions are membrane limited and distinct from mitochondria (M). N = nucleus. Magnifications: (A) ×5,700; (B) ×19,000; (C) ×17,500. (Reprinted from Aguirre et al., 1983.)

that the diseased RPE cells, in spite of their massive hypertrophy, are still able to maintain their photoreceptor-supportive functions. Similar preservation of photoreceptors occurs in both the MPS I (cat) and VII (dog) models, although, in the latter, there is disorientation of cone outer segment disc membranes (Aguirre et al., 1986; Aguirre and Stramm, 1991). Of all the MPS models reported, photoreceptor degeneration occurs only in the MPS VII mouse (Lazarus et al., 1993).

The interphotoreceptor matrix in MPS VII. β-glucuronidase, the enzyme deficient in MPS VII, is involved in the degradation of the three principal GAGs present in the RPE: chondroitin sulfate (CS), dermatan sulfate (DS), and heparan sulfate (HS). Of these, heparan and chondroitin sulfates have important biological activities in, respectively, mediating cell-to-cell interaction and being an important molecular constituent of the main class of proteoglycans present in the IPM (Stramm et al., 1989; 1990). Of the cells bordering the interphotoreceptor space, it is only the RPE that is involved in the degradation of the CS component of IPM proteoglycans (Stramm et al., 1990). Because of the severe disease that occurs in the RPE from GUSB deficiency, it is plausible that an equally severe abnormality would occur in the IPM. For that reason, we have examined the matrix in normal and mutant animals using a series of antibodies and lectins directed at different molecular constituents of this structure. Surprisingly, we have found only a minor alteration in the matrix (Long et al., 1989; Long and Aguirre, unpublished). The distribution of chondroitin sulfate proteoglycan species (0-S, 4-S, and 6-S) is normal, although there is a condensation of the 6-S molecular species limited to the area of the cone matrix sheath. Within this sheath, some of the cone outer segments show a nonprogressive disorientation of the "coin-stack" organization of the discs. However, the major portion of the matrix and the rod photoreceptors are normal (Fig. 14-24). In contrast, the elegant studies of the MPS VII mouse retina by Lazarus and colleagues have shown that abnormalities of the IPM occur early, and that changes in its biochemical composition or physical structure may be causally associated with the subsequent photoreceptor degeneration (Lazarus et al., 1993).

The topography of RPE disease is not uniform. The lysosomal enzymes serve general "housekeeping" functions in the catabolism of complex macromolecules that are targeted to the lysosomal compartment during the remodeling and turnover of cell membranes and extracellular matrices. Because of their ubiquitous distribution in all tissues, including the RPE, and the presumably uniform function of this cell layer in the eye, one would expect that enzyme deficiency would result in uniform disease expression within the monolayer. However, this is far from the case.

In the MPS VI–deficient mutant, the number of RPE inclusions increases with time, but this increase cannot be considered strictly age dependent, as it is strongly modified by topographic factors which appear to regulate disease expression. A striking feature of the ASB-deficient RPE is the lack of uniformity in the expression of the disease phenotype. This is clearly demonstrated in Figure 14-25, which compares disease in nonpigmented (A) and pigmented (B) RPE cells from equivalent positions in the superior and inferior quadrants of the same adult eye; the nonpigmented RPE becomes massively

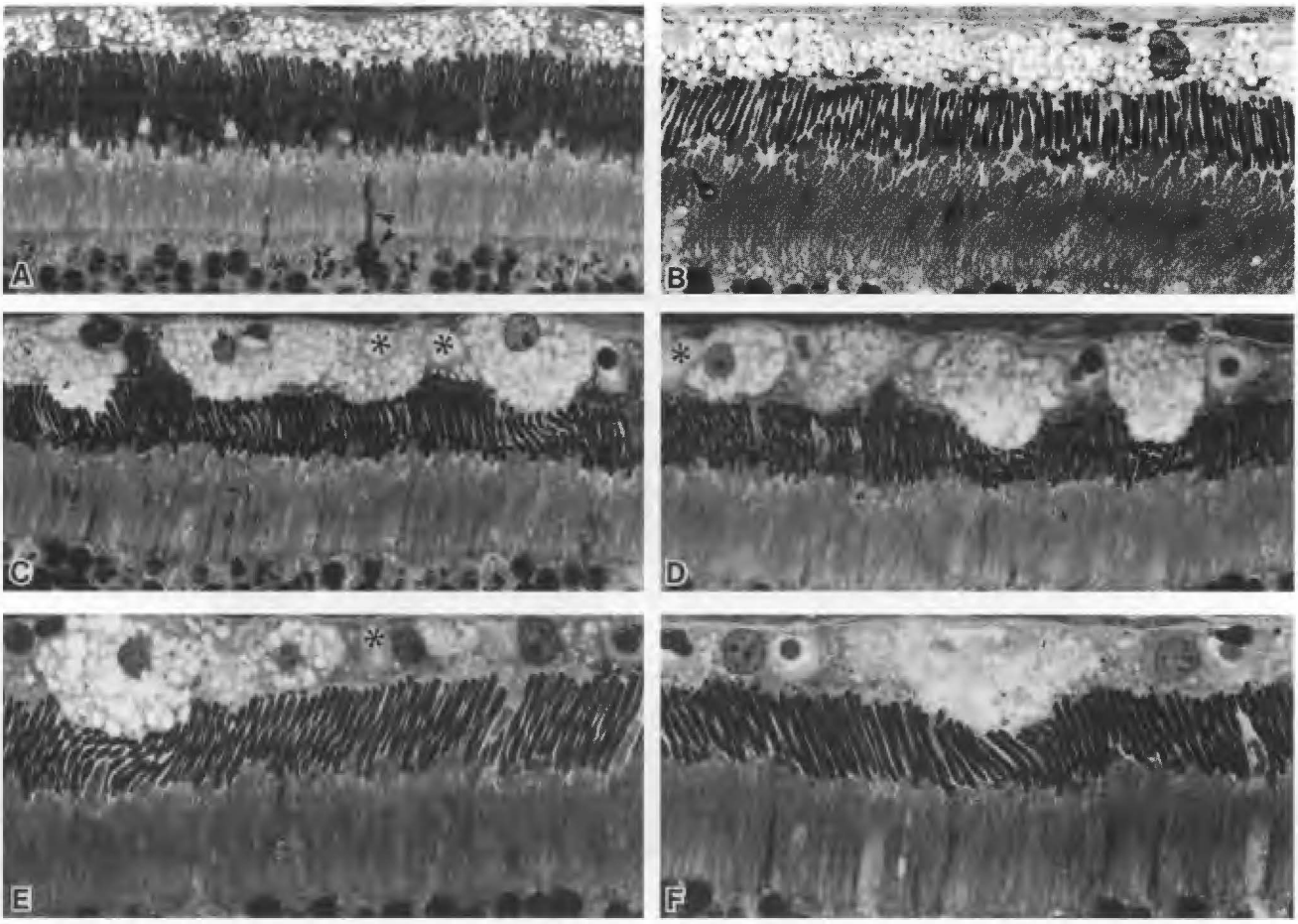

FIGURE 14-21. Nonpigmented RPE from the tapetal zone of MPS VI–affected cats of different ages. (A) 6 months; (B) 9.5 months; (C)–(F) 5 years. (A) vacuolated inclusions fill the cytoplasm without causing hypertrophy. (B) the height of the RPE cells increases concurrent with the accumulation of larger vacuoles. (C)–(F) Hypertrophy of the RPE cells, either singly or in clusters, results in focal disarray of the outer segment layer. Note that photoreceptor disorientation is not accompanied by disease. Arrowheads (A) indicate a necrotic cell that is not associated with the ASB deficiency; asterisks (C) denote normal choriocapillaris indentation of the basal RPE. Magnifications: (A), (B), (E), (F) ×830; (C), (D) ×650. (Reprinted from Aguirre et al., 1983.)

hypertrophied while the pigmented RPE remains normal. In general, two spatial gradients are present in the ASB-deficient RPE (Aguirre et al., 1983). These are (a) central-to-peripheral gradient within the same quadrant: The RPE disease always is more severe in the posterior pole than in the periphery although, with aging, disease in the periphery increases in severity; and (b) quadrant- (pigmentation-) specific distribution: The RPE abnormality is not distributed equally about the optic disc, but has the same disposition as that of nonpigmented RPE cells in the superior, temporal, and nasal meridians. That is, areas of the RPE monolayer that are nonpigmented and over the tapetum lucidum show marked RPE storage, while minimal-to-no storage is present in areas where the RPE is pigmented (Fig. 14-26; compare with Fig. 14-3). In older animals, the relationship between RPE pigmentation and absence of disease decreases in all quadrants, as progressively more pigmented cells accumulate secondary lysosomes and become hypertrophied. The disease phenotype, however, is always less severe in the pigmented RPE.

The lack of uniformity in the response of the RPE to an inherited lysosomal enzyme deficiency raises questions concerning topographic variability in the function and metabolism of the cell layer. It is possible that RPE ASB enzyme activity normally is not the same throughout the monolayer and, in the affected RPE cells, substrate accumulates in those regions having a

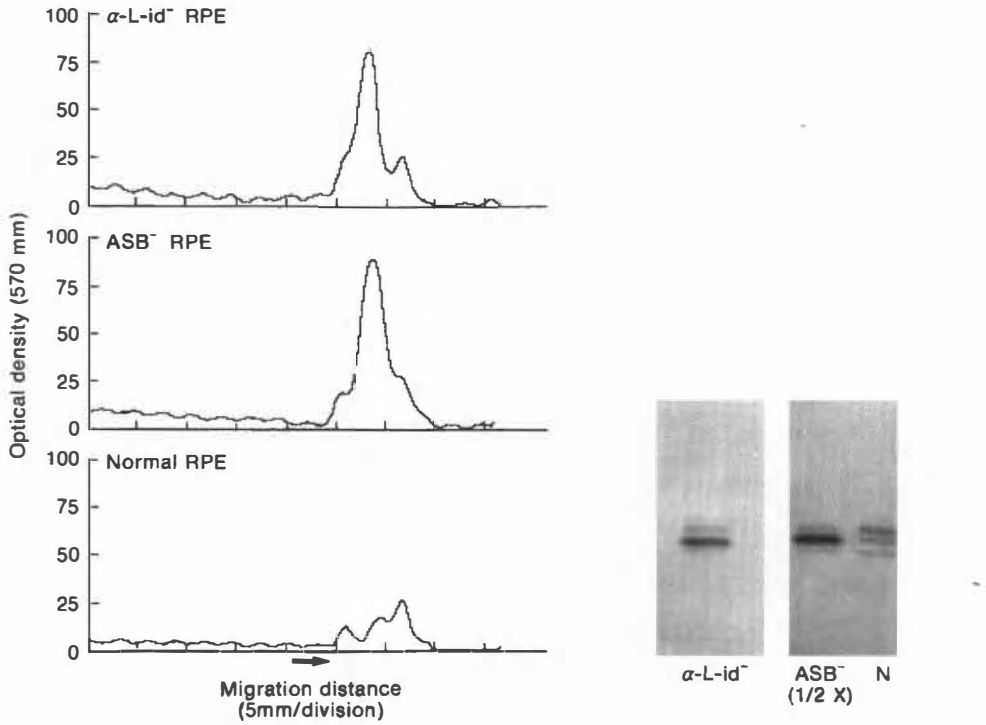

FIGURE 14-22. Scanning densitometry tracing of Alcian Blue–stained GAGs separated by cellulose acetate electrophoresis from freshly isolated RPE cells of a normal cat, and cats affected with MPS I (α-L-id⁻) and MPS VI (ASB⁻). The tracing of the normal RPE cell GAGs shows three distinct peaks, the faster migrating doublet of chondroitin sulfate/dermatan sulfate, and the slower isolated heparan sulfate peak. In both diseases there is an accumulation of GAGs, particularly dermatan sulfate. (Reprinted with modification from Aguirre and Stramm, 1991.)

more profound deficiency. This is not an unreasonable hypothesis, as the activities of several lysosomal enzymes have been shown to exhibit regional variations (Burke and Twining, 1988; Cabral et al., 1990). Other mechanisms that explain the milder disease phenotype of pigmented RPE may be the presence of alternate degradative pathways, a protective action by pigment, or regional differences in GAG metabolism (synthesis, secretion, and/or internalization). Recent in vitro studies, discussed below, indicate that regional differences in GAG metabolism determine the disease topography, and that these differences are not the result of the presence of the tapetum lucidum, but are dependent on the positional origin of the RPE cells.

A lack of spatial uniformity in RPE disease expression is also present in the MPS I feline model. However, because the disease phenotype is not as dramatic as in MPS VI (inclusions are homogeneous rather than vacuolated, and RPE cell hypertrophy is absent), it has been more difficult to ascertain the disease topography. As in the MPS VI model, we have found that accumulations of secondary lysosomes in the α-L-iduronidase-deficient RPE occur primarily in the superior quadrant where the RPE is not pigmented. In this area, the inclusions occupy approximately 18% of the cytoplasmic space. In contrast, RPE cells from the inferior quadrant accumulate a much smaller number of inclusions, and these occupy no more than 5%–6% of the cytoplasmic area. With the exception of melanin, which is not present in the superior (central and equatorial) quadrant, there are no differences in the presence and distribution of other cellular organelles (Stramm et al., 1989).

In vitro expression of RPE disease. Biochemical studies on the RPE are difficult to perform; only small quantities of tissue can be obtained from a single eyecup, and the material is often contaminated by other cell types. In vitro studies overcome these limitations by allowing the preparation and amplification of pure populations of RPE cells. The use of a controlled tissue culture environment allows for the precise determination of the role of metabolic/degradative pathways in normal RPE function. The in vitro systems also are amenable to studies of the regulation of selected pathways, both at the cel-

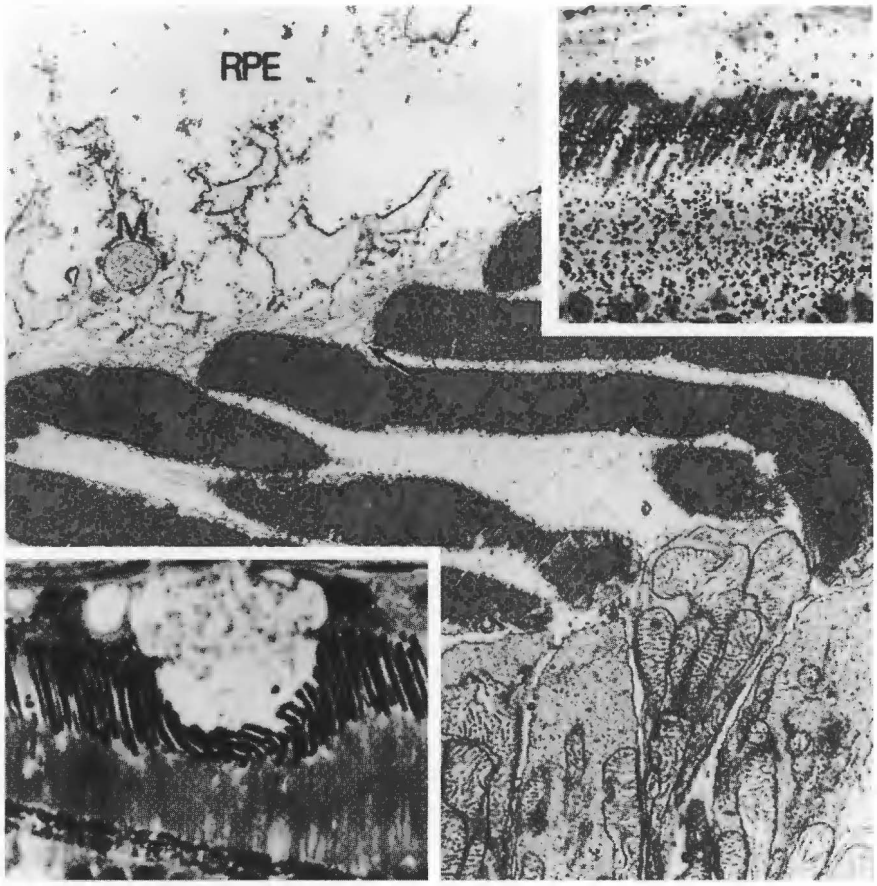

FIGURE 14-23. The RPE in feline MPS VI. Focal disorientation of outer segments opposite a massively hypertrophied RPE cell *(lower inset)*. The internal lamellar organization of the outer segments is normal *(main figure)*, but the RPE cytoplasm is full of vacuolated inclusions, and few organelles are recognizable (M = mitochondrion). Three days after the intravitreal injection of ^{3}H-leucine *(upper inset)*, a band of silver grains is present in the autoradiogram midway along the outer segment length in rods located opposite hypertrophied and diseased RPE cells. This indicates that renewal is normal in spite of severe RPE disease. Arrow in main figure indicates apical microvilli of the RPE. Magnification: ×10,000 for main figure; insets ×850. (Reprinted from Aguirre et al., 1986.)

lular and molecular level, and are useful for developing methodologies for correction of the metabolic defects at the gene level. Other chapters in this book discuss the use of tissue culture to study RPE function and metabolism. In this section, we address the use of in vitro methods in the study of inherited lysosomal deficiencies in the RPE; this topic has been reviewed previously (Aguirre and Stramm, 1991). Of the four lysosomal storage diseases studied in our laboratories (MPS I [dog and cat], VI [cat] and VII [dog]; α-mannosidase deficiency [cat]), all show in vitro retention of the morphologic, biochemical and molecular characteristics of the disease (Aguirre et al., 1995; Ray et al., 1996; Ray et al., 1997; Stramm et al., 1985, 1986, 1989, 1990). Studies presented in this section focus on the disease present in the MPS VI cat model.

MPS VI in vitro disease. Primary cultures of RPE cells initiated from the entire eyecup of cats with MPS VI show that there is a profound decrease of ASB activity, typically 5%–10% of normal (Stramm et al., 1985). This low level, termed *residual enzyme activity,* is insufficient to prevent the morphological manifestations of the disease, and the MPS VI–affected cells accumulate intracellular inclusions identical to those found in situ (Fig. 14-27). In RPE cultures from heterozygotes, the activity of ASB is reduced to approximately 50% of normal. Since these cells are phenotypically normal, both in vitro and in vivo, it appears that this level of enzyme activity is sufficient to prevent expression of the disease. One can conclude, therefore, that ASB activity must be reduced below some critical level in the MPS VI RPE before disease is expressed morphologically. One also may

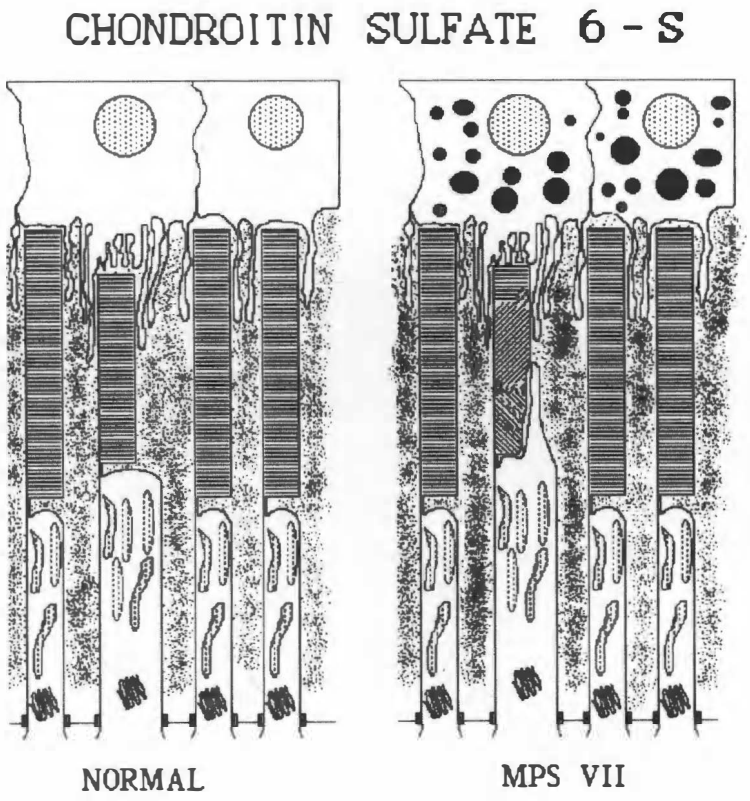

FIGURE 14-24. Schematic illustration of IPM layer immunocytochemical labeling with antibody directed against the 6–0 species of chondroitin sulfate proteoglycan in normal and MPS VII–affected dog retinal sections. In both there is diffuse and similar labeling throughout the IPM. In the MPS VII retina, however, there is a condensation also of immunoreactivity in the matrix around the cone inner and outer segments, and intense labeling of the inclusions present in the RPE. Note the disorientation of the cone outer segment discs, and the extension of a long calyceal process. (Long and Aguirre, unpublished.)

infer from these observations that it may not be necessary to restore 100% of the deficient enzyme activity to restore normal function to the diseased cells.

In a previous section, we showed that the topography of the RPE disease in MPS VI was not uniform, and that cells in the posterior pole exhibited massive intracellular storage while those in the far periphery showed little or no accumulation of undegraded substrate. Within the posterior pole, however, storage of undegraded substrate was more severe in the superior than in the inferior regions. To examine the factors that contribute to the region-specific distribution of RPE disease, we have studied the in vitro RPE isolated from regionally defined areas of the monolayer. In contrast to the isolation method that harvests cells from the entire eyecup (Stramm et al., 1983), regional cultures isolate cells from topographically preselected regions by using small glass cylinders or cloning rings to demarcate the sampled area (Stramm et al., 1985; see Aguirre and Stramm, 1991 for review). A limitation of the method is that only a small sample of cells can be harvested, but, when seeded at a high density, they are highly differentiated and remain pigmented if isolated from the nontapetal regions of the eye.

MPS VI-topographic preservation of disease in vitro. Regional cultures have been initiated from cells isolated from the superior and inferior regions of the eye. We have found that the accumulation of inclusions, representing stored substrate in secondary lysosomes, occurs primarily in cultures initiated from the posterior pole and superior equatorial regions, and not in those initiated from the inferior regions or periphery (Fig. 14-28). This region-specific in vitro disease phenotype is identical to what is observed in situ, and reflects differences in substrate accumulation that are topographically determined. However, disease is not the result of regional

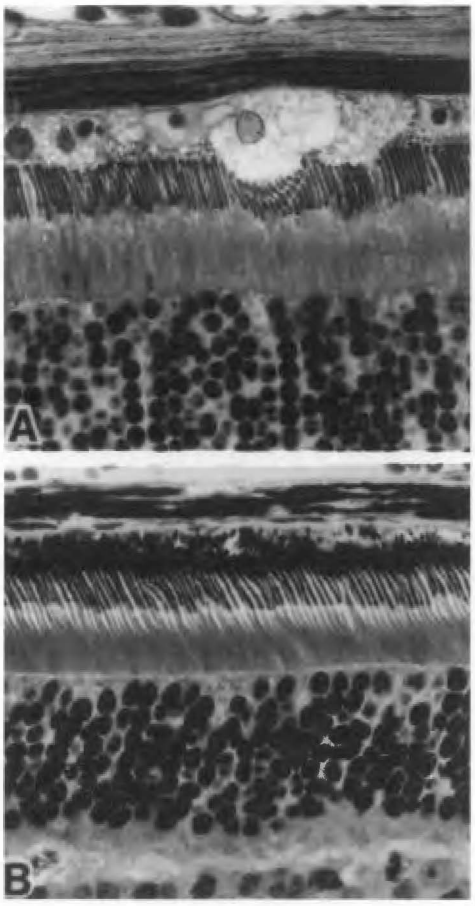

FIGURE 14-25. Sections from the tapetal (A—pigment epithelium not pigmented) and nontapetal (B—pigment epithelium pigmented) zones of a cat with MPS VI. As a result of arylsulfatase B deficiency, the nonpigmented RPE becomes massively hypertrophied (A) and accumulates cytoplasmic vacuolated inclusions. The pigmented RPE remains normal (B). Magnification ×420. (Reprinted from Aguirre et al., 1986.)

differences in expression of the deficient (ASB) enzyme. For example, cell cultures initiated from the inferior and peripheral regions of the eye, which show no substrate storage, have equally deficient ASB activity as cultures from the superior regions and posterior pole, areas which exhibit massive substrate accumulation. This is similar to what occurs in normals, where ASB activity is uniform, but high, throughout the monolayer (Stramm et al., 1986).

Regional differences in RPE metabolism of GAGs determine disease topography. To determine the factors that regulate the topography of disease expression in MPS VI, we have examined the regional metabolism of GAGs in the RPE using an in vitro approach. The extent of radiolabeled GAG accumulation was dependent on the topographic origin of the cells. The accumulation of GAGs within the cell layer was much greater in cultures initiated from the superior region of the eye than in cultures from the inferior region (Fig. 14-29). This is in agreement with our in vivo and in vitro morphologic results (Aguirre et al., 1983; Stramm et al., 1986). In contrast to the cell layer, the media from affected cultures initiated from the inferior region of the eye contained much higher levels of DS/CS than cultures from the superior region, and this difference in the release of newly synthesized GAGs into the media between regions was sustained during the 72-hour chase period. Associated with the accumulation of GAGs, there was a significant increase of collagen production in nonpigmented cultures from the superior quadrant (Stramm et al., 1991).

Our studies show that the region-specific alterations in both cell layer storage of GAGs and the release of GAGs into the media are maintained in vitro in the presence of a lysosomal enzyme deficiency that uniformly affects both regions of the RPE. This finding indicates that additional pathways for GAG turnover exist in the RPE, and are more active in the less severely diseased regions. The alternate pathways do not appear to operate in a regionally selective manner in normal RPE, as evidenced by similar GAG synthesis and secretion profiles in cultures initiated from different areas of the eye. In the disease, however, the function of these pathways appears to be selectively increased in cells derived from specific regions of the eye. Such regionally selective processes indicate that the RPE, although a monolayer, must not be considered to be homogeneous in its function and metabolism. This is of critical importance for the studies of RPE diseases which are expressed in a topographically specified site, such as AMD.

α-Mannosidosis

Our studies of the RPE in the mucopolysaccharidoses have illustrated the importance of the lysosomal-degradative pathways for the turnover of GAGs located in the RPE cell coat, or in the extracellular matrices that surround this cell layer (see Aguirre and Stramm, 1991 for review). Our results emphasize also that RPE disease per se is not causally associated with visual cell disease and neuroretinal degeneration. It could be argued that lysosomal degradation of RPE GAGs, although important for the turnover and remodeling of cell surface and matrix proteoglycans, is not sufficient by itself to cause visual cell disease when a degradative pathway is impaired by an inherited disease. However, similar preservation of photoreceptor integrity is main-

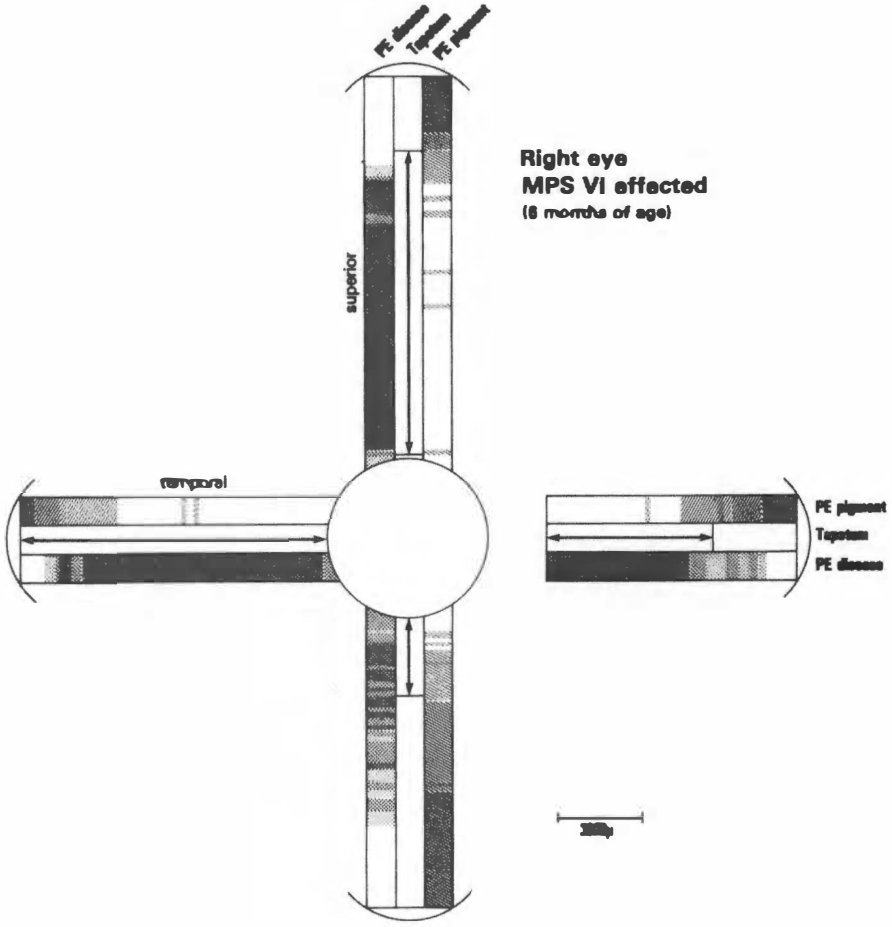

FIGURE 14-26. Schematic representation of the distribution of PE disease, pigmentation and the presence of the tapetum lucidum in the eye of a young MPS VI–affected cat. For comparison with the normal see Figure 14-3. The eye is drawn to scale based on observations of sequential 150 μm fields extending from the disc to the ora serrata *(curved line)*. Note that the tapetum is present primarily in the superior, nasal, and temporal meridians. The pigment epithelium is not pigmented in areas where the tapetum is present. Disease in the pigment epithelium, characterized by the accumulation of vacuolated inclusions and cellular hypertrophy, is more severe in areas where the cell layer is not pigmented. This is most dramatic in the superior meridian. *Key:* arrows indicate the presence of tapetum; RPE pigmentation varies from absent (empty) to moderate (density present in the far periphery); RPE disease varies from normal (empty) to moderate (darker shading indicates that >50% of the cell volume is occupied by vacuolated inclusions and hypertrophy is present). (For details refer to Aguirre et al., 1983, from which this figure was reprinted.)

tained in another lysosomal-storage disorder which is critically involved in rhodopsin degradation.

Acidic α-mannosidase is one of several lysosomal exoglycosidases which sequentially remove sugars from the nonreducing ends of glycoproteins (see Aguirre et al., 1986 for review of animal models of mannosidosis and fucosidosis). Since rhodopsin is the predominant mannose-containing glycoprotein presented to the RPE for degradation, enzyme deficiency results in the progressive accumulation of complex N-linked mannose pentasaccharides (DeGasperi et al., 1991; Alroy et al., 1991). The RPE disease in this mutant is far more severe and far more rapidly progressive than in the comparable mutants with defects in GAG degradation. The cytoplasm is full of secondary lysosomal inclusions, and, other than compacted and often distorted nuclei, it is difficult to identify cellular organelles (Fig. 14-30). In all other respects, however, the RPE appears to function normally. The participation of the RPE in the outer segment renewal process is evident by the accumulation of phagosomes in the apical cytoplasm, even though the degradation of rhodopsin containing outer segment material is incomplete (Aguirre, Haskins, and Ray, unpublished; Aguirre et al., 1995). The outer segments are

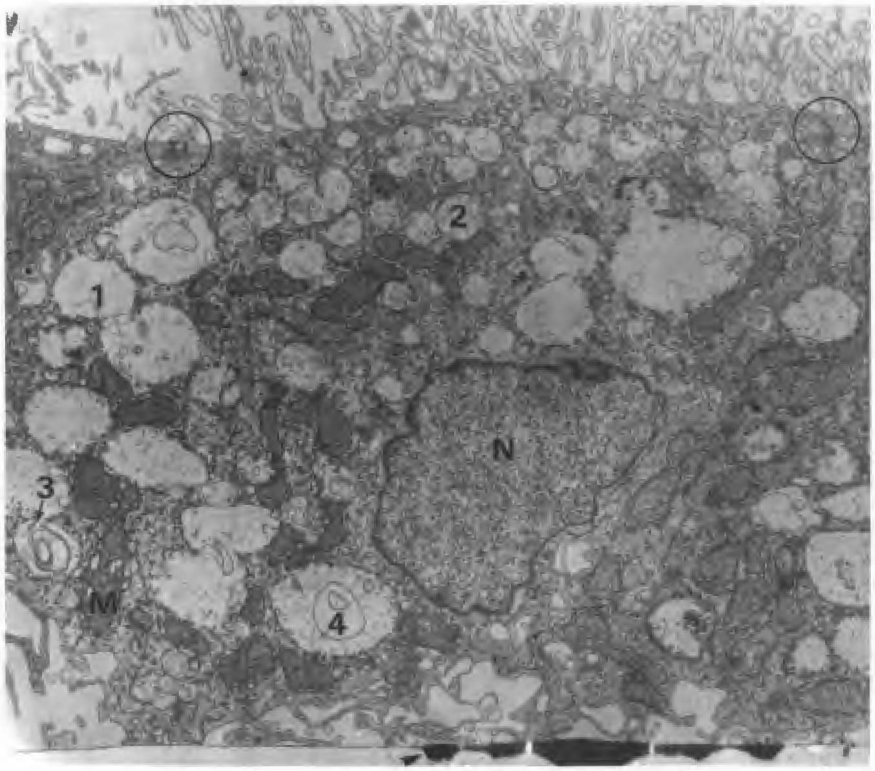

FIGURE 14-27. MPS VI–affected cat RPE after 14 days in tissue culture retains a differentiated phenotype as well as the essential features of the disease (compare with Figure 14-20). There is accumulation of storage in secondary lysosomes; the inclusions appear electron lucent (1), granular (2), lamellar (3), or mixed (4). N = nucleus, M = mitochondria, circle = apicolateral junctions, arrowhead = culture plate. Magnification ×9,400. (Reprinted from Stramm et al., 1985.)

structurally normal, but their average length is reduced by approximately 40%–50%. Similar changes in the RPE have been described in cattle with hereditary α-mannosidase deficiency (Jolly et al., 1987).

The α-mannosidase-deficient mutant has a short lifespan, and most animals die in their first year. It is likely that such a severe deficiency, if sustained for years in an animal or for decades in a human, would eventually result in photoreceptor degeneration secondary to RPE disease. What is more difficult to evaluate, however, is the effect of a less severe but long-term change in the activity of α-mannosidase or another RPE lysosomal enzyme as the result of aging (Wyszynski et al., 1989; Boulton et al., 1994). While there may be an effect on the RPE and neuroretina, our studies in the mutant animals would suggest that the effect is likely to be complex, and modified by other factors, both genetic and environmental, which play a role in the aging eye. Such issues are particularly relevant to a complex disorder such as AMD in man, and continuing studies of the RPE system in these animal models are crucial to clearly defining the importance of the lysosomal degradative pathways in the metabolic pathways of this cell layer.

Experimental Therapy of the RPE in Lysosomal Storage Disorders

Following the in vitro demonstration that soluble "corrective factors" are released into the media and reverse substrate storage in diseased cells (Fratantoni et al., 1968), various strategies have been used to treat the lysosomal storage disorders. Therapy has been directed toward restoring the deficient enzyme function by enhancing residual activity (Vine et al., 1982), by providing normal enzyme directly, or, indirectly, by transplanting bone marrow or other cells (Krivit et al., 1984; Summers et al., 1989; Wenger et al., 1986; Haskins et al., 1991; Akle et al., 1985). More recently, gene therapy using in vivo or ex vivo correction has been accomplished experimentally and in clinical trials. Because the disease may be variable within and between the different clinical entities, and most patients show the disease pheno-

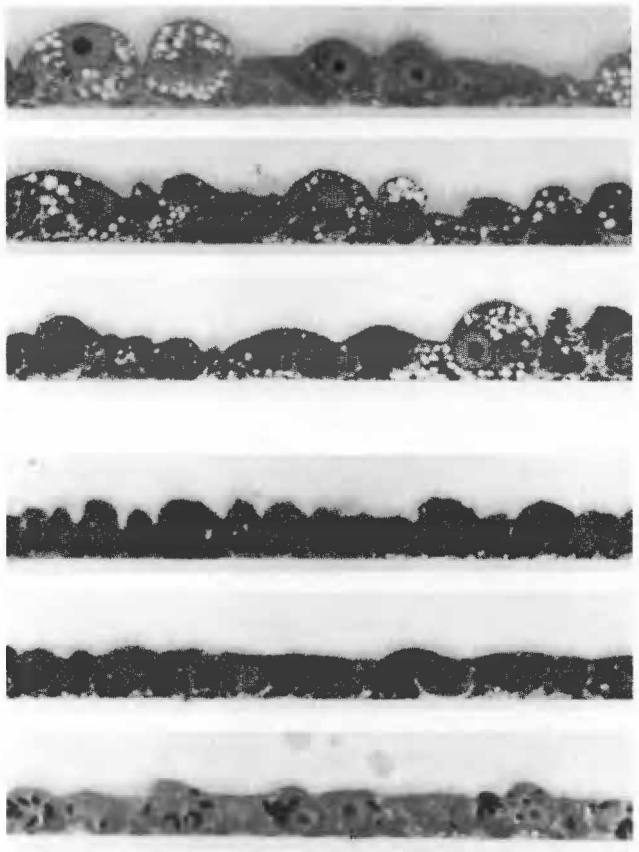

FIGURE 14-28. MPS VI–affected cat RPE cells after 14 days in primary culture. The cells were isolated from defined regions of the eye. The top three sections are of cultures initiated from the superior equatorial region; the three lower sections are from the inferior equatorial region. Although the cultures have equal and deficient levels of ASB activity, only the cells isolated from the superior region are diseased. Magnification ×800. (Reprinted from Aguirre and Stramm, 1991.)

type at the time therapy is initiated, it has been difficult to establish criteria by which the success of therapy can be evaluated. Determination of enzyme activity in the serum or leukocytes provides an objective measurement, but one that may not be appropriate, as the assays generally are made using artificial rather than natural substrates. Consequently, the presence of normal activity in the blood does not necessarily mean that normal degradative function is occurring in the lysosomal compartment of the other affected tissues. In collaboration with associates (M. Haskins and J. Wolfe) at the University of Pennsylvania, our laboratories have examined the effect of bone marrow transplantation (BMT) on the RPE disease phenotype, and have begun experimental gene therapy studies. These areas are discussed below.

Correction of RPE disease phenotype following bone marrow transplantation. Our laboratories have examined the RPE in animal models of MPS VI (cat), VII (dog), and α-mannosidosis (cat) following successful BMT (see Haskins et al., 1991 for review). Within each disease, the results were consistent, but demonstrated that the response to BMT was disease specific. This response appears to be dependent on the amount of enzyme that is

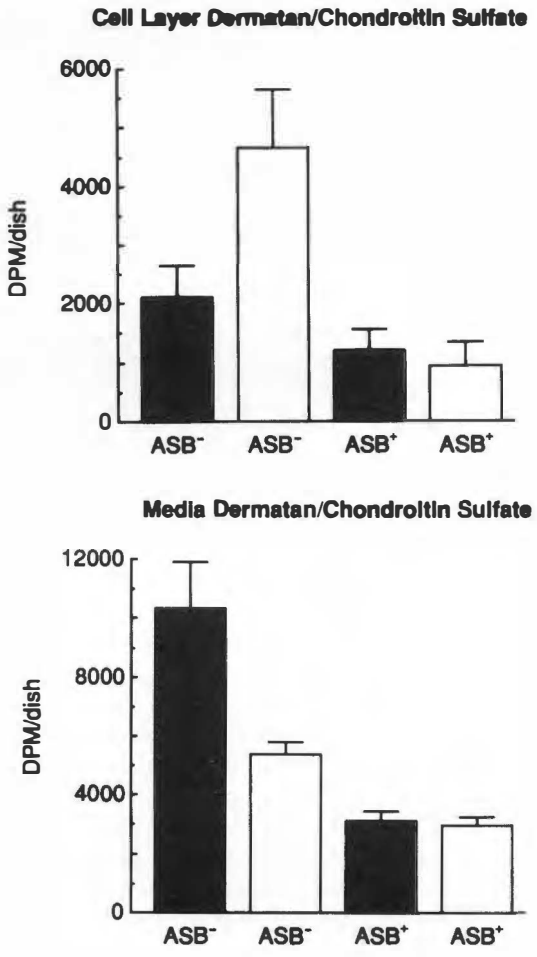

FIGURE 14-29. Cell layer *(A)* and media *(B)* GAGs (dermatan sulfate/chondroitin sulfate; DS/CS) at the end of a 72-hour period of labeling with $^{35}SO_4$. Accumulation of radio-labeled DS/CS in the RPE is significantly elevated in MPS VI–affected (ASB^-) cultures initiated from the superior region of the eye ($P < 0.02$). No regional differences are present in the normal (ASB^+) RPE. Release to the media of radiolabeled DS/CS at the end of a 72-hour labeling period is significantly elevated in MPS VI–affected (ASB^-) cultures initiated from the inferior region of the eye ($P < 0.0005$). Although not as dramatic, release of ^{35}S-DS/CS also was significantly elevated in affected cultures initiated from the superior region of the eye ($P < 0.01$). No regional differences were present in the normal (ASB^+) cultures. Mean ±SEM. Cultures from superior (nonpigmented) region = open bars; cultures from inferior (pigmented) regions = dark bars. (Reprinted from Stramm et al., 1991.)

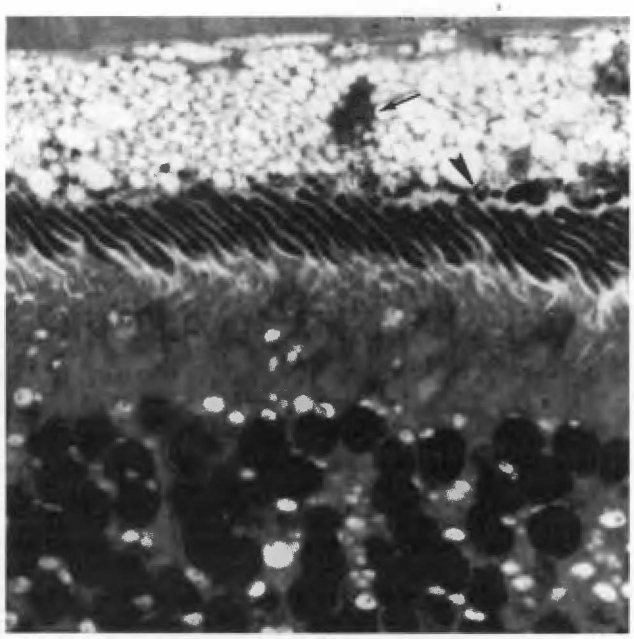

FIGURE 14-30. RPE disease is severe in a young cat affected with α-mannosidase deficiency. The RPE cells are hypertrophied, and the cytoplasm is full of vacuolated inclusions representing incompletely digested substrate that has been leached during tissue processing. The RPE nucleus is indented *(arrow)* by the inclusions that surrounded it; phagosomes *(arrowhead)* are prominently located in the RPE apical region. Although the rod outer segments are shortened, the photoreceptors are intact, but they accumulate inclusions in the inner segment and perinuclear region. Magnification ×1,250. (Aguirre, Haskins and Ray, unpublished.)

normally present extracellularly, and released by the transplanted cells.

Even though MPS VI–affected animals have shown improvement in some tissues after BMT (Gasper et al., 1984), we have not observed any modification of the RPE disease phenotype (Aguirre, Haskins, and Thrall, unpublished). In these animals, the RPE cells continue to hypertrophy as they progressively accumulate cytoplasmic vacuolated inclusions. A similar lack of correction has been found in the cornea, either following BMT (Aguirre, unpublished) or after reciprocal corneal transplantation where MPS VI–affected corneal buttons were transplanted to corneas of genetically normal animals (Aguirre et al., 1992). In order to correct the disease in the RPE and other tissues following BMT, the normal enzyme has to be released from the hematopoietically derived donor cells and has to enter the target cells by a receptor-mediated internalization process with subsequent targeting to the lysosomal compartment. There, the active enzyme is able to degrade stored substrate and prevent the subsequent GAG accumulation in the secondary lysosomes. Lack of correction of the RPE disease could result from one or a combination of different mechanisms: low levels of enzyme in the extracellular compartments, failure of diffusion of enzyme from the vascular compartment to the RPE, or failure of the affected RPE cells to internalize the secreted extracellular enzyme. Based on in vitro studies of the RPE, it appears that lack of correction results from the extremely low availability of ASB in the extracellular compartment. Unlike other lysosomal enzymes, ASB activity is primarily intracellular, with very little release to the extracellular compartment (Ray, unpublished).

In contrast, MPS VII–affected dogs show moderate correction of the RPE disease phenotype after long-term BMT. Many areas of the RPE monolayer show absence of storage, while others show small clusters of cells with cytoplasmic vacuolated inclusions (Fig. 14-31, B). Overall, there is no cellular hypertrophy, and BMT results in marked improvement of the RPE disease (Aguirre, Ray, and Haskins, unpublished). Associated with the BMT, there is a dramatic clearing of the cornea, and generalized improvement of the multiorgan disease that is normally present in canine MPS VII (Haskins et al., 1992). Similar studies have been carried out in the mouse model of MPS VII. Dramatic improvement of the disease phenotype was observed in all tissues except the RPE and retina, presumably because the high doses of irradiation given in the perinatal period prior to BMT resulted in complete retinal degeneration (Sands et al., 1993).

We have found that the most remarkable correction of RPE storage occurs following BMT in the feline model of α-mannosidosis. Eighteen months after transplantation, the RPE disease is completely reversed—the cytoplasmic inclusions disappear, cell size returns to normal, and cellular contours are restored (Fig. 14-31, A). As a result of the correction of the RPE disease, the photoreceptor outer segments resume normal orientation and elongate (Aguirre and Haskins, unpublished). As in the MPS VII–treated animals, there is correction of the storage in other organs, particularly the CNS, and the severe, progressive neurologic disease is prevented (Haskins, unpublished; Walkley et al., 1994). The success of correction of the RPE disease phenotype in both models probably results in part from the high levels of extracellular enzyme present following BMT. We have found that the RPE in culture has a very high level of cellular GUSB and α-mannosidase activity, and that it releases into the media catalytically active protein (Ray et al., 1997; Ray, unpublished). It is this extracellular enzyme that presumably is involved in the correction of disease in distant target tissues. These studies demonstrate that RPE disease can be treated by the systemic route as long as the corrective factor being supplied to the diseased cells is available in the extracellular environment.

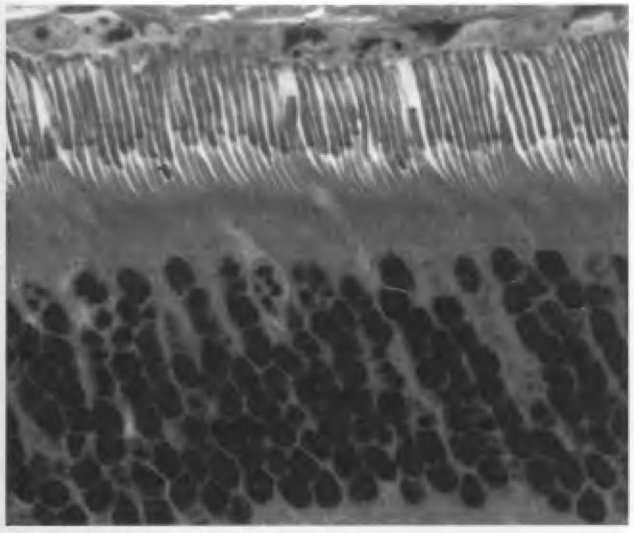

A

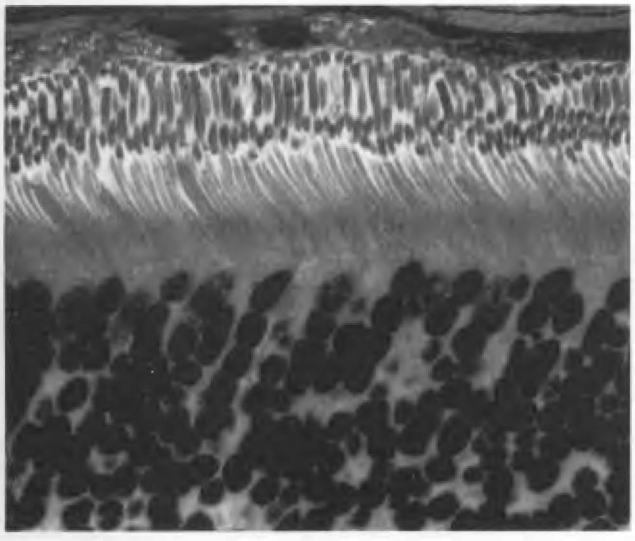

B

FIGURE 14-31. Improvement of RPE disease following long term bone marrow transplantation in a cat with α-mannosidosis *(A)*, and a dog with MPS VII *(B)*; the transplantation intervals are 2 years and 18 months, respectively. In α-mannosidosis *(A)*, the RPE is normal and the photoreceptors have elongated and are now of normal length (compare with Figure 14-30). In contrast, the treated MPS VII dog still shows some accumulation of vacuolated inclusions in the RPE, but no hypertrophy. At this stage the RPE would show marked hypertrophy and the cytoplasm would be full of vacuolated inclusions. Magnification ×800. (Aguirre and Haskins, unpublished.)

Gene therapy of RPE disease in lysosomal storage disorders. The prospects of genetically altering cells and/or organisms that have inherited defects have been improved by the recent advances in molecular biology. In order to genetically engineer the cells, the foreign DNA sequence or gene must not only be introduced into the cell, but also needs to be expressed. Microinjection, electroporation, and calcium phosphate (or dextran sulfate) coprecipitation of DNA have been the traditional methods by which foreign DNA has been transferred into cells. However, each of these methods has inherent limitations. In some cases, a large number of cells need to be injected; in others, the efficiency of transfection and/or expression is low.

The use of retroviral vectors to mediate gene transfer has overcome many of the limitations inherent in other methods of DNA transfer. By altering the structure of internal retroviral sequences, these vectors lack the polymerase and glycoprotein genes essential for replication, and contain instead the foreign DNA that is to be transferred. The deleted sequences, or *trans* acting functions, are provided by a packaging cell line which determines the host range and viral titers produced (Miller and Buttimore, 1986). These retroviral vectors are infective but replication incompetent, and they usually result in the high-efficiency transfer of the foreign DNA. Their disadvantage, however, is that the transferred DNA integrates randomly into the host cell chromosomes.

For most of our studies we have used retroviral vectors which have internal promoters and the cDNA sequences to be transferred (Armentano et al., 1987; Wolfe et al., 1990) (Fig. 14-32) These vectors are designed to use two different promoters (the strong promoter from the retroviral 5′ long-terminal repeat [LTR] and an independent internal promoter) to regulate the expression of two different genes: the *neo* gene and the transferred cDNA. The *neo* gene confers resistance to the neomycin analog G-418, and provides a means for selecting in vitro those cells infected and transduced by the retroviral vector; that is, only transduced cells will survive when G-418 is added to the culture media. We also have used other vectors without internal promoters or selectable marker genes, and have found them to be

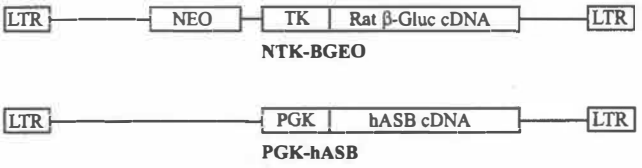

FIGURE 14-32. Retroviral vectors used to mediate cDNA transfer to the RPE. The NTK-BGO vector contains the rat β-glucuronidase cDNA driven by the herpes simplex thymidine kinase (TK) promoter, and the *neo* gene is used for selection of the transduced cells. A similar vector contains the SV-40 promoter to regulate the rat GUSB cDNA expression (see Wolfe et al., 1990, for details). The PGK-hASB vector has the human arylsulfatase B cDNA under the control of the mouse phosphoglucokinase-1 (PGK) promoter, but no selectable marker. (LTR) = long terminal repeat. (Ray et al., 1995.)

equally effective in transferring and expressing a foreign DNA in cultured RPE cells (Fig. 14-32).

In vitro correction of RPE disease in MPS VII (dog) and MPS VI (cat). The rat GUSB cDNA has been transferred in vitro to the RPE of MPS VII–affected dogs using one of two different N2–derived retroviral vectors that contain the entire coding sequence of the rat GUSB cDNA (Nishimura et al., 1986; Wolfe et al., 1990). The difference between the vectors is in the internal promoter used to drive the heterologous cDNA; these are the simian virus 40 (SV-40) and the herpes simplex thymidine kinase (TK) promoters, which are cloned upstream from the rat GUSB cDNA (Fig. 14-32). Both the SV-40 and TK promoters are constitutive promoters with no RPE specificity, yet the level of expression of the gene they regulate is sufficient to correct the inherited RPE defect (see below). It appears, therefore, that nonspecific promoters can be used in the RPE to regulate the expression of a gene that subserves a critical degradative function. Use of these vectors in high concentration (2×10^6 CFU/ml) results in high efficiency of RPE cell transduction without any impairment of cellular growth, metabolism, or viability (Stramm et al., 1990; Wolfe et al., 1990; Ray et al., 1992).

Following retroviral mediated GUSB cDNA transfer, the MPS VII–affected RPE cells show complete restoration of GUSB activity. This represents approximately a three- to five-hundred-fold increase in activity from the levels measured in untreated affected cells. The effect is specific, as the activity of other lysosomal enzymes remains normal and unchanged (Table 14-5; Ray, unpublished). These results have been confirmed in separate experiments using RPE cells from different affected dogs and the same vector constructs. We have found that the GUSB activity present in the vector-treated RPE cells is catalytically active on the natural substrate, and corrects the block in GAG degradation. Following 72 hours of continuous labeling with $^{35}SO_4$, the synthesized GAGs retained by the cell layer of the vector-treated cells are the same as in normal. In contrast, the untreated, affected cells accumulate heparan and chondroitin sulfates (Figs. 14-33, 14-34). The restoration of normal GAG-degradative function in the vector-treated cells occurs specifically in the cell layer compartment, as there are no changes in the media GAGs to indicate increased secretion or enhanced extracellular degradation. The localization of GUSB activity in the lysosomal compartment of the MPS VII vector-treated cells has been demonstrated histochemically (Wolfe et al., 1990).

Similar studies have been carried out in MPS VI cat RPE cells having a deficiency of ASB (Ray et al., 1995). Transduction of RPE cells was done using a retroviral vector containing the human ASB cDNA driven by the mouse phosphoglucokinase-1 promoter (Fig. 14-32). In the affected cells, the ASB activity was only 5%–10% of normal, but, following transduction, there was a hundredfold increase in enzymatic activity. Restoration of ASB activity resulted in a remarkable decrease in the storage of dermatan sulfate, the GAG that accumulates in the MPS VI RPE and other tissues.

TABLE 14-5. *Lysosomal enzyme activities in cultured MPS VII–affected and vector-treated RPE cells*

Group	β-glucuronidase	α-L-iduronidase (α-mannosidase)
Experiment # 1		
MPS VII	5%*	(88%)
Experiment # 2		
MPS VII	0.3%*	107%
MPS VII/TK1	117%	103%
Experiment # 3		
MPS VII	0.2%*	88%
MPS VII/TK1	71%	84%
MPS VII/SV8	102%	118%

Table reproduced from Aguirre and Stramm, 1991 and contains data from Wolfe et al., 1990 and Stramm et al., 1990.

Enzyme activities determined as nmol of substrate cleaved/hour/mg protein and expressed as % of normal control values. Each determination is based on four to ten different samples of three separate experiments: Experiment 1—primary cultures; Experiments 2 and 3—second passage cultures.

*Within experiment comparison between affected and normal or treared cells, $p < 0.001$, t-test. TK1 and SV8-cells infected with vectors NTK-BG-A1 and NSV-BG-A8 having the rat GUSB cDNA under the control, respectively, of the thymidine kinase and SV-40 promoters (Wolfe et al., 1990).

In vivo correction of RPE disease in the MPS VII mouse. The MPS VII mouse model has been used extensively to explore different treatment modalities aimed at correcting the lysosomal enzyme deficiency, and arresting or reversing the pathologic sequela. Transgenic MPS VII mice that overexpress the human GUSB cDNA in a heterozygous manner show complete reversal of the storage disease (Kyle et al., 1990). Retroviral vectors also have been used to transduce enzyme deficient hematopoietic stem cells or fibroblasts with the normal GUSB cDNA, followed by transplantation of these cells into MPS VII mice. Treatment results in variable degrees of tissue-specific correction of the disease phenotype, but there have been no reports of the correction of the ocular lesions (Wolfe et al., 1992; Maréchal et al., 1993; Moullier et al., 1993). In regards to the eye, the most dramatic correction of the RPE disease in vivo has been effected by the adenoviral-mediated transfer of the human GUSB cDNA to ocular tissues following the intravitreal injection of the viral vector. In short-term ex-

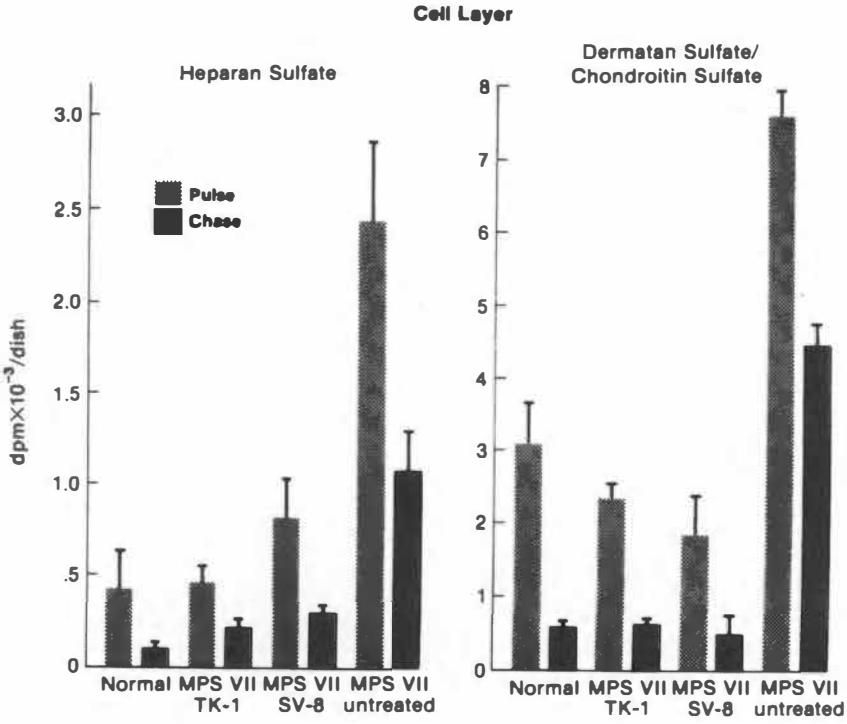

FIGURE 14-33. Cell layer GAGs in normal, MPS VII–affected, and vector-treated affected cells (MPS VII/TK-1, MPS VII/SV-8) following a 72-hour labeling period (pulse) with $^{35}SO_4$, or after a 24-hour chase. The two vector constructs were similar except for the internal promoter driving the rat GUSB cDNA: TK-1 = herpes simplex thymidine kinase promoter, SV-8 = simian virus 40 promoter (see Wolfe et al., 1990, for details). In the MPS VII–untreated cells, newly synthesized radio-labeled GAGs (heparan sulfate and chondroitin sulfate) accumulate in the cell layer at the end of the 72-hour pulse and remain elevated after a 24-hour chase period. In contrast, the vector-treated cells have normal levels of GAGs in the cell layer at the two time periods examined. Enzyme digestion and deamination indicates that the increased radioactivity in the dermatan sulfate/chondroitin sulfate peak of the MPS VII cells is only in chondroitin sulfate. (Reprinted from Aguirre and Stramm, 1991.)

periments that lasted up to three weeks, reversal of the RPE storage began after one week, and, by three weeks, the MPS VII RPE was indistinguishable from normal (Li and Davidson, 1995). It is not clear from these studies if the adenoviral-vector-mediated cDNA transfer directly corrected the affected RPE cells, or whether cells located outside the RPE–photoreceptor interface were corrected, and secreted GUSB enzyme that diffused into the subretinal space and cross-corrected the diseased RPE. Another issue not established from these studies is the duration of correction. Since adenoviral vectors do not stably integrate into the host cell's genetic material, it is likely that long-term stability of expression will not occur, thus necessitating repeated treatments.

These studies indicate the feasibility of using vector mediated cDNA transfer to correct inherited defects of the RPE. In vitro, there is high efficiency of transduction of RPE cells, and the retroviral-vector-corrected cells show stable and long-term expression of the transferred cDNA (J. Ray, unpublished). In vivo, the recent studies using adenoviral vectors are extremely encouraging, and illustrate the possibilities of gene therapy for the treatment of diseases of the RPE and other posterior segment structures. Some of the issues of gene therapy in the RPE have been discussed previously (Aguirre and Stramm, 1991).

RPE LIPOIDAL EPITHELIOPATHY

Aging Monkey

We and others have noted the presence of clusters of yellow flecks and dots present in the foveomacular region of aged rhesus monkeys that are maintained in long-term toxicologic studies (Fine and Kwapien, 1978; Bellhorn et al., 1981). These abnormalities have been described clinically as "pigmentary abnormalities of the macula" or "lipoidal degeneration" and represent a common aging response of the rhesus monkey RPE. Similar lesions have been described in cynomolgus monkeys (Feeney-Burns et al., 1981). In the rhesus monkey,

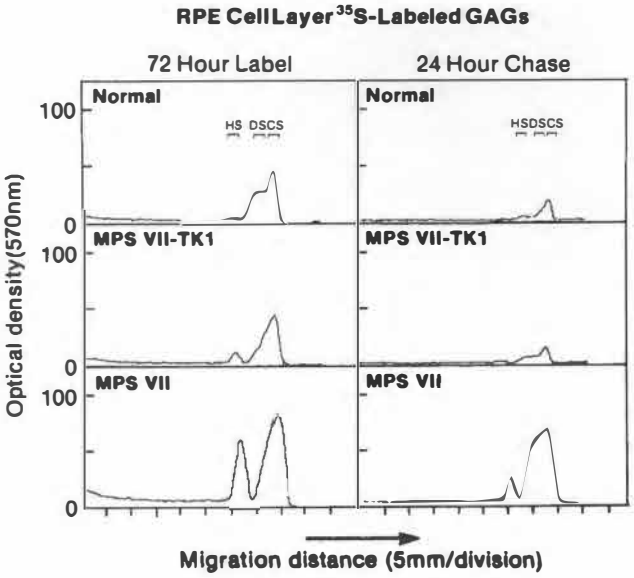

FIGURE 14-34. Scanning densitometer tracings of $^{35}SO_4$-labeled RPE cell layer GAGs after continuous labeling for 72 hours or after a 24-hour chase period. Each densitometer tracing represents the cell layer GAGs of one culture of normal, MPS VII–affected, or TK 1–vector-treated affected cells (MPS VII–TK1) for each labeling period. The markers indicate where the different GAGs run on the scan. The MPS VII–affected RPE shows two prominent peaks of radioactivity consisting of HS and a DS/CS doublet. After the 24-hour chase period, the levels of radioactivity decrease, but never approximate those of the normal or treated cells. (Reprinted with modification from Stramm et al., 1990.)

the lesions are found in both males and females, and appear to increase in severity with aging. The mildest form is characterized by a slight unevenness in macular pigmentation. Later, the macula has a finely stippled or a salt-and-pepper appearance. In the most severe form, the foveomacular region has variable numbers of yellowish flecks (hypopigmented spots) which result in loss of the foveal reflex (Bellhorn et al., 1981). Fluorescein angiographic studies have reported conflicting findings. One study indicates that the hypopigmented spots result in window defects visible on angiography; the window effect being caused by vacuolization of individual RPE cells (Fine and Kwapien, 1978). A second study has not been able to confirm these findings, and no association between the location and extent of the hypopigmented spots and angiographically visible fluorescent foci has been established (Bellhorn et al., 1981). These foveomacular pigmentary abnormalities cause no impairment of function as assessed by retinal testing with electroretinography and visual evoked responses (Bellhorn et al., 1981). Morphologically, the affected RPE cells and adjacent photoreceptors remain intact (Fine and Kwapien, 1978; Fine, 1981; Aguirre and Bellhorn, unpublished).

In glutaraldehyde/osmium-fixed retinas embedded in plastic, light microscopic abnormalities are readily apparent in some RPE cells located in the foveomacular region. The affected cells contain light brown to dark brown inclusions which, when numerous, completely fill the cell. These abnormalities are extremely difficult to detect in eyes that are conventionally fixed, embedded in paraffin, and sectioned at 5–6 μm. By electron microscopy, the affected RPE cells accumulate intracytoplasmic inclusions (Fine and Kwapien, 1978; Fine, 1981; Aguirre and Bellhorn, unpublished). The vacuoles have a distinct limiting membrane, and, in most cases, have low electron density and a homogeneous appearance; in some cells, the inclusions are electron lucent and empty (Fig. 14-35). When few in number, they usually are located basally. As their number increase, the inclu-

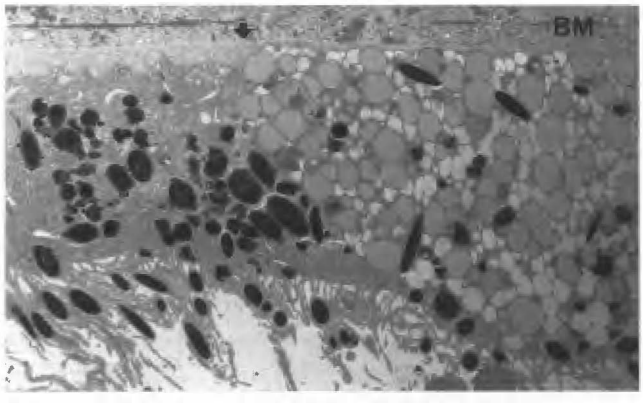

A

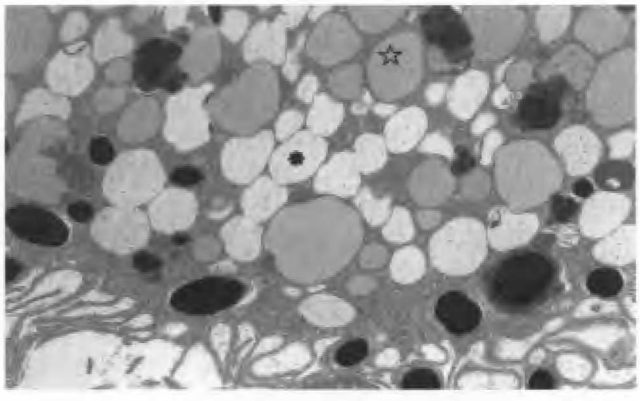

B

FIGURE 14-35. Macular RPE of an aged rhesus monkey. Upper panel (A) shows an RPE cell *(right of vertical arrow)* whose cytoplasm is full of lipoidal inclusions of varying electron density. The cell on the left is unaffected, and contains melanin granules and lipofuscin and melanolipofuscin inclusions. The lower panel (B) shows that the lipoidal inclusions are homogeneous *(open star)* or vacuolated (*). BM = Bruch's membrane. Magnifications: upper panel ×3,500; lower panel ×8,600. (Aguirre and Bellhorn, unpublished.)

sions are located in the basal and central zones, often in close proximity to lysosomal and/or lipofuscin granules. The lipid origin of these inclusions has been confirmed by using osmium tetroxide fixation for electron microscopy, or glutaraldehyde fixation prior to cryosectioning and oil red O staining (Fine, 1981). It is likely that these lipid inclusions have a similar origin to those identified in the RPE of human eyes (El Baba, et al., 1986).

Congenital Stationary Night Blindness (CSNB) in the Dog

Lipoidal epitheliopathy also has been described in the RPE of Swedish briard dogs having congenital night blindness (Narfström et al., 1994). The disease, initially described as a stationary disorder analogous to human CSNB, is now considered to have a progressive component (Narfström et al., 1989b; Wrigstad, 1994). In general, affected dogs have an ERG of normal waveform, but showing a marked diminution of the response amplitudes, similar to a "Riggs-type" ERG in man. The ERG recorded under DC conditions shows complete absence of the a-, b-, and c-waves, with the latter waveform being replaced by a very slow negative potential which develops when the stimulus intensity is greater than 3 log units above the normal b-wave threshold. The authors interpret the abnormalities in the a- and b-waves as representing a delay in rod phototransduction, while the lack of a c-wave was ascribed to the morphologic abnormalities identified in the RPE (Nilsson et al., 1992).

Microscopic examination of the RPE showed the presence of large inclusions in the central and midperipheral tapetal regions in dogs as early as 3.5 months of age. By light microscopy, the inclusions are single to multiple; depending on the fixative used, they are vacuolated or appear homogeneous and stain intensely with crystal violet or other lipid stains (R. Riis, personal communication, 1995). Ultrastructurally, the inclusions are electron lucent vacuoles with a more homogeneous cortex which often contains membranous debris (Wrigstad et al., 1992; 1994). Unlike the lipoidal inclusions found in the aging monkey RPE, a single limiting membrane was absent or not distinct in some of the vacuoles. With aging, the inclusions increase in number and are found in the peripheral RPE cells. The striking feature of some of the lipid inclusions is their immense size (Fig. 14-36).

At this time, the association between the lipoidal changes in the RPE and the primary photoreceptor defect is unknown. That this interesting RPE abnormality is not an incidental finding is demonstrated by the presence of similar RPE lesions in unrelated briard dogs with CSNB, both in France and the United States. However, the causal association between the RPE and photoreceptor pathology is not clear. The ERG results indicate a widespread transduction disorder of all photoreceptors. In contrast, the RPE lipid storage, although prominent, is not present uniformly in all cells, and the severity of the RPE pathology and photoreceptor dysfunction are not correlated.

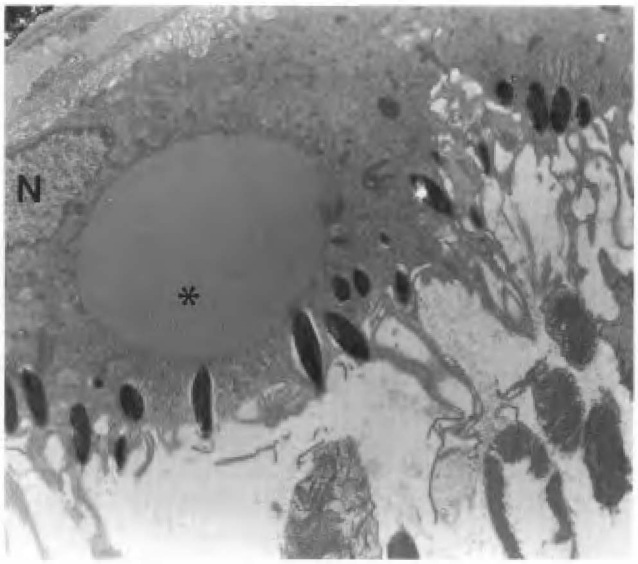

FIGURE 14-36. Nontapetal RPE of adult briard dog with congenital stationary night blindness. Note the extremely large and homogeneous lipid inclusion (*) present in the RPE which dwarfs the cell nucleus (N). The retina is artifactually detached. Magnification ×5,200. (Photograph courtesy of Dr. Ron Riis.)

RPE AUTOFLUORESCENT INCLUSION EPITHELIOPATHY

Retinal Pigment Epithelial Dystrophy (RPED)

Central progressive retinal atrophy (CPRA) is a specific pigment epithelial dystrophy recognized in several breeds of dogs (Parry, 1954; Aguirre and Laties, 1976), which is now termed *retinal pigment epithelial dystrophy* (RPED) (Bedford, 1984). Ophthalmoscopically, the disease is characterized by the accumulation of irregular foci of light brown pigment over the tapetal zone; with time, these foci increase in size and become distributed throughout the tapetal fundus (Plate 14-VII). In the end stages of the disease, the pigmentation decreases or forms clusters around the margins of foci of retinal atrophy.

Using conventional histologic methods, the earliest

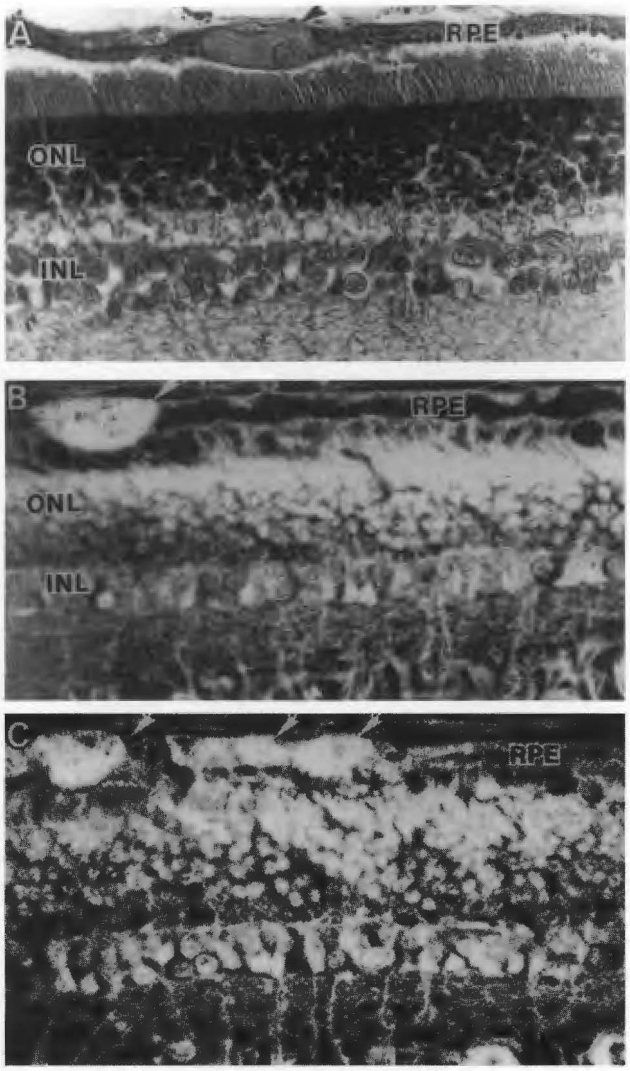

FIGURE 14-37. Retinal pigment epithelial dystrophy (RPED) in the dog. (A) In the early stages of the disease, there is focal hypertrophy of the RPE *(arrowhead)* with accumulation of granular light brown material in the cytoplasm. (B) This material is intensely autofluorescent *(white arrow)*. Note that the rest of the RPE layer is normal. (C) With time, more cells in the monolayer become diseased *(white arrowheads)*. Opposite the hypertrophied cells, the photoreceptor inner and outer segments are disoriented and compressed. The outer and inner nuclear layers (ONL and INL) show normal levels of autofluorescence for fixed tissues. Magnifications: (A) and (B) ×280; (C) ×225.

recognizable lesion is in the RPE. Individual cells become hypertrophied and accumulate a light brown granular material in the cytoplasm. Opposite the hypertrophied cells, the photoreceptor outer segments are shortened. Gradually, the focal lesion spreads in the RPE monolayer, and more cells become hypertrophied (Fig. 14-37). In the end stages of the disease, the hypertrophied RPE cells form multicellular cell nests; at this time, there is focal degeneration of the photoreceptors followed by complete retinal degeneration with intraretinal migration of non-melanin-containing cells. Fluorescent microscopy of unstained retinal sections indicates that the diseased RPE cells, either located on Bruch's membrane or migrating intraretinally, contain a bright autofluorescent lipopigment similar to ceroid or lipofuscin (Fig. 14-37B, C). Recent studies reported in abstract form suggest that the pigments that accumulate in the disease vary by breed, and differ from those that accumulate in the aging human RPE in that they are the result of peroxidation of rod outer segment lipids (Watson and Bedford, 1992; P. Watson, personal communication, 1993).

Most current studies of RPED have been carried out in the briard dog breed in the United Kingdom (Bedford, 1984; Lightfoot, 1988) (Note that RPED differs from the CSNB, which also is reported in briards.). These have demonstrated that rod outer segment renewal is normal, as is acid phosphatase activity in the RPE. In contrast, affected dogs are hypercholesterolemic and systemically deficient in vitamin E and taurine (P. Bedford, personal communication, 1996; Watson et al., 1993).

The clinical and histologic features of RPED are similar to vitamin E deficiency retinopathy in dogs, either naturally acquired (Hayes et al., 1970) or produced experimentally (Riis et al., 1981). In all three diseases, the RPE cells become hypertrophied and accumulate lipofuscin inclusions. In the experimental deficiency, however, lipofuscin accumulation and RPE hypertrophy occur after there is the beginning of photoreceptor outer segment degeneration visible by electron microscopy, and the disease course is much more rapid (Riis et al., 1981). This suggests that the target cell for the disease may be the photoreceptor, even though the most dramatic manifestation of the disease is in the RPE.

The similarities between RPED and vitamin E deficiency may explain its unique geographic distribution. The disease was once prevalent in the United States, but now is extremely rare, and only sporadic cases are identified. In Western Europe, particularly the United Kingdom, by contrast, the disease has had a very high prevalence until recently, and many breeds of dogs have been affected. Because of the possibility that RPED is associated with antioxidant deficiency, the disease frequency in young dogs has been markedly reduced with the widespread use of vitamin E supplementation (P. Bedford, personal communication, 1996). It is not clear at this time, however, whether the disease represents a strictly nutritional deficiency, or is an inherited defect that becomes manifested clinically by inadequate diets.

Equine Motor Neuron Disease (EMND)

A spontaneous neuronopathy has been recently identified in adult horses which bears a striking resemblance to the sporadic form of amyotrophic lateral sclerosis of man (Cummings et al., 1990). The disease is a progressive degeneration of motor neurons of the spinal cord and brainstem which results in muscle atrophy, weakness, and wasting; it is generally fatal. Studies have suggested an association between vitamin E deficiency and EMND, since affected animals have been found to have marked decreases in plasma vitamin E levels (Divers et al., 1994), and they have demonstrated ceroid lipopigment accumulation in the endothelial cells of small vessels in the spinal cord (Cummings et al., 1995).

Characteristic lesions of the RPE have been found in most animals with clinical abnormalities indicative of EMND; in all cases, the ocular abnormalities have always been found in association with the neurologic disease. Fundus examination reveals a horizontal linear or mosaic pattern of pigmentation, located either close to the optic disc or throughout the fundus. These lesions are bilateral, but may vary in severity between the two eyes (Riis et al., 1995). The fundus abnormalities are the result of accumulation of an autofluorescent lipopigment within hypertrophied RPE cells. Initially, the hypertrophied cells occur in foci with no apparent photoreceptor disease. Later, there is degeneration of the photoreceptor cells and inner retinal layers, and macrophages accumulate in the interphotoreceptor space and migrate intraretinally. Autofluorescent lipopigments are found in the hypertrophied RPE and in macrophages. By electron microscopy, the RPE lipopigments are typical of lipofuscin and ceroid (Fig. 14-38) (Cummings et al., in press; R. Riis, personal communication, 1995)

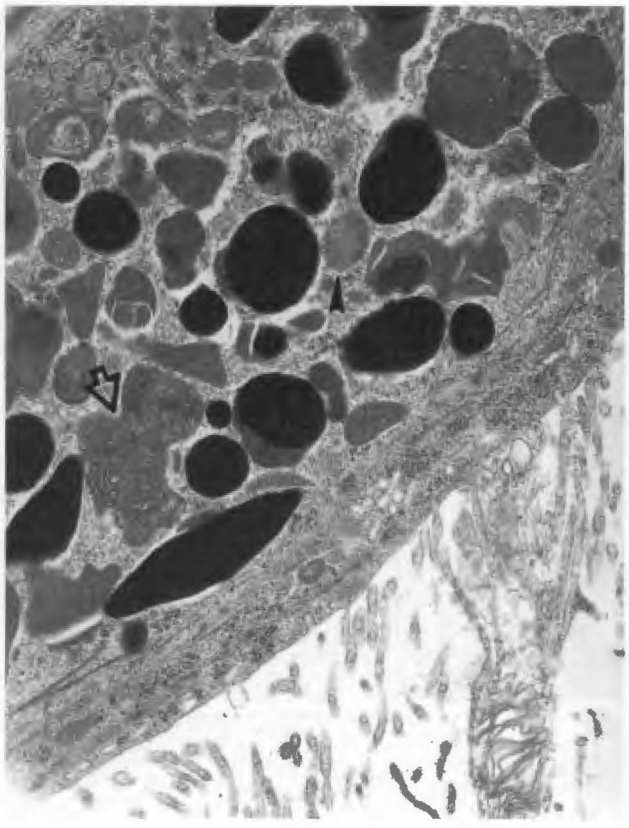

FIGURE 14-38. RPE cell from horse affected with equine motor neuron disease (EMND). Melanin granules and numerous lipofuscin *(arrowhead)* and ceroid *(open arrow)* inclusions are present in the cytoplasm. Magnification ×8500. (Photograph courtesy of Drs. R. Riis and J. Cummings.)

Neuronal Ceroid Lipofuscinosis (NCL)

The neuronal ceroid lipofuscinoses in man are a group of diseases divided into distinct syndromes based on clinical and pathologic criteria; in general, four syndromes have been recognized (infantile, late infantile, juvenile, and adult), and each has a complex of eponyms. Although the diseases have a broad spectrum of neurologic abnormalities, the common denominator is the accumulation of autofluorescent lipopigments in neurons and other cells (Jolly and Palmer, 1995). Except for the infantile form of the disease, which is caused by mutations in the palmitoyl protein thioesterase gene, the molecular basis of NCL is unknown (Vesa et al., 1995). The same diversity of clinical disease and ocular abnormalities also occurs in animals with NCL (Aguirre et al., 1986; Jolly and Palmer, 1995; Jolly et al., 1994). A common clinical manifestation in both man and animals is the presence of blindness, which occurs at approximately the same time as the clinical syndrome with which it is associated. With some exceptions (see below), the blindness is cortical in origin, since photoreceptor structure and function generally are preserved.

In sheep, an early adult onset, acute form of NCL has been described. Animals develop normally for several months after birth, and then show progressive neurologic abnormalities, visual deficits, and blindness; death occurs by approximately two years of age. Blindness in sheep is the result of a progressive degeneration of the photoreceptor cells, particularly the rods. In affected animals, there is a marked loss of rod-mediated ERG responses until they disappear soon after one year of age; cone responses, on the other hand, remain normal until that time and decay thereafter. These functional abnormalities are reflected in the pathology of the retina, which demonstrates a progressive rod-cone degenerative process. The RPE remains relatively normal

throughout the disease, but accumulates numerous electron-dense membranous cytoplasmic structures which are autofluorescent. However, these inclusions are smaller and less numerous than elsewhere in the retina (Graydon and Jolly, 1984). Additionally, RPE function, as determined by the response to azide, remains normal even in blind, terminal animals (R. Jolly, personal communication, 1984). Extensive photoreceptor degeneration with preservation of the RPE also has been found in Devon cattle with NCL (Jolly et al., 1992).

In contrast, most canine forms of NCL are distinguished by blindness of nonretinal origin (see Jolly et al., 1994 for review). Of these, the best characterized disease is that found in the English setter which has an early adult onset with an acute course (see Koppang, 1992 for review). In this breed, retinal function is initially normal at a time when neurologic abnormalities are present. Thereafter, ERG responses become reduced (Berson and Watson, 1980; Aguirre et al., 1986), and, in the very late stages of the disease, the DC recorded ERG shows a severe depression of the responses. At this time, there is a decrease in amplitude and eventual disappearance of the ERG c-wave, and a reduction in the standing potential (Nilsson et al., 1983). These findings suggest an impairment of RPE function.

Retinal abnormalities associated with NCL have been reported in the Tibetan terrier (Riis et al., 1992), miniature schnauzer (Smith et al., 1996) and Polish Owczarek Nizinny (Wrigstad et al., 1995) dog breeds. In Tibetan terriers night blindness is the primary clinical abnormality recognized in young animals. In contrast, NCL in the Nizinny breed appears clinically similar to RPED, and the fundus shows the accumulation of irregular foci of light brown pigment over the tapetal zone which, histologically, reflects the storage of autofluorescent lipopigments in hypertrophied RPE cells . In these three breeds, the clinical manifestations of NCL are initially retinal (photoreceptor or RPE), with neurological abnormalities occurring later in life.

As in humans and other animal models of NCL, autofluorescent lipopigment inclusions accumulate in the RPE cells and other retinal and CNS neurons of affected English setter dogs. However, the association between neuronal lipopigment storage and cell death is not known. Since there is no degeneration of the retina or RPE cells in many different animals with this disease, even though significant storage is present (Neville et al., 1980), the causal association between lipopigment storage, cell dysfunction, and cell death is not clear at this time. This will require identification of the molecular defects present in these different diseases, and characterization of the biochemical abnormalities resulting from the gene defect(s).

MACULAR ABNORMALITIES AND DRUSEN IN MONKEYS

Macular degeneration is uncommon in the subhuman primate. With few exceptions, abnormalities of the macula occur sporadically, and are reported as single case studies. Attempts to determine if macular degeneration occurs naturally in primates have resulted in surveys of monkey colonies (Stafford, 1974; El-Mofty et al., 1978; Nicolas et al., 1996), the most extensive of these undertaken at the Cayo Santiago colony, a part of the Caribbean Primate Center (El-Mofty et al., 1978; 1980; Engel et al., 1988; Dawson et al., 1989). In their initial survey, El-Mofty and colleagues (1978) reported two types of macular anomalies which were age related and affected approximately half of the 105 animals examined: (a) a macular pigmentary disorder showing various degrees of irregularity in the distribution and intensity of pigmentation, and (b) multiple discrete small white spots that mainly clustered in the paramacular area. The pigmentary abnormalities probably are the lipoidal epitheliopathy described in a preceding section, while the paramacular white spots were interpreted by the authors as drusen. A repeat study of a larger group of animals confirmed the previous observations and found that over 80% of old animals had macular lesions (El-Mofty et al., 1980). However, some young animals one to three years of age also showed similar lesions of equal severity, suggesting a heritable component to the disorder. A separate and independent survey of this colony has been undertaken, and confirmed the presence of macular drusen which, histologically, are nearly identical to similar lesions found in the human eye. Although this limited sample did not show any animals with the exudative form of AMD or disciform scars (Engels et al., 1988), a larger sampling reported older animals with end-stage disciform changes (Dawson et al., 1989).

In a study by Feeney-Burns and colleagues (1981), the authors examined the retinas of cynomolgus monkeys with macular abnormalities visible by ophthalmoscopy or fluorescein angiography. Lipoidal epitheliopathy, misshapen foveal depressions, RPE depigmentation, and exudative foci underneath the RPE were found. Surprisingly, morphologic examination of the macular region of animals considered clinically normal showed retinal pathology limited to the macular region. These consisted of degeneration of parafoveal cones, ballooning and disarray of foveolar cone outer segment disc membranes, and accumulation of lamellar, osmiophilic material in the inner and outer segments. The authors emphasized the importance of thoroughly characterizing the normalcy of primate populations before their use in experimental studies.

Drusen have been reported in monkeys, either limited to the macular region, or uniformly distributed throughout the fundus (Barnett et al., 1972; Stafford, 1974; El-Mofty et al., 1980; Ishibashi et al., 1986). The histologic appearance of the lesions is quite characteristic, and similar to comparable abnormalities in man. As noted previously, the incidence of macular and paramacular druse increases with aging. Generalized drusen of the fundus have been found in baboons and rhesus monkeys, usually at a young age, suggesting that these lesions may be present congenitally or develop in the perinatal period. They occur as large, single or multiple nodules which are overlaid by an extremely thin and attenuated RPE. Other than disorientation of the apposed photoreceptor cells, there is surprisingly minimal pathology of the retina (Barnett et al., 1972; Aguirre, unpublished).

A bilateral macular degeneration associated with widespread outer retinal disease has been reported in a colony of captive reared Guinea baboons (Vainisi et al., 1974). In the propositus, the maculae were atrophic, with a reticular yellow metallic appearance, and prominent window defects were evident on angiography (Plate 14-VIII). The RPE and retina were absent in the macular region; more peripherally, there was photoreceptor degeneration with RPE preservation. Additional studies on animals from this colony have shown that the disease is likely to be hereditary, but the mode of inheritance has not been established. In young animals, the initial clinical abnormalities are restricted to the macula (subtle depigmentation in the fovea surrounded by a hyperpigmented ring); histologically, the RPE is normal, but disease is present in the photoreceptors and is more widespread. There is initially degeneration of parafoveal rods and cones which subsequently spreads to involve those photoreceptors in the equator and periphery. In animals with advanced macular degeneration, there is extensive degeneration and loss of the photoreceptor and outer nuclear layers in the equator and periphery (Tso et al., 1983; Santos-Anderson et al., 1983). Unfortunately, a colony of this potentially important animal model for human retinal disease is no longer extant.

ORNITHINE-δ-AMINO TRANSFERASE DEFICIENCY IN CATS

Deficiency of the mitochondrial matrix enzyme ornithine-δ-amino transferase (OAT) causes a retinal degeneration in man and cats. In man, the disease is termed *gyrate atrophy of the choroid and retina* because of the characteristic fundus lesions. In contrast, cats with OAT deficiency have a generalized retinal degeneration (Plate 14-IX) that is clinically indistinguishable from that present in animals affected with PRA, the group of primary photoreceptor degenerative diseases.

In cats the disease has been found sporadically, and is characterized by hundredfold elevation in plasma ornithine levels with overflow ornithinuria (Valle et al., 1981; 1983; Rosenzweig et al., 1990). This results from deficiency of OAT in tissues, and enzyme deficiency is confirmed in cultured fibroblasts. A suggestion of autosomal recessive inheritance is based on the finding that presumably heterozygous animals have reduced OAT activity levels that are intermediate between affected and normal cats (Giger, personal communication, 1995). In one animal, OAT was pyridoxine responsive, but long-term oral supplementation with this vitamin did not affect the progression of retinal degeneration (Aguirre, unpublished). Histologic examination of the retina shows complete atrophy of the RPE and photoreceptor cells, and end-stage retinal degeneration (Fig.

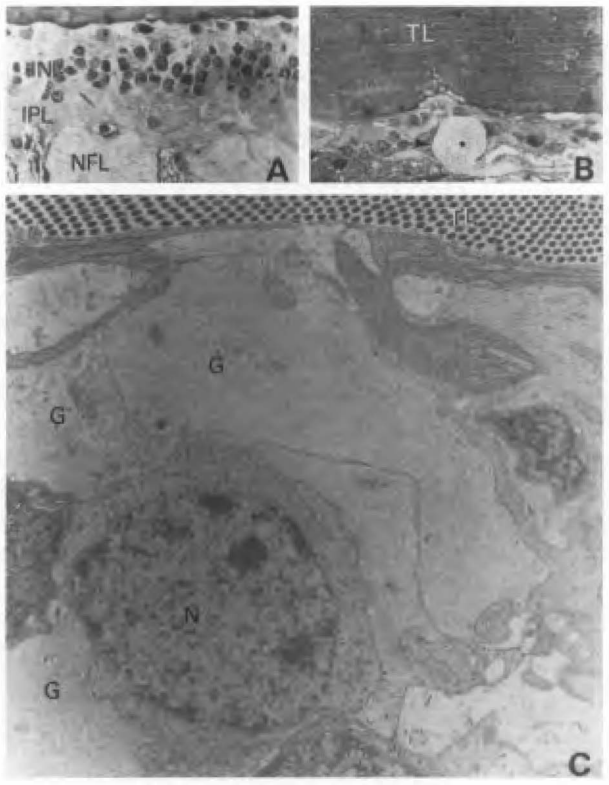

FIGURE 14-39. Light (A and B) and electron (C) micrographs of the tapetal retina from an adult cat with ornithine-δ-amino transferase deficiency. (A) Retina in the posterior pole shows loss of RPE and photoreceptor layers, with preservation of inner retina (INL, IPL, NFL). (B) Tapetal region (TL) showing a very thin and gliotic retina with a prominent ganglion cell. (C) Unidentified neuron (N) surrounded by prominent glial fibers (G) is located adjacent to the tapetum lucidum (TL). Magnifications: (A) and (B) ×400, (C) ×9,600. (Reprinted from Valle et al., 1981.)

14-39) (Valle et al., 1981). Such extensive atrophy of the outer retina is unusual for retinal-degenerative disorders in cats or other animals.

THE RPE AND ECTOPIC PHOTORECEPTOR NUCLEI

Subretinal displacement of photoreceptor nuclei has been found in many different animal species. In the rat, the displacement reflects a general mechanism of cell loss that is influenced, to some extent, by aging and environmental exposure to high ambient light intensities (Lai et al., 1978; Lai 1980). A similar process occurs in humans and has been associated with age-related degenerative disorders of the eye, diabetes, or systemic infections (Lai et al., 1982). In most cases, the distinct cytologic characteristics of the photoreceptor nuclei help to distinguish them from the phagocytic cells that invade the subretinal space during the degenerative phase of primary photoreceptor diseases (see "Photoreceptor degeneration, RPE pigmentation, and interphotoreceptor space phagocytic cells," above).

The presence of ectopically located photoreceptor nuclei in the subretinal space is supposed to represent two different cell death mechanisms: in situ death followed by displacement, and the outward movement of photoreceptors with their subsequent death in the subretinal space (Lai et al., 1982). Recent studies in dogs with inherited cone degeneration question the loss of viability of the ectopically located photoreceptor cell nuclei, particularly cones (Gropp et al., 1996).

We have previously identified a canine model for rod monochromatism in man (Aguirre and Rubin, 1974; 1975). The disease was initially termed *hemeralopia,* but, in order to prevent etymological controversy, the name and gene locus identification were changed to *cone degeneration* (Long and Aguirre, 1991). Cone degeneration *(cd)* is a rare, autosomal recessive disorder found originally in the Alaskan malamute breed, and characterized by specific functional and structural abnormalities limited to the cone photoreceptors. The disease is unique in being the only model for selective cone degeneration in man. In the *cd* retina, cones become dysfunctional early in life, show disorganization and loss of outer segments, and accumulate 100 Å neurofilament bundles in the inner segment and perinuclear cytoplasm; degeneration of cones occurs subsequently.

An unusual feature of *cd* is the manner in which cone

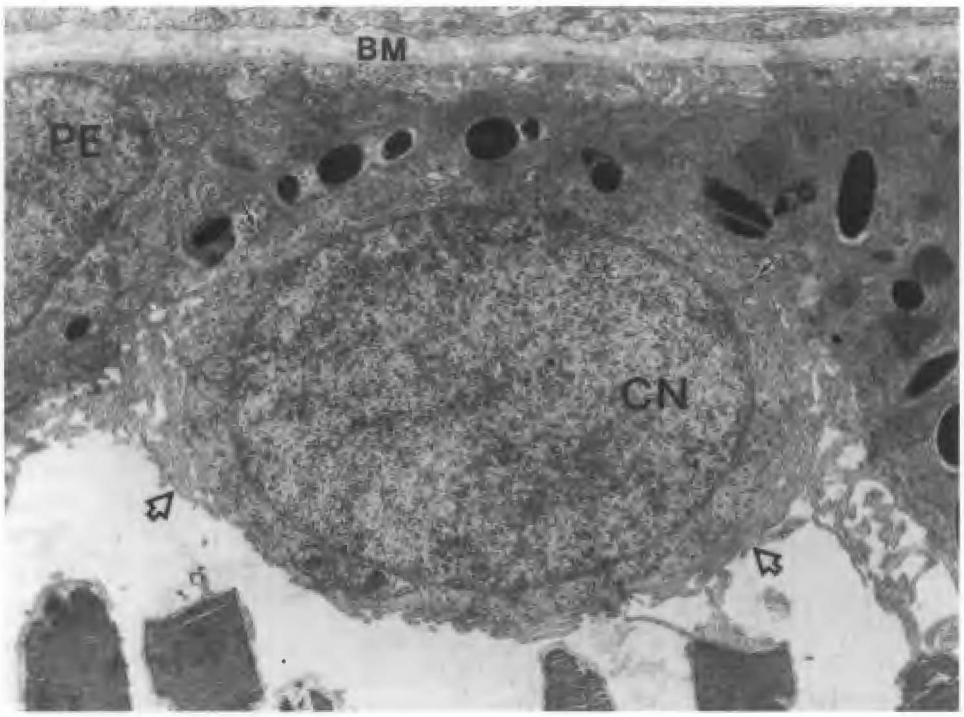

FIGURE 14-40. Ectopically located cone nucleus (CN) adjacent to the retinal pigment epithelium (PE) in an adult dog with hereditary cone degeneration *(cd)*. The ectopic nucleus is surrounded by a rim of cytoplasm, and indents the apical border of the PE, bringing the apically located melanin granules closer to the basal PE surface and Bruch's membrane (BM). The ectopic nucleus is surrounded by the apical microvilli of the PE *(open arrows)*. Note the distinct separation between the cytoplasmic membranes of the PE and the ectopic cone nucleus *(black/white arrows)*. Magnification ×10,500. (Reprinted from Gropp et al., 1996.)

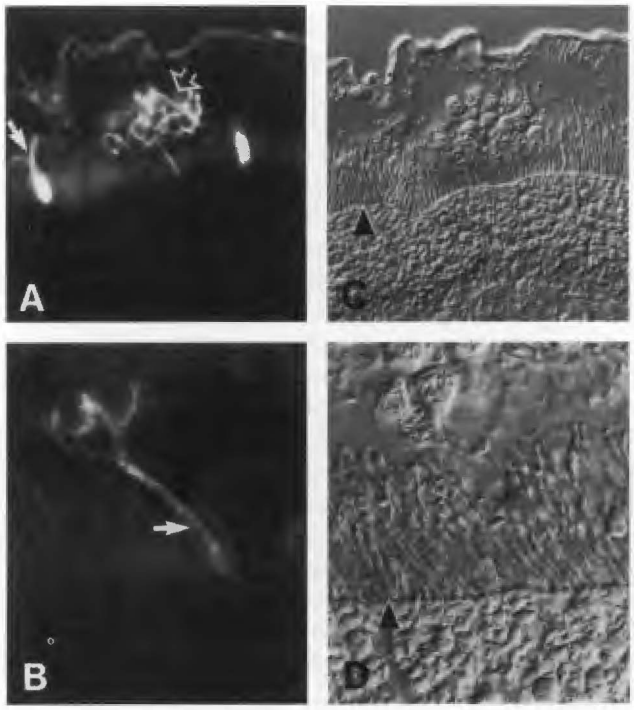

FIGURE 14-41. Paired PNA fluorescence and Nomarski (A, C and B, D) photomicrographs of the *cd* retina from an adult affected dog. Groups of PNA-positive cone somata are clustered ectopically in the subretinal space (A) *(open arrow)*. Some cells extend PNA positive processes (B) *(arrow)* proximally to the external limiting membrane (marked by arrowheads in C and D). Distinct cone matrix sheaths are still present (A) *(arrow)*. Artefactual detachment of the retinal pigment epithelial layer accentuates the ectopically located cone nuclei. Magnifications: (A) and (C) ×250; (B) and (D) ×750. (Reprinted from Long and Aguirre, 1991.)

loss evolves. Unlike other models of photoreceptor degeneration, where nuclear pyknosis and apoptotic cell death follow disease and degeneration of the outer and inner segments (Chang et al., 1993; Portera-Cailliau et al., 1994), this process does not occur, at least initially, in the *cd* retina. Diseased cones undergo slow extrusion of the nucleus into the inner segment, displacement into the interphotoreceptor space, and final placement adjacent to the RPE (Fig. 14-40). In this position, the ectopically located nuclei indent the RPE surface, but cause no further response (Gropp et al., 1996). Cone extrusion also occurs in complete typical rod monochromatism in man, the disease for which *cd* serves as an animal model (Larsen, 1921; Harrison et al., 1960; Falls et al., 1965). In the retinas of humans affected with this disorder, there is loss of cones as well as the presence of ectopic cone nuclei which are located in the inner segment, in the interphotoreceptor space, and adjacent to the RPE (Falls et al., 1965).

Examination of *cd*-affected retinas embedded in plastic and sectioned at 1 μm suggests that the ectopic cone

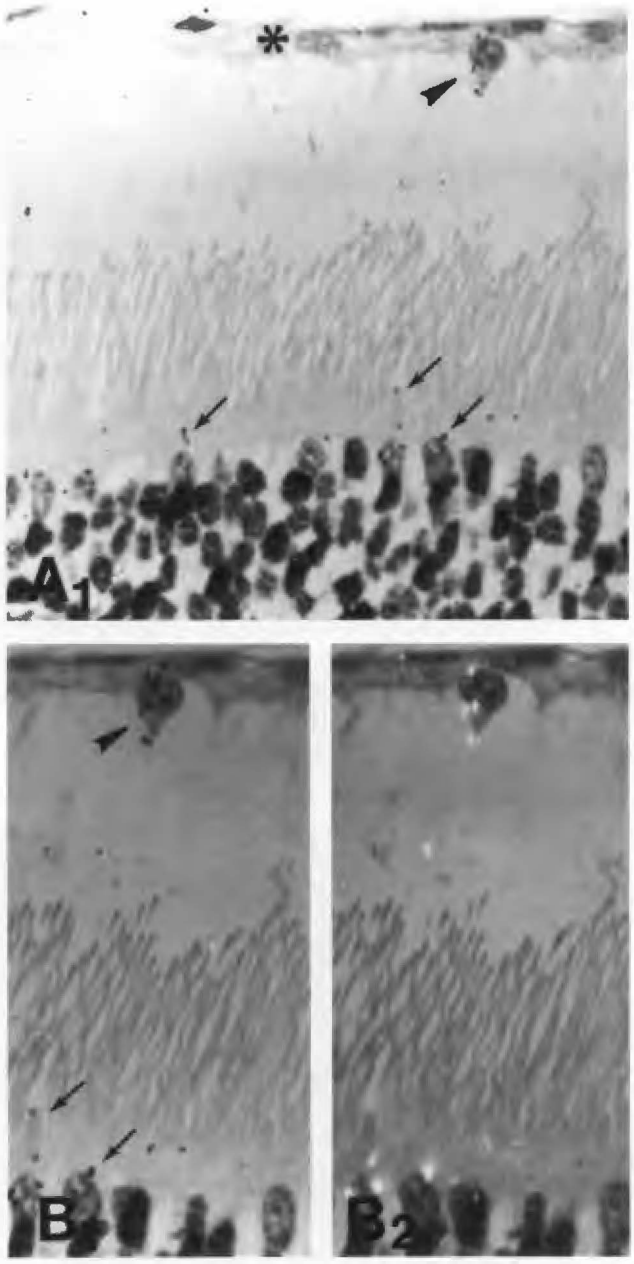

FIGURE 14-42. Brightfield (A_1, B_1) and combined brightfield/epipolarization (B_2) photomicrographs of the *cd* retina from a young affected dog hybridized with ^{3}H-labeled antisense human red/green cone opsin cRNA probe. The ectopically located cone nuclei *(arrowheads)* are located adjacent to the retinal pigment epithelium (A_1, *; see B_1 for higher magnification), and have an accumulation of silver grains in the perinuclear cytoplasm. The remaining cones in the photoreceptor layer *(arrows,* A_1, B_1) have silver grains that cluster in the perinuclear cytoplasm or the proximal inner segment. The intensity of the hybridization signal in all cones is normal. Magnifications: (A_1) ×800; (B_1) and (B_2) ×1000. (Reprinted from Gropp et al., 1996.)

nuclei are separated from the photoreceptor layer. However, in thicker sections (10 μm) reacted with peanut agglutinin (PNA) lectin to identify the extracellular cone matrix domains, some of the subretinal nuclei appear to be connected to the external limiting membrane, and, in some cases, form cellular aggregates in the subretinal space (Fig. 14-41—Long and Aguirre, 1991). Additionally, in situ hybridization using a red/green cone pigment cRNA probe indicates normal cone opsin gene expression (Fig. 14-42). Based on the presence of cone pigment mRNA transcripts, and immunoreactivity (using cone-specific antibodies) of intensity equal to that found in normally placed cone cells, we consider these ectopic cone nuclei viable (Gropp et al., 1996). With aging, there is progressive loss of cone nuclei from their normal position in the photoreceptor layer, and the oldest retina examined had the greatest number of ectopic cone nuclei located at the level of the RPE. Whether the ectopically located cone nuclei eventually degenerate or remain viable is not known at this time. However, their position adjacent to the RPE monolayer fails to elicit any histologically evident cellular response.

ACKNOWLEDGMENTS

The studies presented in this chapter have been supported in part by NIH grants EY-01244, -06855, -07705 and -11,142, DK-25759 and NS-33526, The Foundation Fighting Blindness, The Morris Animal Foundation, The Seeing Eye, Inc., the American Federation for Aging Research and the Starr Foundation.

REFERENCES

Acland GM, Aguirre GD. 1987. Retinal degenerations in the dog: IV. Early retinal degeneration *(erd)* in Norwegian elkhounds. Exp Eye Res 44:491–521.

Acland GM, Ray K, Aguirre GD. 1995. Exclusion of the cyclic GMP-PDE beta subunit gene as a candidate in the prcd-dog. Invest Ophthalmol Vis Sci 36:S891.

Acland G, Fletcher RT, Gentleman S, Chader G, Aguirre G. 1989. Non-allelism of three genes (*rcd* 1, *rcd* 2 and *erd*) for early-onset hereditary retinal degeneration. Exp Eye Res 49:983–998.

Acland G, Blanton SH, Hershfield B, Aguirre G. 1994. XLPRA: A canine retinal degeneration inherited as an x-linked trait. Am J Med Gen 52:27–33.

Aguirre GD. 1978. Retinal degenerations in the dog. L Rod dysplasia. Exp Eye Res 26:233–253.

Aguirre G. 1986. Phagocytic cells in the interphotoreceptor space: correlation with disease stage in canine progressive rod-cone degeneration. In: Agardh E, Ehinger B, eds, Retinal Signal Systems, Degenerations and Transplants. New York: Elsevier, 193–200.

Aguirre GD, Acland GM. 1988. Variation in retinal degeneration phenotype inherited at the *prcd* locus. Exp Eye Res 46:663–687.

Aguirre G, Acland G. 1991. Inherited retinal degeneration in the Labrador retriever dog. a new animal model of RP? Invest Ophthalmol Vis Sci 32(Suppl):889.

Aguirre GD, Laties A. 1976. Pigment epithelial dystrophy in the dog. Exp Eye Res 23:247–256.

Aguirre G, O'Brien P. 1986. Morphological and biochemical studies of canine progressive rod-cone degeneration: ^{3}H-fucose autoradiography. Invest Ophthal Vis Sci 27:635–655.

Aguirre GD, Rubin LF. 1974. Pathology of hemeralopia in the Alaskan malamute dog. Invest Ophthalmol 13:231–235.

Aguirre GD, Rubin LF. 1975. The electroretinogram in dogs with inherited cone degeneration. Invest Ophthalmol 14:840–847.

Aguirre GD, Rubin LF. 1979. Diseases of the retinal pigment epithelium in animals. In: Zinn K, Marmor M, eds, The Retinal Pigment Epithelium. Cambridge (MA): Harvard University Press; 334–356.

Aguirre G, Stramm L. 1991. The RPE: a model system for disease expression and disease correction. Prog Retinal Res 11:153–191.

Aguirre GD, Lolley R, Farber D, Fletcher T, Chader G. 1978. Rod-cone dysplasia in Irish setter dogs: a defect in cyclic GMP metabolism in visual cells. Science 201:1133–1134.

Aguirre G, Alligood J, O'Brien P, Buyukmihci N. 1982a. Pathogenesis of progressive rod-cone degeneration in miniature poodles. Invest Ophthal Vis Sci 23:610–630.

Aguirre G, Farber D, Lolley R, O'Brien P, Alligood J, Fletcher RT, Chader G. 1982b. Retinal degenerations in the dog: III. Abnormal cyclic nucleotide metabolism in rod-cone dysplasia. Exp Eye Res 35:625–642.

Aguirre G, Stramm L, Haskins, M. 1983. Feline mucopolysaccharidosis: VI. General ocular and pigment epithelial pathology. Invest Ophthal Vis Sci 24:991–1007.

Aguirre G, Stramm L, Haskins M, Jezyk P. 1986. Animal models of metabolic eye disease. In: Renie W, Goldberg M, eds, Goldberg's Genetic and Metabolic Eye Disease. Boston: Little, Brown 139–167.

Aguirre G, Raber I, Yanoff M, Haskins M. 1992. Reciprocal corneal transplantation fails to correct mucopolysaccharidosis VI corneal storage. Invest Ophthalm Vis Sci 33:2702–2713.

Aguirre G, Ray J, Pearce-Kelling S, Stramm L, Haskins M. 1995. Lysosomal α-mannosidase is essential for retinal pigment (RPE) degra-dative function. Invest Ophthal Vis Sci 36:S816.

Akle C, McColl I, Dean M, Adinolfi M, Brown S, Fensom A, Marsh J, Welsh K. 1985. Transplantation of amniotic epithelial membranes in patients with mucopolysaccharidoses. Expl Clin Immunogenet 2:43.

Akhmedov NB, Piriev NI, Ray K, Acland, GM, Aguirre GD, Farber DB. 1997. Structure and analysis of transducin β3-subunit, a candidate for inherited cone degeneration (*cd*) in the dog. Gene 194:47–56.

Alroy J, Bachrach A Jr, Thalhammer JC, Panjwani N, Richard R, DeGasperi R, Warren CD. 1991. Clinical, neurophysiological biochemical and morphological features of eyes in Persian cats with mannosidosis. Virchows Archiv B Cell Pathol 60:173–180.

Anderson R, Maude M, Alvarez R, Nilsson SE, Narfström K, Acland G, Aguirre G. 1991. Plasma lipid abnormalities in *prcd*-affected miniature poodles and Abyssinian cats. In: Hollyfield JG, Anderson RE, Lavail MM, eds, Degenerative Retinal Disorders: Clinical and Laboratory Investigations. Boca Raton, Fla.:CRC Press, 131–142.

Armentano D, Yu S-F, Kantoff PW, von Ruden T, Anderson WF, Gilboa E. 1987. Effect of internal viral sequences on the utility of retroviral vectors. J Virol 61:1647–1650.

Barbehenn E, Gagnon C, Noelker D, Aguirre G, Chader G. 1988. Inherited rod-cone dysplasia: abnormal distribution of cyclic GMP in visual cells of affected Irish setters. Exp Eye Res 46:149–159.

Barnett KC, Curtis R. 1985. Autosomal dominant progressive retinal atrophy in Abyssinian cats. J Hered 76:168–170.

Barnett KC, Heywood R, Hague P. 1972. Colloid degeneration of the retina in a baboon. J Comp Pathol 82:117–118.

Bedford PGC. 1984. Retinal pigment epithelial dystrophy (CPRA): a study of the disease in the briard. J Small Anim Pract 25:129–138.

Bellairs R, Harkness LR, Harkness RD. 1975. The structure of the tapetum in the eye of the sheep. Cell Tiss Res 157:73.

Bellhorn RW, Bellhorn MB, Swarm RL, Impellizzeri CW. 1975. Hereditary tapetal abnormality in the beagle. Ophthal Res 7:250–260.

Bellhorn RW, King CD, Aguirre GD, Ripps H, Siegel IM, Tsai HC. 1981. Pigmentary abnormalities of the macula in rhesus monkeys: clinical observations. Invest Ophthalmol Vis Sci 21(6):771–781.

Bernstein MH, Pease DC. 1959. Electron microscopy of the tapetum lucidum of the cat. J Biophys Biochem Cytol 5:35–53.

Berson EL, Rosner B, Sandberg MA, Dryja TP. 1991. Ocular findings in patients with autosomal dominant retinitis pigmentosa and a rhodopsin gene defect (PRO-23-HIS). Arch Ophthalmol 109:92–101.

Berson EL, Watson G. 1980. Electroretinograms in English setters with neuronal ceroid lipofuscinosis. Invest Ophthalmol Vis Sci 19: 87–89.

Boulton M, Moriarty P, Jarvis-Evans J, Marcyniuk B. 1994. Regional variation and age-related changes of lysosomal enzymes in the human retinal pigment epithelium. Br J Ophthalmol 78:125–129.

Bowes C, Li T, Danciger M, Baxter LC, Applebury ML, Farber DB. 1990. Retinal degeneration in the *rd* mouse is caused by a defect in the β subunit of rod cGMP-phosphodiesterase. Nature 347:677–680.

Bowes C, Li T, Frankel WN, Danciger M, Coffin JM, Applebury ML, Farber DB. 1993. Localization of a retroviral element within the *rd* gene coding for the beta subunit of cGMP phosphodiesterase. Proc Nat Acad Sci USA 90:2955–2959.

Budinger JM. 1961. Diphenylthiocarbazone blindness in dogs. Arch Pathol 71:304.

Burke J, Twining S. 1988. Regional comparisons of cathepsin D activity in bovine retinal pigment epithelium. Invest Ophthalmol Vis Sci 29:1789–1793.

Burkhardt JK, Wiebel FA, Hester S, Argon Y. 1993. The giant organelles in beige and Chediak-Higashi fibroblasts are derived from late endosomes and mature lysosomes. J Exp Med 178:1845–1856.

Burns MS, Bellhorn RW, Impellizzeri CW, Aguirre GD, Laties AM. 1988. Development of hereditary tapetal degeneration in the beagle dog. Curr Eye Res 7:103–114.

Bussow H. 1980. The tapetal cell: a unique melanocyte in the tapetum lucidum cellulosum of the cat (Felis domestica L): an electron microscopic, cytochemical and chemical study. Anat Embryol 158:289–302.

Butturini U, Grignolo A, Baronchelli A. 1953. "Diabete" da ditizone aspetti metabolici oculari ed istologici. G Clin Med 34:1253–1347.

Cabral L, Unger W, Boulton M, Lightfoot R, McKechnie N, Grierson I, Marshall J. 1990. Regional distribution of lysosomal enzymes in the canine retinal pigment epithelium. Invest Ophthalmol Vis Sci 31:670–676.

Chader GJ. 1991. Animal mutants of hereditary retinal degeneration: General considerations and studies on defects in cyclic nucleotide metabolism. Prog Vet Comp Ophthalmol 1:109–126.

Chader GJ, Fletcher RT, Sanyal S, Aguirre G. 1985. A review of the role of cyclic GMP in neurological mutants with photoreceptor dysplasia. Curr Eye Res 4:811–819.

Chang GQ, Hao Y, Wong F. 1993. Apoptosis: final common pathway of photoreceptor death in *rd, rds,* and rhodopsin mutant mice. Neuron 11:595–605.

Clements PJM, Gregory CY, Petersoe-Jones SM, Sargan DR, Bhattacharya SS. 1993. Confirmation of the rod cGMP phosphodiesterase β subunit (PDEβ) nonsense mutation in affected rcd-1 Irish setters in the UK and development of a diagnostic test. Curr Eye Res 12:861–866.

Cloyd GG, Wyman M, Shadduck JA, Winrow MJ, Johnson GR. 1978. Ocular toxicity srudies with zinc pyridinethione. Toxicol Appl Pharmacol 45:771–782.

Collier LL, Prieur DJ, King EJ. 1984. Ocular melanin pigmentation anomalies in cats, cattle, mink, and mice with Chediak-Higashi syndrome: histologic observations. Curr Eye Res 3:1241–1251.

Collier LL, King EJ, Prieur DJ. 1985a. Tapetal degeneration in cats with Chediak-Higashi syndrome. Curr Eye Res 4:767–773.

Collier LL, King EJ, Prieur DJ. 1985b. Aberrant melanosome development in the retinal pigmented epithelium of cats with Chediak-Higashi syndrome. Exp Eye Res 41:305–311.

Collier LL, King EJ, Prieur DJ. 1986. Age-related changes of the retinal pigment epithelium of cats with Chediak-Higashi syndrome. Invest Ophthalmol Vis Sci 27:702–707.

Cummings JF, DeLahunta A, George C, Fuhrer L, Valentine BA, Cooper BJ, Summers BA, Huxtable CR, Mohammed HO. 1990. Equine motor neuron disease. Cornell Vet 80:357–379.

Cummings JF, DeLahunta A, Mohammed HO, Divers TJ, Summers BA, Valentine BA, Jackson CA. 1995. Endothelial lipopigment as an indicator of α-tocopherol deficiency in two equine neurodegenerative diseases. Acta Neuropathol 90:262–272.

Cummings JF, DeLahunta A, Mohammed HO, Divers TJ. In press. The histopathology of equine motor neuron disease (ENMD). Equine Vet J.

Curtis R, Barnett KC, Leon A. 1987. An early-onset retinal dystrophy with dominant inheritance in the Abyssinian cat. Invest Ophthalmol Vis Sci 28:131–139.

Dawson WW, Engel HM, Hope GM, Kessler MJ, Ulshaffer RJ. 1989. Adult-onset macular degeneration in the Cayo Santiago macaques. PR Health Sci J 8:111–115.

DeGasperi R, Daher SA, Daniel PF, Winchester BG, Jeanloz RW, Warren CD. 1991. The substrate specificity of bovine and feline lysosomal alpha-D-mannosidases in relation to alpha-mannosidosis. J Biol Chem 266:16556–16563.

Divers TJ, Mohammed HO, Cummings JF, Valentine BA, deLahunta A, Jackson CA, Summers BA. 1994. Equine motor neuron disease: findings in twenty-eight horses and proposal of a pathophysiological mechanism for the disease. Equine Vet J 26:409–415.

Dorey C, Wu G, Ebenstein D, Garsd A, Weiter J. 1989. Cell loss in the aging retina: relationship to lipofuscin accumulation and macular degeneration. Invest Ophthalmol Vis Sci 30:1691–1699.

Dryja TP, Li T. 1995. Molecular genetics of retinitis pigmentosa. Hum Mol Genet 4:1739–1743.

Dryja TP, Berson EL, Rao VR, Oprian DD. 1993. Heterozygous missense mutation in the rhodopsin gene as a cause of congenital stationary night blindness. Nat Genet 4:280–283.

Dryja TP, Finn JT, Peng YW, McGee TL, Berson EL, Yau KW. 1995. Mutations in the gene encoding the α subunit of the rod cGMP-gated channel in autosomal recessive retinitis pigmentosa. Proc Natl Acad Sci USA 92:10177–10181.

Edwards RB, Szamier RB. 1977. Defective phagocytes of isolated rod outer segments by RCS rat retinal pigment epithelium in culture. Science 197:1001–1003.

El Baba FE, Green WR, Fleischmann J, Finkelstein D. 1986. Clinicopathologic correlation of lipidization and detachment of the retinal pigment epithelium. Am J Ophthalmol 101:576–583.

El-Mofry A, Gouras P, Eisner G, Balazs EA. 1978. Macular degeneration in rhesus monkey (Macaca mulatta). Exp Eye Res 27:499.

El-Mofty AAM, Eisner G, Balazs EA, Denlinger JL, Gouras P. 1980. Retinal degeneration in rhesus monkeys, Macaca mulatta: survey of three seminatural free-breeding colonies. Exp Eye Res 31:146–166.

Engel HM, Dawson WW, Ulshafer RJ, Hines MW, Kessler MJ. 1988. Degenerative changes in maculas of rhesus monkeys. Ophthalmologica 196:143–150.

Falls HF, Wolter JR, Alpern M. 1965. Typical total monochromacy: a histological and psychophysical study. Arch Ophthal 74:610–616.

Farber DB, Lolley RN. 1974. Cyclic guanosine monophosphate: Elevation in degenerating photoreceptor cells of the C3H mouse retina. Science 186:449–451.

Farber DB, Danciger JS, Aguirre G. 1990. Early mRNA defect in Irish setter dog retina. Invest Ophthalmol Vis Sci (Supp). 31:310.

Farber D, Danciger JS, Aguirre G. 1992. The β-subunit of cyclic GMP phosphodiesterase is deficient in canine rod-cone dysplasia 1. Neuron 9:349–356.

Feeney-Burns L, Ellersieck MR. 1985. Age-related changes in the ultrastructure of Bruch's membrane. Am J Ophthalmol 100:686–697.

Feeney-Burns L, et al. 1981. Maculopathy in cynomolgus monkeys: a correlated fluorescein angiographic and ultrastructural study. Arch Ophthalmol 99:664–672.

Feeney-Burns L, Hilderbrand ES, Eldridge S. 1984. Aging human RPE: morphometric analysis of macular, equatorial and peripheral cells. Invest Ophthalmol Vis Sci 25(1):195–200.

Fine BS. 1981. Lipoidal degeneration of the retinal pigment epithelium. Am J Ophthalmol 91:469–473.

Fine BS, Kwapien RP. 1978. Pigment epithelial windows and drusen: an animal model. Invest Ophthalmol Vis Sci 17:1059.

Fishman GA, Stone EM, Gilbert LD, Sheffield VC. 1992. Ocular findings associated with a rhodopsin gene codon 106 mutation: glycine-to-arginine change in autosomal dominant retinitis pigmentosa. Arch Opthhalm 110:646–653.

Fratantoni J, Hall C, Neufeld E. 1968. Hurler and Hunter syndromes: mutual correction of the defect in cultured fibroblasts. Science 612: 500.

Gao H, Hollyfield JG. 1992. Aging of the human retina. Invest Ophthalmol Vis Sci 33(1):1–17.

Gasper PW, Thrall MA, Wenger DA, Macy DW, Ham L, Dornsife RE, McBiles K, Quackenbush SL, Kesel ML, Gillette EL, Hoover EL. 1984. Correction of feline arylsulfatase B deficiency (mucopolysaccharidosis VI) by bone marrow transplantation. Nature 312:467–469.

Gorin MB, To AC, Narfström K. 1995. Sequence analysis and exclusion of phosducin as the gene for the recessive retinal degeneration of the Abyssinian cat. Bioch Biophys Acta 1260:323–327.

Gorin MB, Snyder S, Narfstrom K, Curtis R. 1993. The cat RDS transcript: candidate gene analysis and phylogenetic sequence analysis. Mamm Genome 4:544–548.

Graydon RJ, Jolly RD. 1984. Ceroid-lipofuscinosis (Batten's disease): sequential electrophysiologic and pathologic changes in the retina of the ovine model. Invest Ophthalmol Vis Sci 25:294–301.

Gropp KE, Szél A, Huang JC, Acland GM, Farber DB, Aguirre GD. Selective absence of cone outer segment β_3-transducin immunoreactivity in hereditary cone degeneration (*cd*). Exp Eye Res 63:285–296.

Hageman GS, Johnson LV. 1991. Structure, composition and function of the retinal interphotoreceptor matrix. In: Osborne N, Chader GJ, eds, Progress in Retinal Research, vol. 10 Oxford: Pergamon Press.

Harrison R, Hoefnagel D, Hayward JN. 1960. Congenital total color blindness: a clinicopathological report. Arch Ophthalmol 64:685–692.

Haskins M, Baker H, Birkenmeier E, Hoogerbrugge P, Poorthuis B, Sakiyama T, Shull R, Taylor R, Thrall M, Walkley S. 1991. Transplantation in animal model systems. In: Desnick R, ed, Therapy of Genetic Disease. New York: Churchill Livingston.

Haskins M, Chieffo C, WangP, Just C, Evans S, Aguirre G. 1992. Bone marrow transplantation in canine mucopolysaccharidosis VII (beta-glucuronidase deficiency). Am J Hum Genet 49:435.

Hayasaka S. 1974. Distribution of lysosomal enzymes in the bovine eye. Jpn J Ophthalmol 18:233–239.

Hayes KC, Rousseau JE, Hegsted DM. 1970. Plasma tocopherol concentrations and vitamin E deficiency in dogs. J Am Vet Med Assoc 157(1):64–71.

Heckenlively JR, Rodriguez JA, Daiger SP. 1991. Autosomal dominant sectoral retinitis pigmentosa: two families with transversion mutation in codon 23 of rhodopsin. Arch Ophthalmol 109:84–91.

Herron WL, Riegel BW, Myers OE, Rubin ML. 1969. Retinal dystrophy in the rat—a pigment epithelial disease. Invest Ophthal 8:595–604.

Huang J, Mieziewska K, Philp N, van Veen T, Aguirre G. 1993. Diethylene glycol distearate (DGD): a versatile embedding medium for retinal cytochemistry. J Neurosci Meth 47:227–234.

Huang J, Chesselet M-F, Aguirre G. 1994. Decreased opsin mRNA and immunoreactivity in progressive rod-cone degeneration (*prcd*): Cytochemical studies of early disease and degeneration. Exp Eye Res 58:17–30.

Huang SH, Pittler SJ, Huang X, Oliveira L, Berson EL, Dryja TP. 1995. Autosomal recessive retinitis pigmentosa caused by mutations in the α subunit of rod cGMP phosphodiesterase. Nature Genetics 11:468–471.

Humphries P, Kenna P, Farrar GJ. 1992. On the molecular genetics of retinitis pigmentosa. Science 256:804–808.

Ishibashi T, Sorgente N, Patterson R, Ryan SJ. 1986. Pathogenesis of drusen in the primate. Invest Ophthalmol Vis Sci 27:184–193.

Jacobson SG, Kemp CM, Narfstrom K, Nilsson SE. 1989. Rhodopsin levels and rod-mediated function in Abyssinian cats with hereditary retinal degeneration. Exp Eye Res 49:843–852.

Jolly RD, Palmer DN. 1995. The neuronal ceroid-lipofuscinoses (Batten disease): comparative aspects. Neuropathol Appl Neurobiol 21:50–60.

Jolly RD, Shimada A, Dalefield RR, Slack PM. 1987. Mannosidosis: ocular lesions in the bovine model. Curr Eye Res 6:1073–1079.

Jolly RD, Gibson AJ, Healy PJ, Slack PM, Birtles MJ. 1992. Bovine ceroid-lipofuscinosis: pathology of blindness. New Zealand Vet J 40:107–111.

Jolly RD, Palmer DN, Studdert VP, Sutton RH, Kelly WR, Koppang N, Dahme G, Hartley WJ, Patterson JS, Riis RC. 1994. Canine ceroid-lipofuscinoses: a review and classification. J Sm Anim Pract 35:299–306.

Kaiser JA. 1963. Tapetal depigmentation in dogs produced by ethylenediamines. Fed Proc 22:369.

Kajiwara K, Berson EL, Dryja TP. 1994. Digenic retinitis pigmentosa due to mutations at the unlinked peripherin/RDS and ROM1 loci Science 264:1604–1608.

Kajiwara K, Hahn LB, Mukai S, Travis GH, Berson EL, Dryja TP. 1991. Mutations in the human retinal degeneration slow gene in autosomal dominant retinitis pigmentosa. Nature 354:480–484.

Koppang N. 1992. English setter model of neuronal ceroid-lipofuscinosis in man. Am J Med Genet 42:599–604.

Krivit W, et al. 1984. Bone-marrow transplantation in the Maroteaux-Lamy syndrome (mucopolysaccharidosis type VI). New Eng J Med 311:1606–1611.

Kyle JW, Birkenmeier EH, Gwynn B, Vogler C, Hoppe PC, Hoffman JW, Sly WS. 1990. Correction of murine mucopolysaccharidosis VII by a human B-glucuronidase transgene. Proc Nat Acad Sci USA. 87:3914–3918.

Lai Y-L. 1980. Outward movement of photoreceptor cells in normal rat retina. Invest Ophthalmol Vis Sci 19:849–856.

Lai Y-L, Jacoby RO, Jonas AM. 1978. Age-related and light-associat-

ed retinal changes in Fischer rats. Invest Ophthalmol Vis Sci 17:634–638.

Lai Y-L, Masuda K, Mangum RL, Macrae DW, Fletcher G, Yung-Pin L. 1982. Subretinal displacement of photoreceptor nuclei in human retina. Exp Eye Res 34:219–228.

Landers RA, Tawara A, Varner HH, Hollyfield JG. 1991. Proteoglycans in the mouse interphotoreceptor matrix. IV. Retinal synthesis of chondroitin sulfate proteoglycan. Exp Eye Res 52:65–74.

Larsen H. 1921. Demonstration mikroskopischer Präparate von einem monochromatischen Auge. Z Augenheilkunde 46:228–229.

LaVail MM. 1980. Degenerate retinal disorders: interaction of environmental light and pigmentation with inherited retinal degenerations. Vision Res 20:1172–1177.

LaVail MM, Battelle B. 1975. Influence of eye pigmentation and light deprivation on inherited retinal dystrophy in the rat. Exp Eye Res 21:167–192.

LaVail MM, Pinto LH, Yasumura D. 1981. The interphotoreceptor matrix in rats with inherited retinal dystrophy. Invest Ophthalmol Vis Sci 21:658–668.

Lazarus HS, Sly WS, Kyle JW, Hageman GS. 1993. Photoreceptor degeneration and altered distribution of interphotoreceptor matrix proteoglycans in the mucopolysaccharidosis VII mouse. Exp Eye Res 56:531–541.

Leon A, Curtis R. 1990. Autosomal dominant rod-cone dystrophy in the *rdy* cat. 1. Light and electron microscopic findings. Exp Eye Res 51:361–381.

Leon A, Hussain AA, Curtis R. 1988. Rod-cone dysplasia in the *rdy* cat: electrophysiology and biochemistry. Invest Ophthalm Vis Sci 29(suppl):143.

Li T, Davidson B. 1995. Phenotype correction in retinal pigment epithelium in murine mucopolysaccharidosis VII by adenovirus-mediated gene transfer. Proc Nat Acad Sci USA 92:7700–7704.

Li L, Turner JE. 1988. Inherited retinal dystrophy in the RCS rat: prevention of photoreceptor degeneration by pigment epithelial cell transplantion. Exp Eye Res 47:911–917.

Lightfoot, RM. 1988. Retinal pigment epithelial dystrophy in the dog. PhD dissertation. University of London.

Long KO, Haskins ME, Aguirre GD. 1989. Photoreceptor-RPE interface in β-glucuronidase deficiency: an anatomical and immunocytochemical study. Invest Ophthalmol Vis Sci 30(suppl):3.

Long K, Aguirre G. 1991. The cone matrix sheath in the normal and diseased retina. Exp Eye Res 52:699–713.

Maréchal V, Naffakh N, Danos O, Heard JM. 1993. Disappearance of lysosomal storage in spleen and liver of mucopolysaccharidosis VII mice after transplantation of genetically modified bone marrow cells. Blood 82:1358–1365.

Massa T, Davis GJ, Schiavo D, Sinha DP, Szot RJ, Black HE, Schwartz E. 1984. Tapetal changes in beagle dogs. II. Ocular changes after intravenous administration of a macrolid antibiotic rosaramicin. Toxicol Appl Pharmacol 72:195–200.

McLaughlin ME, Sandberg MA, Berson EL, Dryja TP. 1993. Recessive mutations in the gene encoding the β-subunit of rod phosphodiesterase in patients with retinitis pigmentosa. Nat Genet 4:130–134.

McLaughlin ME, Ehrhart TL, Berson EL, Dryja TP. 1995. Mutation spectrum of the gene encoding the β subunit of rod phosphodiesterase among patients with autosomal recessive retinitis pigmentosa. Proc Nat Acad Sci USA 92:3249–3253.

Mieziewska K. 1993. The interphotoreceptor matrix: a study of structure and composition in normal and degenerating retinas. PhD dissertation. University of Göteborg, Faculty of Natural Sciences.

Mieziewska K, van Veen T, Murray J, Aguirre G. 1991. Rod and cone specific domains in the interphotoreceptor matrix. J Comp Neurol 308:371–380.

Miewziewska K, van Veen T, Aguirre G. 1993a. Development and fate of interphotoreceptor matrix components during dysplastic photoreceptor differentiation: a lectin cytochemical study of rod-cone dysplasia 1. Exp Eye Res 56:429–441.

Mieziewska K, van Veen T, Aguirre G. 1993b. Structural changes of the interphotoreceptor matrix in an inherited retinal degeneration: A lectin cytochemical study of progressive rod-cone degeneration (*prcd*). Inv Ophthalm Vis Sci 34:3056–3066.

Miller AD, Buttimore C. 1986. Redesign of retrovirus packaging cell lines to avoid recombination leading to helper virus production. Mol Cell Biol 6:2895–2902.

Moullier P, Bohl D, Heard J-M, Danos O. 1993. Correction of lysosomal storage in the liver and spleen of MPS VII mice by implantation of genetically modified skin fibroblasts. Nat Genet 4:154–159.

Mullen RJ, LaVail MM. 1976. Inherited retinal dystrophy: primary defect in pigment epithelium determined with experimental rat chimeras. Science 192:799–801.

Nakaizumi Y. 1964. The ultrastructure of Bruch's membrane. II. Eyes with a tapetum. Arch Ophthalmol 77:388–394.

Narfström K. 1983. Hereditary progressive retinal atrophy in the Abyssinian cat. J Hered 74:273–276.

Narfström K, Nilsson SE. 1986. Progressive retinal atrophy in the Abyssinian cat. Invest Ophthalmol Vis Sci 27:1569–1576.

Narfström K, Nilsson SE. 1989. Morphological findings during retinal development and maturation in hereditary rod-cone degeneration in Abyssinian cats. Exp Eye Res 49:611–628.

Narfström KL, Nilsson SE, Andersson BE. 1985. Progressive retinal atrophy in the Abyssinian cat: studies of the DC-recorded electroretinogram and the standing potential of the eye. Br J Ophthalmol 69:618–623.

Narfström K, Wilen M, Andersson BE. 1988. Hereditary retinal degeneration in the Abyssinian cat: developmental studies using clinical electroretinography. Doc Ophthalmol 69(2):111–118.

Narfström K, Nilsson SE, Wiggert B, Lee L, Chader GJ, van Veen T. 1989. Reduced level of interphotoreceptor retinoid binding protein (IRBP) a possible cause for retinal degeneration in the Abyssinian cat. Cell Tissue Res 257:631–639.

Narfström K, Wrigstad A, Nilsson SEG. 1989. The Briard dog: a new animal model of congenital stationary night blindness. Br J Ophthalmol 73:750–756.

Narfström K, Wrigstad A, Ekesten B, Nilsson SEG. 1994. Hereditary retinal dystrophy in the Briard dog: clinical and hereditary characteristics. Vet Comp Ophthalmol 4(2):85–92.

Neville H, Armstrong D, Wilson B, Koppang N, Wehling C. 1980. Studies on the retina and the pigment epithelium in hereditary canine ceroid lipofuscinosis III. Morphologic abnormalities in retinal neurons and retinal pigmented epithelial cells. Invest Ophthalmol Vis Sci 19:75–86.

Nicolas MG, Fujiki K, Murayama K, Suzuki MT, Mineki R, Hayakawa M, Yoshikawa Y, Cho F, Kanai A. 1996. Studies on the mechanism of early onset macular degeneration in cynomolgus (Macaca fascicularis) monkeys. I. Abnormal concentrations of two proteins in the retina. Exp Eye Res 62:211–219.

Nilsson SEG, Armstrong D, Koppang N, Persson P, Milde K. 1983. Studies on the retina and the pigment epithelium in hereditary canine ceroid lipofuscinosis. IV: Changes in the electroretinogram and the standing potential of the eye. Invest Ophthalmol Vis Sci 24:77–84.

Nilsson SEG, Wrigstad A, Narfström K. 1992. Changes in the DC electroretinogram in briard dogs with hereditary congenital night blindness and partial day blindness. Exp Eye Res 54:291–296.

Nishimura Y, Rosenfeld MG, Kreibich G, Gubler U, Sabatini DD, Adesnik M, Andy R. 1986. Nucleotide sequence of rat preputial gland β-glucuronidase cDNA and in vitro insertion of its encoded

polypeptide into microsomal membranes. Proc Nat Acad Sci USA 83:7292–7296.

Parry HB. 1954. Degenerations of the dog retina VI. Central progressive atrophy with pigment epithelial dystrophy. Br J Ophthal 38:653–668.

Parshall C, Wyman M, Nitroy S, Acland G, Aguirre G. 1991. Photoreceptor dysplasia: an inherited progressive retinal atrophy of miniature schnauzer dogs. Prog Vet Comp Ophtholmol 1:187.

Perou CM, Kaplan J. 1993. Complementation analysis of Chediak-Higashi syndrome: the same gene may be responsible for the defect in all patients and species. Somat Cell Mol Genet 19:459–468.

Pirie A. 1966. Chemistry and structure of the tapetum lucidum. In: Graham-Jones O, ed, Aspects of Comparative Ophthalmology. London: Pergamon Press, 57–68.

Pittler SJ, Baehr W. 1991. Identification of a nonsense mutation in the rod photoreceptor cGMP phosphodiesterase β-subunit gene of the rd mouse. Proc Nat Acad Sci USA 88:8322–8326.

Porrello K, Yasumura D, LaVail MM. 1986. The interphotoreceptor matrix in RCS rats: histochemical analysis and correlation with the rate of retinal degeneration. Exp Eye Res 43:413–429.

Portera-Cailliau C, Sung C-H, Nathans J, Adler R. 1994. Apoptotic photoreceptor cell death in mouse models of retinitis pigmentosa. Proc Nat Acad Sci USA 91:974–978.

Prince JH, Diesem CD, Eglitis I, Ruskell GL. 1960. Anatomy and Histology of the Eye and Orbit in Domestic Animals. Springfield, Charles C. Thomas, page 219.

Ray J, Wolfe J, Haskins M, Aguirre G. 1992. Specificity of β-glucuronidase cDNA to correct inherited defects of the lysosomal system in the RPE. Invest Ophthalmol Vis Sci 33(suppl):909.

Ray J, Wu Y, Haskins M, Salvetti A, Heard JM, Aguirre G. 1995. Enhanced degradation of accumulating GAGs in MPS VI-affected retinal pigment epithelium by arylsulfatase B cDNA transfer. Inv Ophthalmol Vis Sci 36(suppl):S918.

Ray J, DeSanto CM, Sun W, Haskins M, Aguirre G. 1996. Studies on the molecular basis of β-glucuronidase deficiency in mucopolysaccharidosis VII (MPS VII) in the retinal pigment epithelium. Invest Ophthalmol Vis Sci (suppl) 37:5379.

Ray J, Wu Y, Aguirre GD. 1997. Characterization of β-glucuronidase in the retinal pigment epithelium. Curr. Eye Res. 16:131–143.

Ray K, Baldwin V, Acland G, Blanton S, Aguirre G. 1994. Co-segregation of codon 807 mutation of the rod cGMP phosphodiesterase β gene (PDEB) in *rcd1*. Invest Ophthalmol Vis Sci 35:4291–4299.

Ray K, Baldwin V, Acland G, Aguirre G. 1995. Molecular diagnostic tests for ascertainment of genotype at the rod cone dysplasia 1 (rcd1) locus in Irish setters. Curr Eye Res 14:243–247.

Ray K, Acland GM, Aguirre GD. 1996. Nonallelism of *erd* and *prcd* and exclusion of the canine RDS/peripherin gene as a candidate for both retinal degeneration loci. Inv Ophthalm Vis Sci 37:783–794.

Ray K, Baldwin VJ, Zeiss C, Acland GM, Aguirre GD. In press. Canine rod transducin α-1: cloning of the cDNA and evaluation of the gene as a candidate for progressive retinal atrophy. Curr Eye Res 16:71–77.

Riis RC, Sheffy BE, Loew E, Kern TJ, Smith JS. 1981. Vitamin E deficiency retinopathy in dogs. Am J Vet Res 42:74–86.

Riis RC, Cummings JF, Loew ER, de Lahunta A. 1992. Tibetan terrier model of canine ceroid lipofuscinosis. Am J Med Gen 42:615–621.

Riis RC, Rebhun WC, Jackson CA, Loew E, Katz ML, Cummings JF, Mohammed HO, Divers TJ, deLahunta A, Valentine BA. 1995, Fundic lesions in horses affected with equine motor neuron disease. Proc Am Coll Vet Ophthalm 43.

Roque RS, Imperial CJ, Caldwell R. 1996. Microglial cells invade the outer retina as photoreceptors degenerate in Royal College of Surgeons rats. Invest Ophthalmol Vis Sci 37:196–203.

Rosenzweig M, Giger U, Metzler J, Valle DL, Aguirre G. 1990. Ornithine aminotransferase deficiency in a domestic short hair cat. J Vet Int Med 4:116.

Rubin LF, Lipton DE. 1973. Retinal degeneration in kittens. J Am Vet Med Assoc 162:467–469.

Rushton A, Dawson G. 1977. The effect of glycosaminoglycans on the in vitro activity of human skin fibroblast glycosphingolipid B-galactosidases and neuraminidases. Clin Chim Acta 80:133–139.

Sands MS, Barker JE, Vogler C, Levy B, Gwynn B, Galvin N, Sly WS, Birkenmeier E. 1993. Treatment of murine mucopolysaccharidosis type VII by syngeneic bone marrow transplantation in neonates. Lab Invest 68:676–686.

Santos-Anderson RM, Tso MOM, Vainisi SJ. 1983. Heredofamiliar retinal dystrophy in Guinea baboons. II. Electron microscopic observations. Arch Ophthalmol 101:1762–1770.

Schiavo DM, Sinha DP, Black HE, Arthaud L, Massa T, Murphy BF, Szot RJ, Schwartz E. 1984. Tapetal changes in beagles dogs. I. Ocular changes after oral administration of a beta-adrenergenic blocking agent, SCH 19927. Toxicol Appl Pharmacol 72:187–194.

Schiavo DM, Green JD, Traina VM, Spaet R, Zaidi I. 1988. Tapetal changes in beagle dogs following oral administration of CGS 14796C, a potential aromatase inhibitor. Fundam Appl Toxicol 10: 329–334.

Schmidt SY, Aguirre GD. 1985. Reductions in taurine secondary to photoreceptor loss in Irish setters with rod-cone dysplasia. Invest Ophthalmol Vis Sci 26:679.

Smith RIE, Sutton RH, Jolly RD, Smith KR. 1996. A retinal degeneration associated with ceroid-lipofuscinosis in adult miniature schnauzers. Vet Comp Ophthalmol 6:187–191.

Stafford TJ. 1974. Maculopathy in an elderly sub-human primate. Mod Probl Ophthal 12:214–219.

Stramm LE, Haskins ME, McGovern M, Aguirre G. 1983. Tissue culture of cat retinal pigment epithelium. Exp Eye Res 36:91–101.

Stramm L, Haskins M, Desnick RJ, Aguirre G. 1985. Disease expression in cultured pigment epithelium: feline mucopolysaccharidosis VI. Invest Ophthalmol Vis Sci 26:182.

Stramm LE, Desnick RJ, Haskins ME, Aguirre GD. 1986. Arylsulfatase B activity in cultured retinal pigment epithelium: regional studies in feline mucopolysaccharidosis VI. Invest Ophthalmol Vis Sci 27:1050.

Stramm LE, Haskins ME, Aguirre GD. 1989. Retinal pigment epithelial glycosaminoglycan metabolism: intracellular versus extracellular pathways. Invest Ophthalmol Vis Sci 30:2118.

Stramm L, Wolfe J, Schuchman E, Haskins M, Patterson DF, Aguirre G. 1990. β-glucuronidase mediated pathway essential for retinal pigment epithelial degradation of glycosaminoglycans. Disease expression and in vitro disease correction using retroviral mediated cDNA transfer. Exp Eye Res 50:521–532.

Suber ML, Pittler SJ, Qin N, Wright GC, Holcombe V, Lee RH, Craft CM, Lolley RN, Baehr W, Hurwitz RL. 1993. Irish setter dogs affected with rod/cone dysplasia contain a nonsense mutation in the rod cGMP phosphodiesterase β-subunit gene. Proc Nat Acad Sci USA 90:3968–3972.

Summers G, Purple R, Krivit W, Pineda R, Copland G, Ramsay N, Kersey J, Whitley C. 1989. Ocular changes in the mucopolysaccharidoses after bone marrow transplantation. Ophthalmol 96:977.

Tamai M, O'Brien PJ. 1979. Retinal dystrophy in the RCS rat: in vivo and in vitro studies of phagocytic action of the pigment epithelium on the shed rod outer segments. Exp Eye Res 28:399–411.

Travis GH, Brennan MB, Danielson PE, Kozak CA, Sutcliffe JG. 1989. Identification of a photoreceptor-specific mRNA encoded by the gene responsible for retinal degeneration slow (*rds*). Nature 338:70–73.

Tso MOM, Santos-Anderson RM, Vanisi SJ. 1983. Heredofamilial

retinal dystrophy in Guinea baboons. I. A histopathologic Study. Arch Ophthalmol 101(10):1597–1603.

Vainisi S, Beck B, Apple D. 1974. Retinal degeneration in a baboon. Am J Ophthalmol 78(2):279–284.

Valle D, Boison A, Jezyk P, Aguirre G. 1981. Gyrate atrophy of the choroid and retina in a cat. Invest Ophthalmol Vis Sci 20:251.

Valle D, Jezyk P, Aguirre G. 1983. Gyrate atrophy of the choroid and retina. Comp Pathol Bull 15:2.

Vesa J, Hellsten E, Verkruyse LA, Camp LA, Rapola J, Santavuori P, Hofmann SL, Peltonen L. 1995. Mutations in the palmitoyl protein thioesterase gene causing infantile neuronal ceroid lipofuscinosis. Nature 376:584–587.

Vine D, McGovern M, Schuchman E, Haskins M, Desnick R. 1982. Enhancement of residual arylsulfatase B activity in feline mucopolysaccharidosis VI by thiol-induced subunit association. J Clin Invest 69:294.

Vogel M. 1978. Postnatal development of the cat's retina. Adv Anat Embryol Cell Biol 54(4):7–66.

Vogel AW, Kaiser JA. 1963. Ethambutol induces transient change and reconstruction (in vivo) of the tapetum lucidum color in the dog. Exp Mol Pathol 2(suppl):136–149.

Walkley SU, Thrall MA, Dobrenis K, Huang M, March PA, Siegel DA, Wurzelmann S. 1994. Bone marrow transplantation corrects the enzyme defect in neurons of the central nervous system in a lysosomal storage disease. Proc Nat Acad Sci USA 91:2970–2974.

Wang W, Acland GM, Aguirre GD, Ray K. 1995. Exclusion of rhodopsin, and probable exclusion of rds/peripherin, as candidates for canine progressive rod cone degeneration (*prcd*). Invest Ophthalmol Vis Sci 36(suppl):S772.

Watson P, Bedford PGC. 1992. The pigments of retinal pigment epithelial dystrophy in dogs. Vet Pathol 29:5.

Watson P, Simson, KW, Bedford, PGC. 1993. Hypercholesterolaemia in briards in the United Kingdom. Res Vet Sci 54:80–85.

Weleber RG, Carr RE, Murphey WH, Sheffield VC, Stone EM. 1993. Phenotypic variation including retinitis pigmentosa, pattern dystrophy, and fundus flavimaculatus in a single family with a deletion of codon 153 or 154 of the peripherin/RDS gene. Arch Ophthalmol 111:1531–1542.

Wen GY, Sturman JA, Wisniewski HM, Lidsky AA, Cornwell AC, Hayes KC. 1979. Tapetum disorganization in taurine-depleted cats. Invest Ophthalmol Vis Sci 18:1201–1206.

Wen GY, Wisniewski HM, Sturman JA. 1982. Hereditary abnormality in tapetum lucidum of the Siamese cats: A histochemical and quantitative study. Histochemistry 75:1–9.

Wen GY, Sturman JA, Shek JW. 1985. A comparative study of the tapetum, retina and skull of the ferret, dog, and cat. Lab Anim Sci 35:200–210.

Wenger D, Gasper P, Thrall M, Dial S, LeCoteur R, Hoover E. 1986. Bone marrow transplantation in the feline, model of arylsulfatase B deficiency. In: Krivit W, Paul N, eds. Bone Marrow Transplantation for Treatment of Lysosomal Storage Diseases. New York: Liss, 177.

West-Hyde Leigh DVM, Buyukmihci N. 1982. Photoreceptor degeneration in a family of cats. J Am Vet Med Assoc 181:243–248.

Wiggert B, Kutty G, Long K, Inouye L, Gery I, Chader G, Aguirre G. 1991. Interphotoreceptor retinoid-binding protein (IRBP) in progressive rod-cone degeneration (*prcd*). Exp Eye Res 53:389–398.

Wiggert B, van Veen T, Kutty G, Lee L, Nickerson J, Si J-S, Nilsson SEG, Chader GJ, Narfström K. 1994. An early decrease in interphotoreceptor retinoid-binding protein gene expression by Abyssinian cats homozygous for hereditary rod-cone degeneration. Cell Tissue Res 278:291–298.

Wolfe J, Schuchman E, Stramm L, Concaugh E, Haskins M, Aguirre G, Patterson D, Desnick R, Gilboa E. 1990. Restoration of normal lysosomal function in mucopolysaccharidosis type VII cells by retroviral vector-mediated gene transfer. Proc Nat Acad Sci USA 87: 2877–2881.

Wolfe JH, Sands MS, Barker JE, Gwynn B, Rowe LB, Vogler CA, Birkenmeier EH. 1992. Reversal of pathology in murine mucopolysaccharidosis type VII by somatic cell gene transfer. Nature 360: 749–753.

Woodford BJ, Liu Y, Fletcher RT, Chader GJ, Farber DB, Santos-Anderson R, Tso M●M. 1982. Cyclic nucleotide metabolism in inherited retinopathy in collies: A biochemical and histochemical study. Exp Eye Res 34:703–714.

Wrigstad A. 1994. Hereditary dystrophy of the retina and the retinal pigment epithelium in a strain of briard dogs: a clinical, morphologic and electroretinographic study. Linköping University Medical Dissertation #423.

Wrigstad A, Nilsson SEG, Narfström K. 1992. Ultrastructural changes of the retina and the retinal pigment epithelium in briard dogs with hereditary congenital night blindness and partial day blindness. Exp Eye Res 55:805–818.

Wrigstad A, Narfström K, Nilsson SEG. 1994. Slowly progressive changes of the retina and retinal pigments epithelium in briard dogs with hereditary retinal dystrophy: a morphologic study. Doc Ophthalmol 87:337–354.

Wrigstad A, Nilsson SEG, Dubielzig R, Narfström K. 1995. Neuronal ceroid lipofuscinosis in the Polish Owczarek Nizinny (PON) dog. Doc Ophthalmol 91:33–47.

Wyszynski RE, Bruner WE, Cano DB, Morgan KM, Davis CB, Sternberg P. 1989. A donor-age-dependent change in the activity of alpha-mannosidase in human cultured RPE cells. Invest Ophthalmol Vis Sci 30:2341–2347.

Zhao H, Boissy YL, Abdel-Malek Z, King RA, Nordlund JJ, Boissy RE. 1994. On the analysis of the pathophysiology of Chediak-Higashi syndrome: defects expressed by cultured melanocytes. Lab Invest 71:25–34.

Zimmerman W, Godchaux W, Belkin M. 1983. The relative proportions of lysosomal enzyme activities of bovine retinal pigment epithelium. Exp Eye Res 36:151–158.